Spring 4-13-2018

ADSORPTION OF HEAVY METAL CATIONS ON KLASON LIGNIN FROM PAULOWNIA ELONGATA AND KRAFT LIGNIN

Hanchi Chen
hchen23@syr.edu

ADSORPTION OF HEAVY METAL CATIONS ON KLASON LIGNIN FROM PAULOWNIA ELONGATA AND KRAFT LIGNIN

by

Hanchi Chen

A dissertation
submitted in partial fulfillment
of the requirements for the
Doctor of Philosophy Degree
State University of New York
College of Environmental Science and Forestry
Syracuse, New York
April 2018

Department of Paper and Bioprocess Engineering

Approved by:
Shijie Liu, Major Professor
John E. Wagner, Chair, Examining Committee
Bandaru V. Ramarao, Department Chair
S. Scott Shannon, Dean, The Graduate School

Acknowledgements

First I would like to give my best appreciation to my major professor Dr. Shijie Liu, who has given me the best intellectual support and guidance with his extraordinary experiences and knowledge. His great characters of passion, innovation, preciseness, and enthusiasm as a scientist have encouraged me and motivated me to pursue the truth in science. His earnest edification will continually light my future academic path after my graduation.

Special thanks to my committee members, Dr. Bandaru V. Ramarao and Dr. Wendong Tao, who has provided me their times and efforts in my Ph.D. program. My research project and thesis cannot be completed without their professional knowledge and experiences. Thank Dr. Biljana Bujanovic for providing me her knowledge in wood chemistry which are extremely helpful for this research project. Thank Dr. Nirmal Joshee and International Paper Inc. for providing me the raw materials in this study.

I also wish to bring my thanks to Mr. Dave Kiemle, Ms. Deb Driscoll, and Ms. Marlene Braun. It is their efforts in NMR and ICP that resolved plenty of problems in sample characterizations and quantifications.

Thank my group members who have provided me a pleasant environment to study. Thank Dr. Jipeng Yan, Dr. Yang Wang, Dr. Yuanzheng Wang, Dr. Karin Arens, Dr. John Paul, Dr. Alan Shupe, and Dr. Yipeng Xie who as the senior members in this research groups has introduced me to this group and provided their best effort in my training. Thank my group members Xiaolin Qu, Wei Dai, Guoyu Dong, Chenghui Liang, Dorlan D. Curtis, Jiaqi Huang, Jinxia Yuan and Yaoyao Wang. It is their company that makes my life at ESF splendid.

I would like to thank the faculties and staffs in Paper and Bioprocess Engineering Department. I'm especially grateful to Dr. Gary M. Scott who is the first person that introduced me to this college and department. Thank Ms. Lynn C. Mickinkle and Mr. William M. Burry for providing me plenty of help in this department.

Thank Dr. Nirmal Joshee and International Paper Inc. for providing me the lignin raw materials. Thank the financial support from China Scholarship Council. Finally, I would like to thank my family and everyone who helped me during my Ph.D. program, though I could not mention personally one by one.

Table of Contents

List of Figures

List of Tables

Abstract

H. Chen. Adsorption of Heavy Metal Cations on Klason Lignin from *Paulownia Eelongata* and Kraft Lignin, 106 pages, 11 tables, 26 figures, 2018. Harvard style guide used.

Lignin produced from two processes, 1. An acid hydrolysis process: sequential acid hydrolysis of *Paulownia elongata* wood powder (Klason lignin); 2. Kraft pulping process: black liquor (Kraft lignin), were studied for their heavy metal adsorption affinities. Both lignin samples were effective in removing Pb(II), providing the industrial application potential of lignin in treating lead-contaminated wastewater.

Hot water treatment of woody biomass is a typical biorefinery process that can result in lignin extraction for potential applications. Hot-water treatment was thus evaluated for its impact on the heavy metal adsorption affinities of Klason lignin. It was found hot water treatment can either enhance or weaken the lignin adsorption capacity depending on the severity of the treatment. Samples with long duration of treatment encountered a substantial loss in the adsorption ability. Depolymerization and condensation lignin reaction schemes under acidic and high temperature environment were summarized and applied to explain the affinity changes.

The adsorption mechanism was further studied with Kraft lignin. The Pb(II) adsorption affinity of Kraft lignin was found to follow an "S" dependency on the environmental pH, indicating the existence of more than one ion-exchanging functional groups involved in the adsorption process. NMR characterization of Kraft lignin discovered phenolic hydroxyl groups and carboxyl groups as ion-exchanging functional groups. Other chemical structures in Kraft lignin such as aldehyde groups, ketone groups, ether bond, and aromatic rings are also considered as adsorption functional group because of their potential to complex with heavy metal cations. In order to explain the process from a mechanistic point of view, an novel adsorption theory named "1-n cooperative adsorption theory" was proposed which considered the existence of multiple active sites and the interaction of one adsorbate to multiple sites. The derived model evaluated the effect of temperature and pH on the adsorption affinity, which achieved a significant improvement compared to the Langmuir model. The simulation results show the binding affinity towards Pb(II) is significantly higher than Cd(II) and Ni(II). The new theory also has wide application range to other multivalent interactions including adsorption, flocculation, chelation, and filtration.

Keywords: Heavy metal, Lignin, Hot-water treatment, Non-Langmuir adsorption

H. Chen
Candidate for the degree of Doctor of Philosophy, April 2018
Shijie Liu, Ph.D.
Department of Paper science and Bioprocess Engineering
State University of New York College of Environmental Science and Forestry,
Syracuse, New York

Chapter 1
Introduction

1.1 Background and Objectives

Lignin is a native polymer which is also being produced as the main byproduct from the pulping and biorefinery industries. Now the industrial produced lignin is mainly burned for energy with low value. On the other hand, both pulping and biorefinery industries are in demand in expanding their profit margin. One way to achieve that is to explore extra value for the lignin byproduct. Lignin can be potentially used as adsorbent for treating heavy metal cations in wastewater [1-2]. This is because of the chemical structure of lignin that it contains heavy metal adsorption functional groups such as phenolic hydroxyl group, carboxyl group and electrophilic groups. Heavy metal pollution is one of the most eminent environmental problems nowadays. Most heavy metals are toxic to human beings. On the other hand, people are dependent on heavy metals in producing daily necessities such as electroplates, battery, pigments, tannery and pesticides, which results in the heavy metal exposure to the environment [3-11]. Different heavy metal remediation technologies have been developed such as pH adjustment, chemical precipitation, membrane filtration and electrochemical methods. Some conventional treatment technologies for heavy metals are chemical precipitation, membrane filtration and electrochemical methods [12]. However, these technologies either require large capital investments or high operational costs. The high cost of the treatment process and material is one reason that impedes some industries, especially traditional and small-scale industries, to treat their wastewater properly. Alternatively, adsorption is another effective process in treating heavy metal contaminants with low energy input. Recently, the development of cost-efficient heavy metal treatment materials has been studied in order to reduce the overall cost of the heavy metal treatment process and lignin is one of them. A couple of studies have been conducted upon the heavy metal adsorption by Kraft lignin that concluded Kraft lignin is effective in removing Pb(II), Cd(II) and Cu(II) from wastewater streams

[13-17]. On the other hand, the adsorption mechanism of heavy metal cations on lignin is still obscure. Previously studies have applied ion-exchanging mechanisms in explaining the process, while some other studies indicate the involvedness of complexing between electrophilic groups and heavy metal cations. Due to the complexity of the process, there is yet a mechanistic model describing this process, while the currently applied models are mostly empirical. In the review chapter, we went through the chemical structure of lignin from different origins. Lignin characterization methods was introduced and later applied to our study. The heavy metal pollution sources was discussed in order to achieve a pollution control from the origin. The current status of heavy metal pollution was also reviewed based on different regions around the world. For the heavy metal remediation technologies, chemical precipitation, flocculation, ion exchange chromatography, and bioremediation, are introduced from their mechanisms and their pros and cons. The adsorption process was reviewed from its mechanism to the theories, as well as the previous studies about using lignin as a heavy metal adsorbent.

From the literature review, we observed the lack of study about lignin from the biorefinery field, and there is a potential of using this part of lignin as heavy metal adsorbent [18-20]. So in the first part of the project, Klason lignin originated from *Paulownia elongata* wood powder was evaluated for its adsorption affinities towards Pb(II), Cd(II), and Cu(II). Klason lignin, although it is mostly referred to a quantification method for lignin content, is technically the residue of the acid hydrolysis process. Biorefinery processes such as autohydrolysis, alkaline pretreatment, and oxidative pretreatment can impact on the adsorption affinity due to the alternation of the lignin chemical structure. Hot water treatment, a typical biorefinery process, was evaluated on its impact to the adsorption affinity in this part of study. We observed both the increase and decrease of the adsorption affinity after different severities of treatment, and summarized lignin reactions during

hot water treatment and their effects on the adsorption affinity. NMR characterization was performed and applied to quantify the amount of functional groups before and after hot water treatment. Lignin reaction were summarized and applied to explain the affinity changes after hot water treatment.

It was also observed that current studies have not provided a plausible mechanistic description of the process. In the second part of this study, we performed NMR characterization on Kraft lignin structure, and proposed the binding mechanisms of heavy metal cations on lignin. A novel adsorption theory, "1-n cooperative adsorption theory" in explaining the adsorption process of heavy metal cations on lignin. In the new theory, couple characteristics of a non-ideal adsorption process have been considered: 1. the ununiformed adsorbent surface with active sites at different interactive energy levels (multiple active sites). 2. the binding of one adsorbate to multiple active sites (multivalent interactions). 3. the interaction between active sites in capturing one adsorbate molecule (cooperativity). The proposed theory characterized the adsorption features of heavy metal cations on lignin which is applied to interpret the experimental data with high agreement. The theory itself also has a wider application on other multivalent interactions beside adsorption.

1.2 Outline

Chapter 1: Introduction

This chapter gives an introduction to the background of the problem. It explains the reason and objectives of this study. Meanwhile, it gives readers a general idea about the major contents and achievements in this thesis.

Chapter 2: Literature Review

In this chapter, the characteristics of lignin, the heavy metal pollution problems, and the previous studies about using lignin as heavy metal adsorbent are introduced in the following sessions:

1. Lignin: structure, production, and characterization
2. Heavy metal pollution
3. Heavy metal remediation technologies
4. Heavy metal adsorption on lignin

Chapter 3: The effect of hot water treatment on the adsorption affinity of Klason lignin

This chapter describes the hot-water treatment and its relevance. The raw materials, experimental methods, will be introduced and explained in detail. The experimental results will be provided and the lignin reaction schemes under hot water treatment will be summarized and applied to explain the results.

Chapter 4: Cooperative adsorption of heavy metal cations on Kraft lignin

This chapter describes the theoretical development of this thesis. The raw materials, experimental methods, "1-n cooperative adsorption theory", and the mathematical modeling will be introduced and explained in detail. The experimental results with model interpretation will be provided. Discussion of the parameters obtained will be given in describing the characteristics of the adsorbent surface. Adsorption isotherm will be given providing information about the adsorption capacity with the change of the environmental pH.

Chapter 5: Conclusions

This chapter concludes based on the experimental findings and illustrates the achievement of the initial goals and potential applications.

Chapter 6: Future studies

In this chapter, we will combine the research results obtained from the study and propose further development requirements regarding to this project. Research ideas of the process improvement will be proposed as well in this chapter.

Chapter 2
Literature Review

2.1 Lignin: structure, production, and characterization

Lignin is known as the most abundant aromatic polymer and the second most abundant polymer after cellulose in nature. Lignin provides the strength to plants that its deposition in plant cell wall significantly helps cellulose and hemicelluloses to support the tree from severe environmental conditions. However, lignin is not a desired component in the pulp and paper industry because lignin generates dark color during the pulping process and lignin interferes the hydrogen bonding between fibers which substantially reduces the strength of the product. On the other hand, modern biorefinery technologies are using lignin for different materials such as adsorbents, adhesives, antibiotics, and antioxidants. In either way, it is important to understand the lignin structural and chemical characteristics for a better utilization of lignin. In this session, a brief introduction of monolignols (the monomeric units of lignin), monolignols polymerization, native/industrial lignin, lignin reactions, as well as lignin characterizations will be introduced.

2.1.1 Monolignols and their biosynthesis in lignocellulosic species

Although it has been proposed that lignin is constructed from phenylpropanoid units in 1940 due to its chemical properties, the idea was not accepted until 1954 when Lange analyzed a wood section with UV microscopy [21]. The main structure of a lignin molecule is built from three cinnamyl alcohol derivatives known as coniferyl alcohol ($M1_G$), sinapyl alcohol ($M1_S$) and *p*-coumaryl alcohol ($M1_H$). After polymerization, the three monolignols become the constituents of a lignin molecule to guaiacyl (G), syringyl (S) and *p*-hydroxyphenyl (H) units, respectively [22]. The chemical structures of the three major monolignols and their respective forms in a polymer are shown in Figure 2.1. Besides the three main monolignol precursors, other monomeric phenolic compounds such as phenylaldehyde and hydroxycinnamyl acetate may also be observed in different lignins. The three monolignols are also known as lignin precursors. It should be noted that the double bond in the precursors is saturated after polymerization. The content of each lignin

unit is depending on the species. Softwood lignin consists of majorly G unit and little H unit while hardwood lignin consists of both S unit and G unit with a trace amount of H unit. In monocotyledons, lignin is composed of S, G and H units while the content of H unit is relatively higher than that in higher plants [23]. A lignin molecule is formed through the conjugative and random polymerization between the dehydrogenated oxidized monolignols, so a lignin molecule does not have a regular chemical structure. Lignin models for softwood and hardwood are shown in Figure 2.2 and 2.3 respectively.

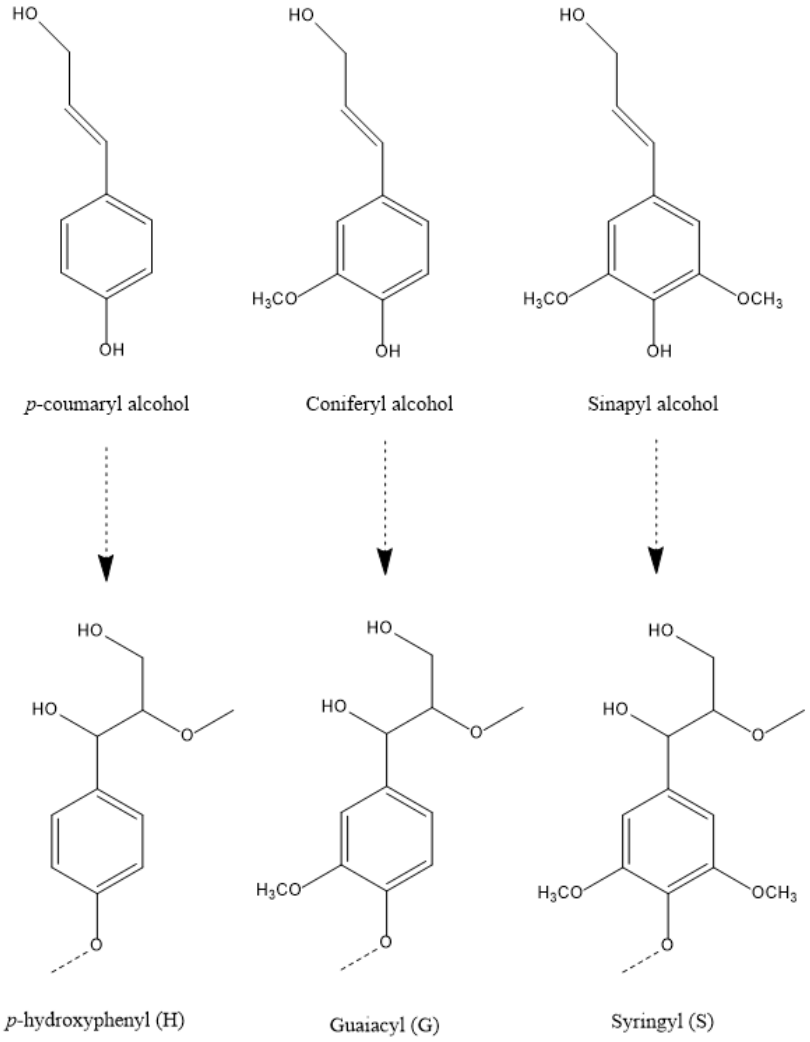

Figure 2.1. The chemical structure of three monolognol precursors and their polymerized forms in lignin [24].

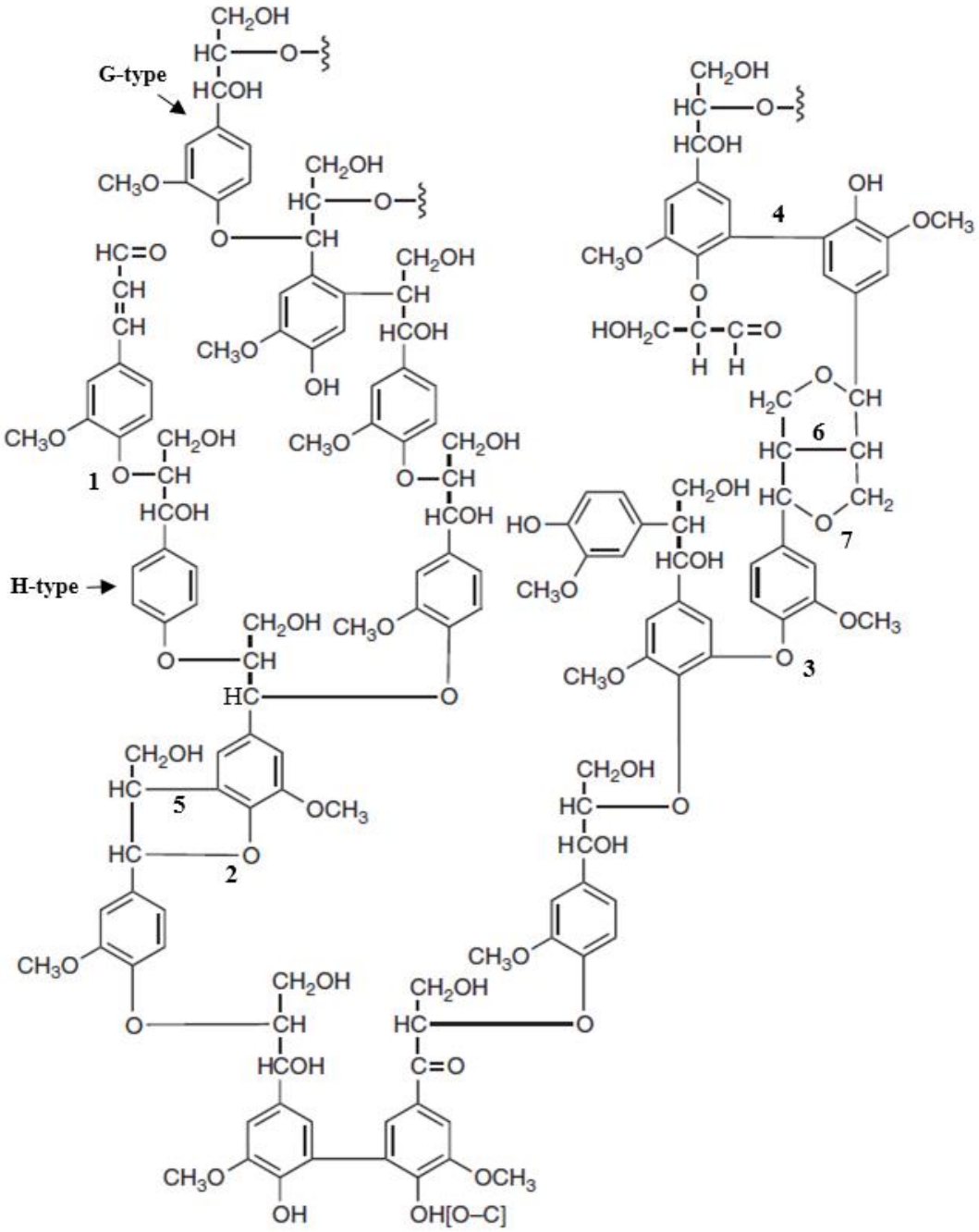

Figure 2.2. A softwood lignin model. Only *p*-hydroxylphenyl (H) and guaiacyl (G) units are presented, where coniferyl alcohol is the major precursor [24].

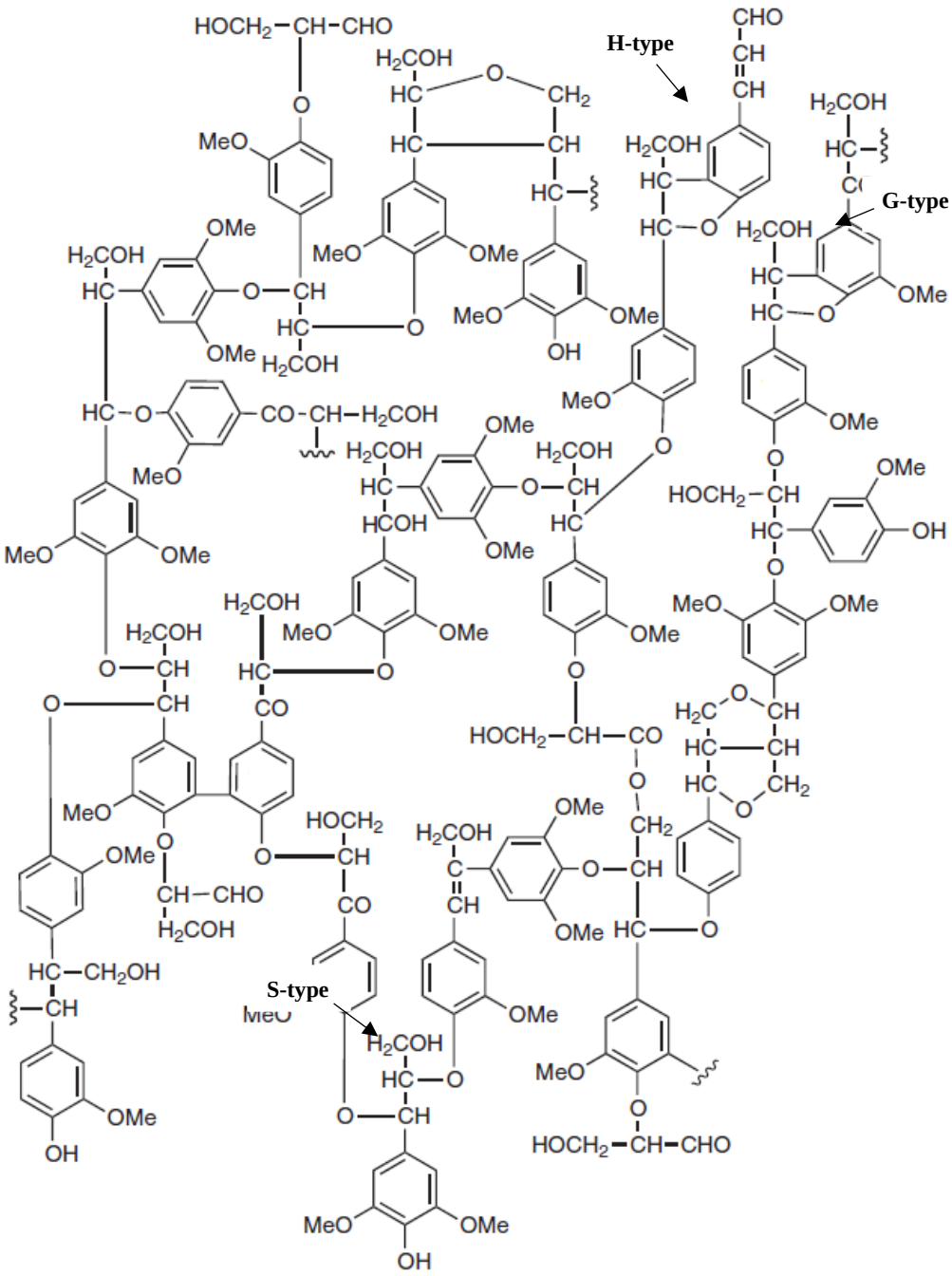

Figure 2.3. A hardwood lignin model based on beech. All H, G, S types of lignin units are presented. The proportion of S and G units is substantially higher than the H unit [24].

How monolignols are synthesized in lignocellulosic species was a controversial topic in the early years, but with the development of genetic cloning as well as the *in vitro* enzymatic assays, researchers are now painting a clearer picture of the lignin biosynthesis pathway. The monolignols synthesis pathway originated from two primary metabolites known as phosphoenolpyruvate (PEP) and erythrose 4-phosphate (E4P), which are the intermediates during the glycolysis and pentose phosphate pathway, respectively [25]. The metabolic synthesis pathway from PEP and E4P to monolignols, shikimate-chorismate pathway and monolignols synthesis pathway, are summarized in Figure 2.4 and 2.5 with the relevant enzymes in each steps of synthesis given in Table 2.1 and 2.2. From the synthetic pathway one can observe that monolignols are synthesized either from phenylalanine or tyrosine as the metabolites from the shikimate-chorismate pathway which have already processed the benzylpropanoid structure. Further synthesis includes the methoxylation on the aromatic ring as well as the deamination and reduction on the propane chain.

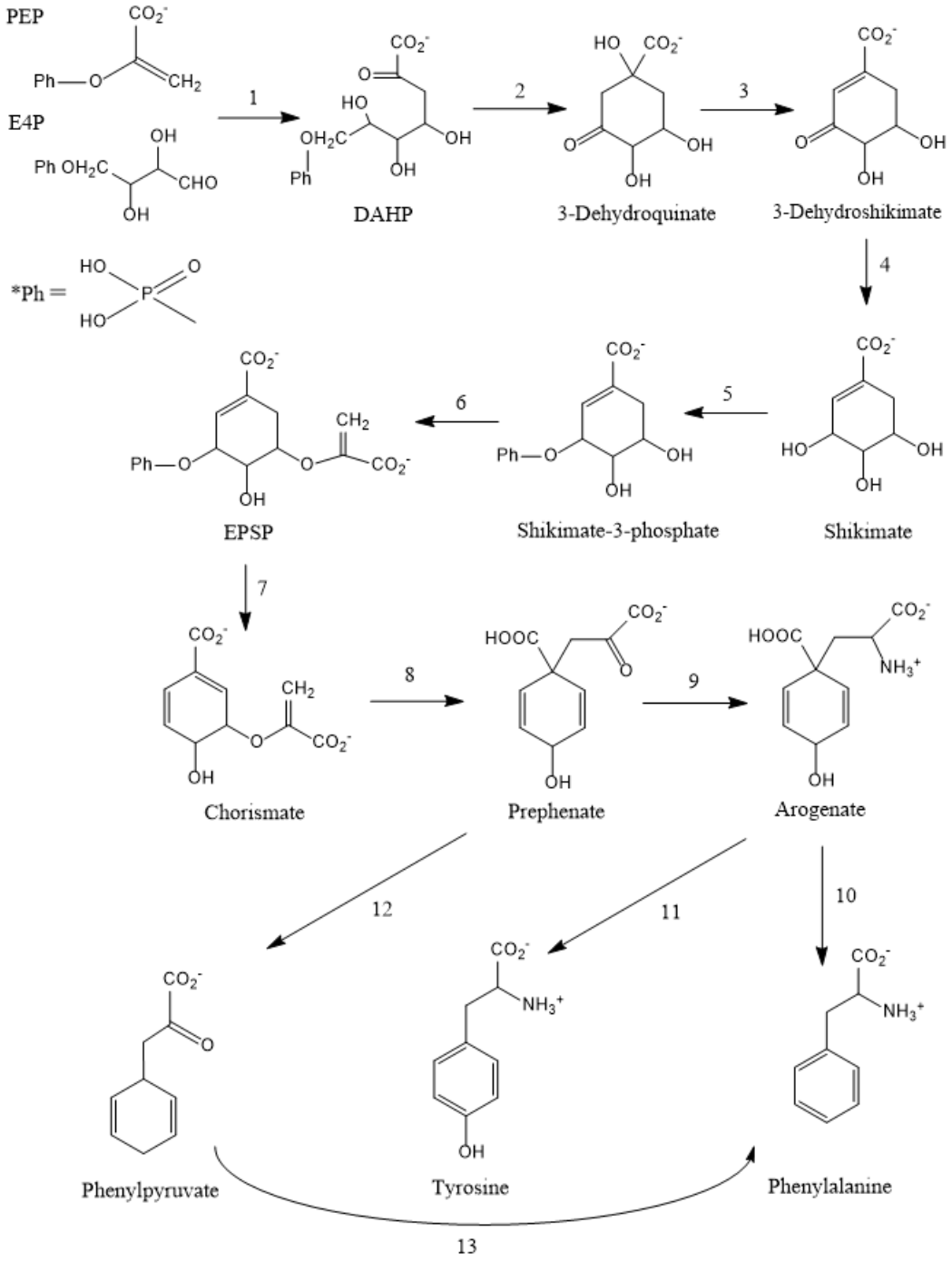

Figure 2.4. The formation of phenylalanine and tyrosine as the starting metabolites for monolignols synthesis through shikimate pathway [26,27].

Table 2.1. The enzymology and the involvement of substrate(s) in each step of the Shikimate pathway [26].

Reaction step	Catalytic enzyme	Substrate(s)
1	DAHP synthase	PEP, E4P
2	Dehydroquinate synthase	DAHP, NAD^+
3	3-dehydroquinate dehydratase	3-dehydroquinate
4	3-hydroxyshikimate reductase	3-hydroxyshikimate, NADPH
5	Shikimate kinase	Shikimate, ATP
6	EPSP synthase	Shikimate-3-phosphate, PEP
7	Chorismate synthase	EPSP
8	Chorismate mutase	Chorismate
9	Prephenate amino transferase	Prephenate, NH_4^+
10	Arogenate dehydratase	Arogenate
11	Arogenate dehydrogenase	Arogenate
12	Prephenate dehydratase	Prephenate
13	Phenylpyruvate aminotransferase	Phenylpyruvate, L-glutamine

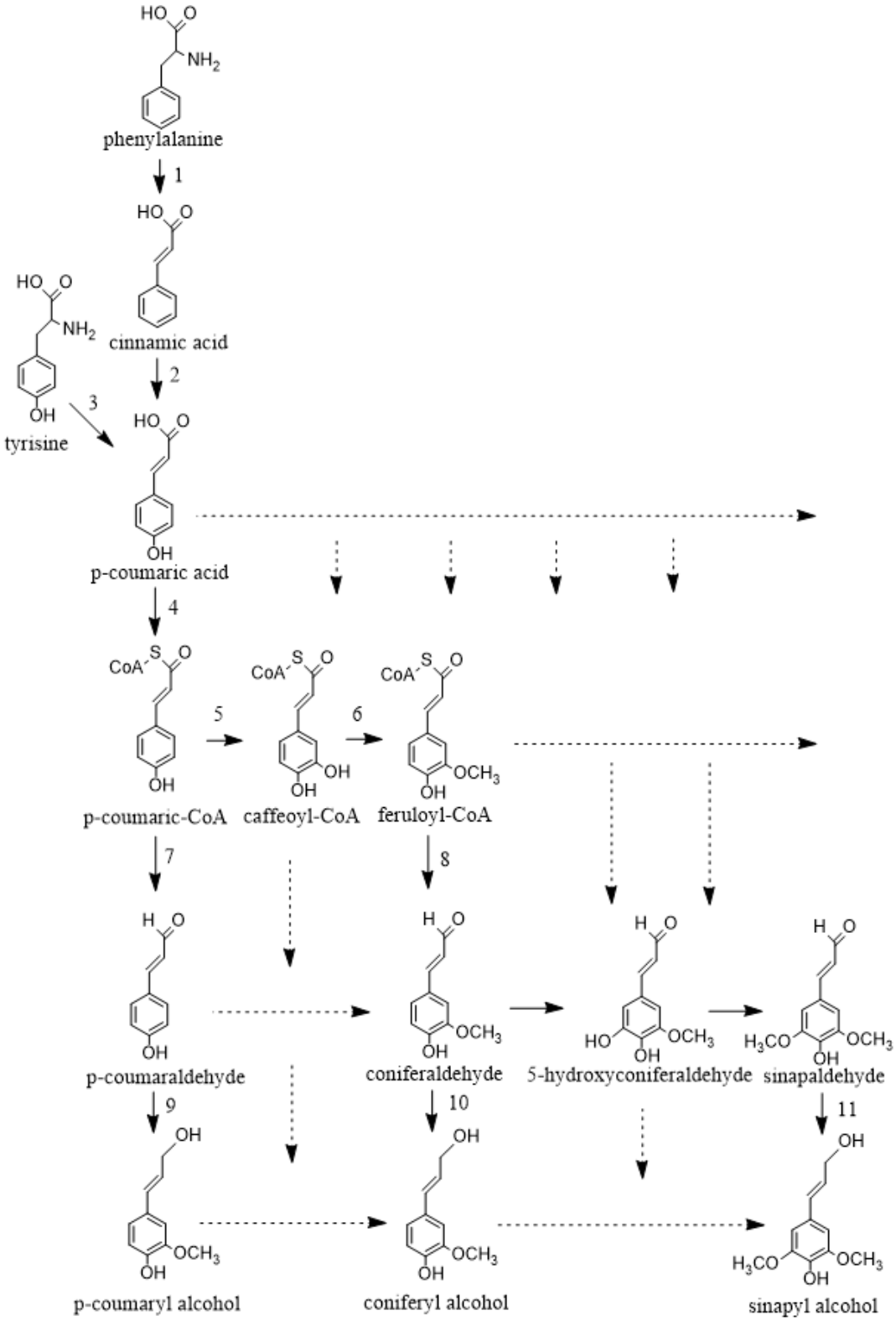
phenylalanine
1
cinnamic acid
2
tyrisine
3
p-coumaric acid
4
p-coumaric-CoA
5
caffeoyl-CoA
6
feruloyl-CoA
7
8
p-coumaraldehyde
coniferaldehyde
5-hydroxyconiferaldehyde
sinapaldehyde
9
10
11
p-coumaryl alcohol
coniferyl alcohol
sinapyl alcohol

Figure 2.5. The biosynthesis pathway from phenylalanine or tyrosine to monolignols. Solid arrows suggest the most favored monolignols biosynthesis route in angiosperms as studied with lignin composition, in vitro enzyme assays and transgenic plants. Dash arrows give the secondary routes for monolignols biosynthesis which were observed in vitro but corresponding enzymes showed lower efficiency to the substrates than the solid route [28].

Table 2.2. The enzymology during the biosynthesis of monolignols [28].

Reaction step	Catalytic enzyme
1	phenylalanine ammonia-lyase
2	cinnamate-4-hydroxylase
3	tyrosine ammonia-lyase
4	4-coumarate CoA ligase
5	quinate shikimate *p*-hydroxycinnamoyltransferase/coumarate 3-hydroxylase
6	caffeoyl-CoA O-methyltransferase
7	cinnamoyl-CoA reductase
8	cinnamoyl-CoA reductase
9	cinnamyl alcohol dehydrogenase/sinapyl alcohol dehydrogenase
10	cinnamyl alcohol dehydrogenase/sinapyl alcohol dehydrogenase
11	cinnamyl alcohol dehydrogenase/sinapyl alcohol dehydrogenase

2.1.2 From monolignols polymerization to lignin structures

Monolignols are synthesized in the cytoplasm of the plant cell. However, as phenolic compounds, monolignols are toxic to the plant cell. Due to the low solubility of monolignols, how monolignols are stored in the cytoplasm and transported to the cell wall becomes an interesting area to be studied. It was first found the monolignol glucosides are accumulated in the cambium suggesting the monolignols are in forms of glucosides in living cells [29]. Later in vitro experiment observed that sinapyl alcohol can be glucosylated to syringin with glycosyltransferases synthesized

from *Arabidopsis* genes [30]. With the phenomenon observed in nature cells as well as in vitro experiment, the currently accepted concept is that monolignols are glucosylated through the phenolic group into monolignol 4-O-β-D-glucosides after their biosynthesis (Figure 2.6). After the synthesis, monolignols are transported to the cell wall in forms of monolignol 4-O-β-D-glucosides either through passive diffusion or facilitative transport. The higher solubility of monolignol 4-O-β-D-glucosides also facilitates the transportation process while reducing the monolignol level in the cytoplasm [24].

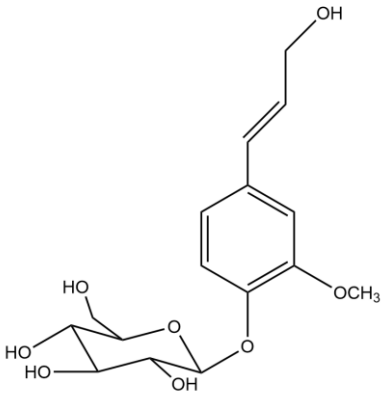

Figure 2.6. The structure of coniferyl glucoside. Monolignol and D-glucose are linked through 4-O-β ether bond.

The polymerization of monolignols is a radical coupling process starts with dehydrogenation. The dehydrogenation produces phenoxy radicals on monolignols, which can be further converted to carbon radicals (Figure 2.7a) and results in the intermolecular reactions between monolignols or oligomers. A class of enzymes such as peroxidase, laccase, and phenol oxidases is considered to be involved in the dehydrogenation process. Peroxidase catalyzes the reaction between hydroperoxide and the phenolic hydroxyl group on monolignols, which generates a phenoxy radical on C4. Hydrogen peroxide can be originated from some oxidases in cells. For examples,

glucose oxidase catalysis the oxidation of glucose to gluconolactone while releases hydrogen peroxide (Eqn a) [31]. Glyoxal oxidase catalyzes the oxidation of glyoxalate and releases hydrogen peroxide (Eqn b) [32]. Other hypothesizes proposed the oxidation of monolignols with NADPH oxidase or through the malate dehydrogenase and peroxidase on the cell wall [33-34]. On the other hand, laccase catalyzes the oxidation of monolignols with oxygen. Other oxidases were involved either catalyzing a different hydroxyl group or a different substrate. In general, no single enzyme is solely responsible for the step of dehydrogenation. In native lignin, it is also observed that some types of reduced structures which cannot be explained by oxidative coupling. Holmgren et al. [35] proposed a non-enzymatic catalysis reducing pathway of β-aryl ether quinone methide by NADH indicating that a part of the monolignol polymerization can be non-enzymatically controlled.

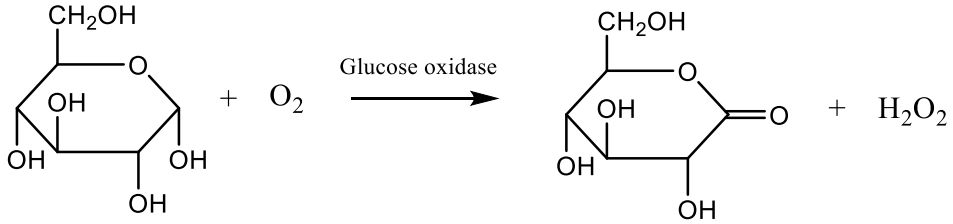

(a)

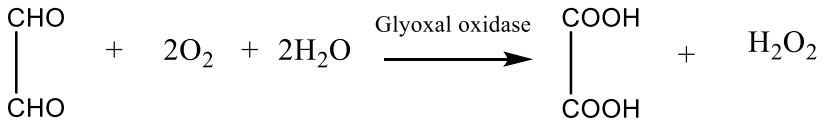

(b)

The polymerization is initially considered as a random process happening in plant cell wall. However, the recent discovery of a class of dirigent proteins suggests the polymerization is actually under biological control [36]. The polymerization of monolignols results in both lignan and lignin. The difference between lignan and lignin lies in two points: Structurally speaking, lignan is formed from the dimerization of monolignols. β-β is the major couplings occurred in lignans which results in the stereospecific structure of lignan [37]. On the other hand, lignin molecules are much polymerized and cross-linked. Functionally speaking, lignin is embedded in cell wall providing

the physical support of a plant. Lignan has other properties such as antioxidant and antibiotic which is more involved in a plant's defense system. The polymerization starts with the dimerization through coupling such as β-O-4', α-O-4', β-β', 5-5' etc. On the other hand, native lignin formation is known to be an end-wise polymerization process. Such process suggest the highest potential of radical location on Cβ, while the coupling occurs stepwise usually between Cβ and the original radical location (phenolic hydroxyl group). This explains why β-O-4' is the major linkage in native lignin while β-β' is the major linkage in in-vitro lignin synthesis [38]. β-O-4' presents about 45%-50% in softwood lignin and 50%-65% in hardwood lignin. 5-5' bond is the condensation linkage which presents about 18%-25% in softwood lignin while only 4%-10% of hardwood lignin due to the high content of synapyl unit [21,38]. Radicals can be further formed from the oxidation of dimers that keeps dimers to further polymerize into lignin molecules. The scheme of radical formation on monolignols are shown in Figure 2.7. The major linkages between monolignols are C-C and C-O bonds as depicted in Figure 2.2, which is further summarized in Table 2.3. The carbons in a monolignol are labeled as α-γ for alkenyl carbons and 1-6 for phenyl carbons.

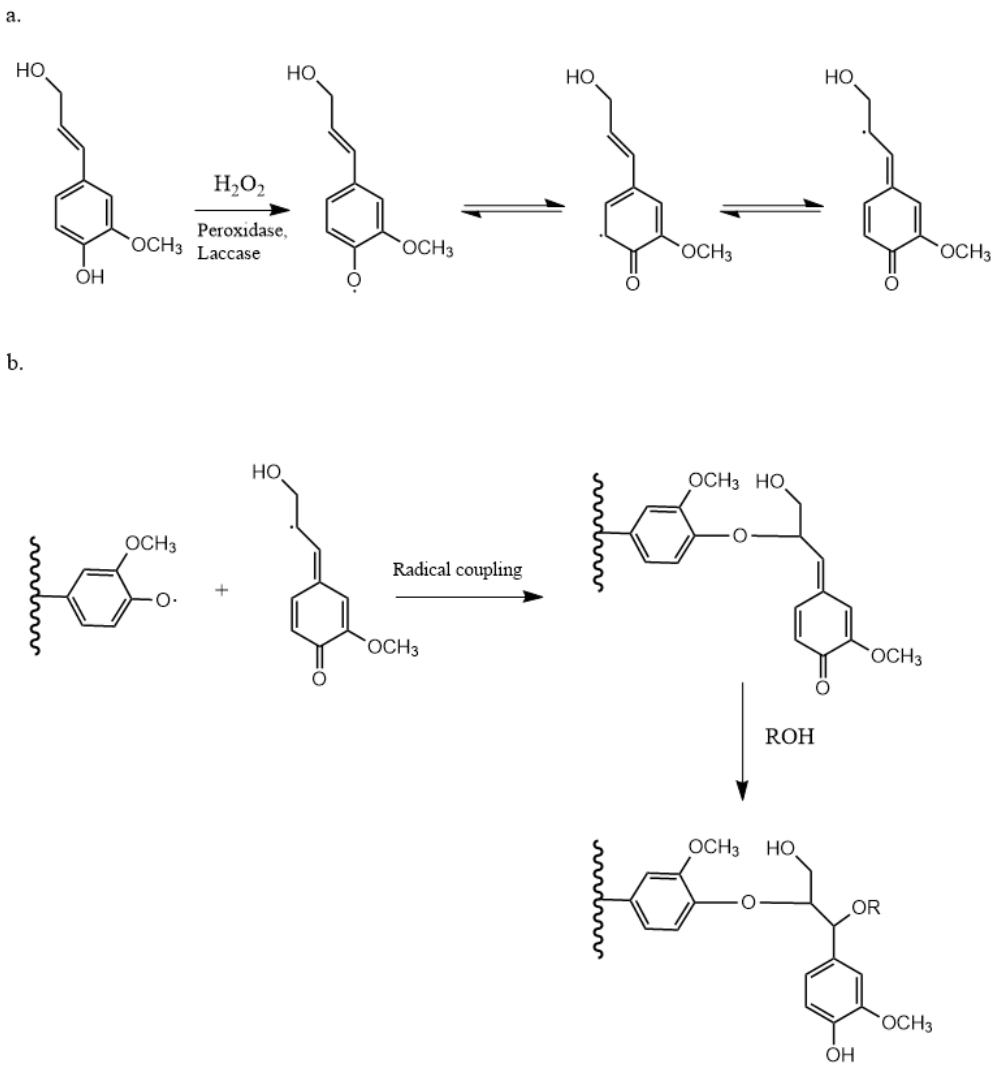

Figure 2.7. (a) Radical formation on the phenolic group, C_5, and C_β on coniferyl alcohol. (b) The scheme of the β-O-4 bond formation through the radical coupling. ROH: H_2O, carbohydrate, phenolic compound [35,39].

Table 2.3. Typical linkages in lignin.

Depiction (Labeled in Figure 2.2)	Linkage-type
1	β-O-4'
2	α-O-4'

3	4-O-5'
4	5-5'
5	β-5'
6	β-β'
7	α-O-γ'

2.1.3 Native and industrial lignin

2.1.3.1 Native lignin in wood formation

As a plant-derived biopolymer, lignin basically exists in every biomass species including trees, grasses, and crops. Principally speaking, the cell wall contains all the lignin in a plant cell. A plant cell wall can be characterized by layers namely as middle lamella (ML), primary wall (P) and secondary wall (S), where the secondary wall is further differentiated as the outer layer (S1), middle layer (S2) and inner layer (S3) (Figure 2.8) [40]. ML and S3 have the highest concentration of lignin among the layers. ML is the intercellular layer that lignin in ML functions as an adhesive that binds cells together. S3 as an inner layer contains lignin that provides the firmness of the cell wall. The lignin content of a biomass varies from species. Generally speaking, wood species contain 18-35 wt% of lignin [41].

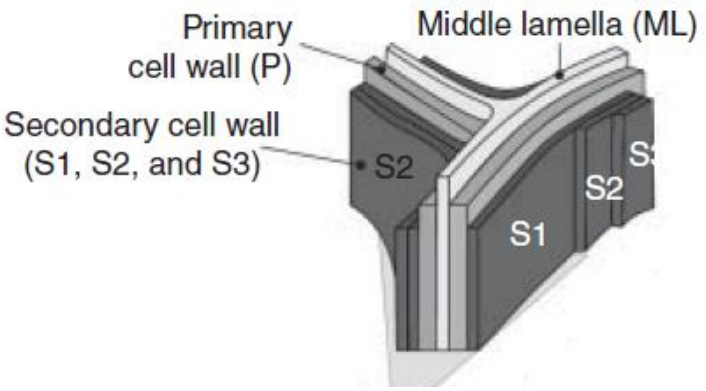

Figure 2.8. Structural model a plant cell wall [40].

2.1.3.2 Kraft lignin

Industrial black liquor is a waste stream that generated from the Kraft pulping industries during the delignification process. Black liquor used to be regarded as the single source of industrial lignin until the recent upraise of the biorefinery industry. However, due to the huge scale difference between the two fields, black liquor is still regarded as the major source of industrial lignin. Every year, more than 500 thousands metric tonnes of lignin are produced through pulping, which poses a significant problem for its disposal regarding the environment constraints [14,17]. The current process is to separate Kraft lignin through evaporation and use the lignin as fuel. Although such process is favorable in energy saving, Kraft lignin contains a certain amount of sulfur that its incineration can cause air pollution. The development of industrial lignin applications is drawing attention from both researchers and industries. To fulfill such goal, it is essential to first understand the origin and structure of Kraft lignin.

The Kraft process is a chemical pulping process which incorporates the use of sodium hydroxide and sodium sulfide. In the cooking step, sodium hydroxide and sodium sulfide solution known as the white liquor is mixed with the wood chips and heated to over 170°C. Under such high temperature and alkalinity, both hemicellulose and lignin are depolymerized and dissolved into the solution, leaving cellulose with loose structure for further processing [42-43]. Specific lignin depolymerization reactions include α-O-4 cleavage with OH^-; β-O-4 cleavage with HS^- (Figure 2.9).

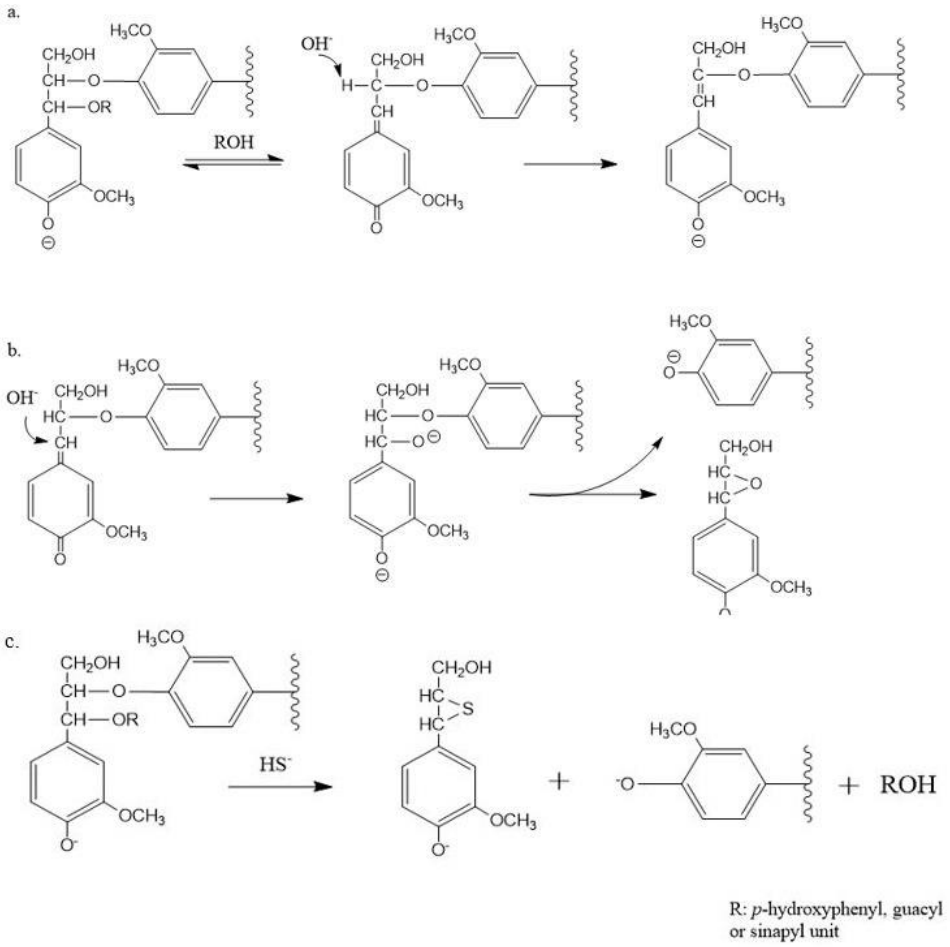

Figure 2.9. Lignin depolymerization reactions happened during Kraft cooking [44-46].

The solution after the cooking step possesses a dark color, known as the black liquor. Due to the lignin reactions, Kraft lignin is structurally different to the native lignin. Kraft lignin can be easily separated from the solution through acidification. Comparing to the native lignin, the Kraft lignin is typically less polymerized and sulfur-containing.

2.1.3.2 Lignin from biorefinery processes

Due to the rich in carbohydrate, the utilization of biomass in the production of renewable bioenergy and biomaterials has been a popular topic since the past decades. Most lignocellulosic biomasses, such as wood, monocotyledons and agriculture residues, possess recalcitrant cell wall

structures that require harsh conditions to be processed. At such conditions, the changes of lignin from its original structure is expected. In this part of the review, lignin structural changes after typical biorefinery processes at acidic, alkaline, and oxidative conditions will be introduced.

2.1.3.2.1 Lignin from biorefinery processes

Typical acidic biorefinery processes are autohydrolysis pretreatments including hot water pretreatment and steam explosion. Acid hydrolysis is another biorefinery process conducted at acidic conditions. However, acid hydrolysis is less studied recently due to its poor cellulose conversion, high equipment requirement, and environmental pollution issues. Autohydrolysis is usually conducted at low pH, high temperature, and potentially pressurized conditions. The presence of acetic acid in the autohydrolysis environment is the main reason for the acidic condition. Some of the acidity can also be contributed through the deprotonation of glucuronic acid and the release of other organic acids such as ferulic acid and cumaric acid in monocotyledons. As softwood has relatively lower acetylation in its hemicelluloses structure and its G lignin structure is easily condensed under acidic pH [47-48], autohydrolysis processes are applied to hardwood species, agriculture residues, and monocotyledons.

Before pretreatment, biomass has highly ordered structure with cellulose and hemicelluloses embedded in lignin. Under high temperature and low pH conditions, the cleavage of glycosidic bonds starts to occur first on the hemicellulose that opens up the cell wall structure that increases the accessibility of chemicals in further processing [49]. Cellulose structure also changed in the autohydrolysis process due to the reduction of polymerization degree as well as crystallinity. Figure 2.10 shows the depolymerization mechanism during autohydrolysis by using xylan as an example. Autohydrolysis processes result in the depolymerization of hemicellulose that is soluble in the forms of oligomers and monomers while cellulose and lignin remain insoluble. Further

degradations of monosaccharides to furfural and hydroxymethylfurfural (HMF) can also occur depending on the severity (temperature and duration) of the pretreatment.

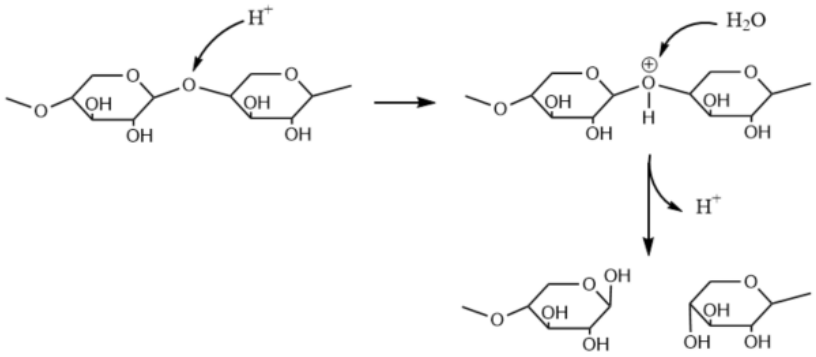

Figure 2.10. Reaction scheme of xylan depolymerization under acid condition [50].

Lignin structural changes during autohydrolysis can be characterized as depolymerization and repolymerization (condensation). The aryl ether bonds in lignin such as α-O-4 and β-O-4 linkages can be cleaved under the acidic environment (Figure 2.11), where the reactivity of α aryl ether bond was reported to be 100 times higher than the β aryl ether bond [51]. This lignin depolymerization process is significantly favored by the high temperature and acidity. Lignin depolymerization results in free phenolic hydroxyl groups and carbon cations that increases the lignin reactivity. One should notice that the cleavage of aryl ether bonds occurs not only between lignin units but also in lignin-carbohydrate complex (LCC) [52]. The cleavage of LCC bonds results in the detachment of fiber from lignin and a better exposure to carbohydrates in the further processing.

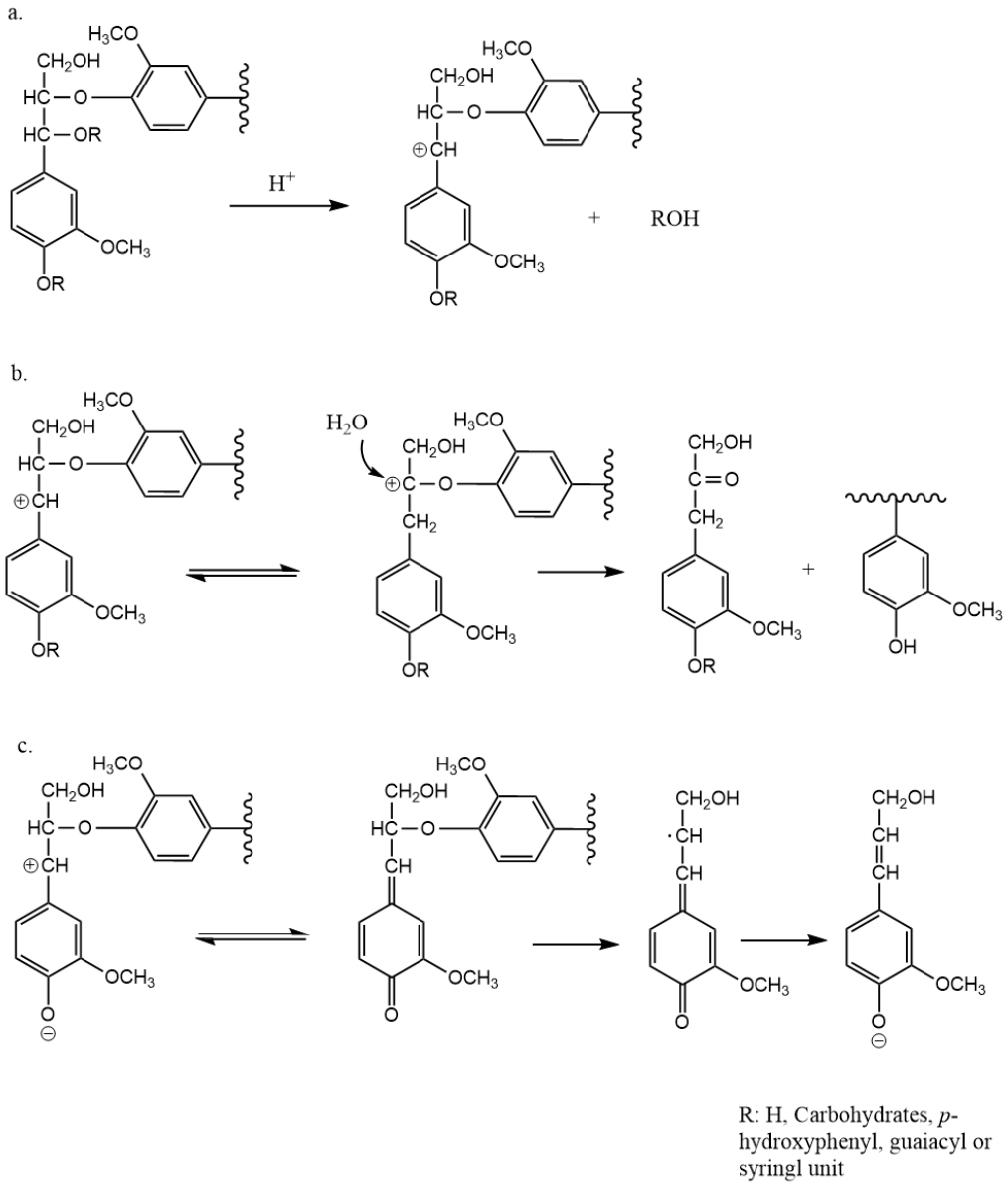

Figure 2.11. (a) The cleavage of α aryl ether bond under acidic condition. A new phenolic hydroxyl group and a carbon cation are generated. (b) The interconversion of carbon cation between C_α and C_β which results in the cleavage of β-O-4 linkage with the attack of water. A new phenolic group and a Hibbert ketone are generated. (c) The cleavage of β-O-4 linkage through radical exchange reaction, which can only occur in units with free PhOH group [53].

In another case, due to the formation of carbon cation on C_α, lignin repolymerization can occur between C_α and C_6 which results in a condensed C-C bond (Figure 2.12). The condensation reaction is also favored by high temperature and low pH. It has been reported that with long autohydrolysis duration, lignin reactions are dominated by condensation. One reason is the decreasing amount of aryl ether linkages at a later stage of pretreatment due to the depolymerization that the only condensation can occur. Li et al. [53] performed steam explosion on aspen wood and observed the decrease of β-O-4 bond with an increase of severity. Hydrothermal pretreatment with high severity and short duration results in the decrease of lignin polymerization degree. Increase of lignin molecular weight was observed with long duration of hydrothermal pretreatment [53-54]. Lignin condensation is not desired during pretreatment as the condensed lignin can attach on the fiber and is highly hydrophobic and recalcitrant, which reduces the accessibility of fibers. Also, the reactivity of condensed lignin is low, which hinders lignin for further application. Some studies have been performed to avoid lignin repolymerization by adding other chemicals such as boric acid which can react with carbon cation before another lignin unit does [55].

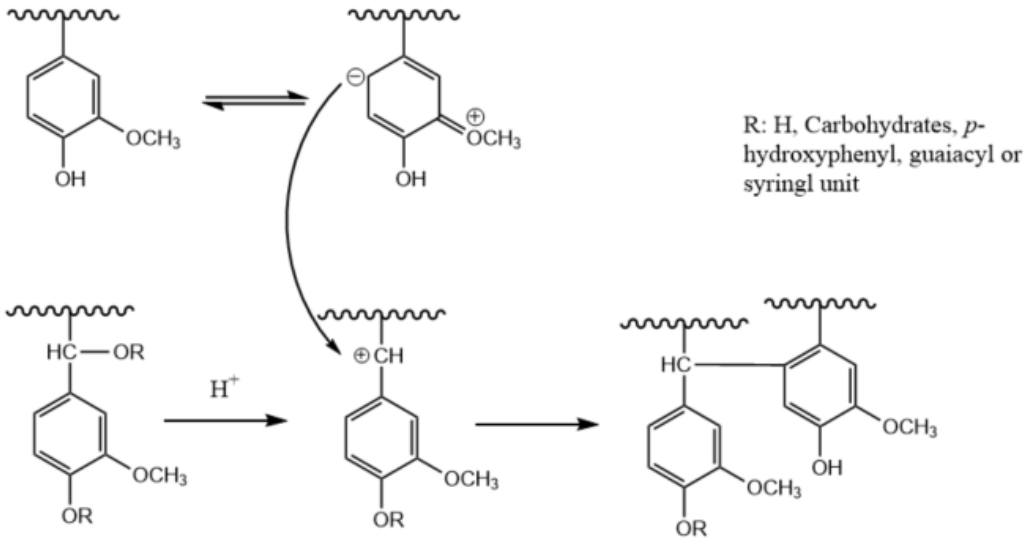

Figure 2.12. Reaction scheme of lignin repolymerization. Condensed C-C bond is formed between C_α and C_6. Repolymerization was reported to be dominant at severity S_0=3.2-4.5 [53,56].

Besides the depolymerization and condensation reactions occurring during autohydrolysis inside of lignin molecules, the formation of pseudo-lignin can also occur with sugar degradation products (SDP) or between SDP and lignin. Studies have been performed to analyze pseudo-lignin structures with GPC, FTIR, and NMR. Carbonyl, carboxylic, aromatic and aliphatic structures are discovered in pseudo-lignin. Pseudo-lignin is not preferred as its formation will increase the recalcitrance of the lignocellulosic materials that impacts on the further hydrolysis efficiency [57-58].

2.1.3.2.2 Alkaline process: alkaline pretreatment

Alkaline pretreatment is the use of basic chemicals to react with the cell wall constituents, mainly lignin, that results in a better exposure of cellulose and hemicellulose. Same with the autohydrolysis pretreatment, alkaline pretreatment can either be heterogeneous and homogeneous, ammonia fiber explosion (AFEX) and alkaline hydrolysis for example. The reaction conditions of alkaline pretreatment can be milder than autohydrolysis. Ammonia fiber explosion (AFEX) is usually carried at below 100°C [59-60]. Homogeneous alkaline pretreatment can be conducted at ambient conditions but longer reaction time, hours to days depending on the lignin content. Sodium hydroxide, potassium hydroxide, and ammonium hydroxide are all found to be effective in the alkaline pretreatment. Recently, the use of calcium hydroxide has been studied to be an effective and cheap alkaline pretreatment chemical. One major difference between the AFEX and alkaline hydrolysis is the solid removal ratio. AFEX can keep almost all materials in the solid for with only limited removal of hemicellulose and lignin. Hemicelluloses and lignin are depolymerized after the AFEX and hemicelluloses are deacetylated. On the other hand, the solid removal is significant

in the alkaline pretreatment mainly because of the dissolution of lignin. Depolymerization of hemicellulose and cellulose was also observed due to the peeling reaction [61].

Lignin depolymerization occurred mainly during the alkaline pretreatment process, which is similar to the delignification reactions in the Kraft pulping process. Lignin depolymerization scheme is similar to the Kraft delignification process as shown in Figure 2.9 (a) and (b). One should notice that the cleavage of aryl ether bond can only happen on the lignin units with free phenolic hydroxyl groups and new phenolic hydroxyl groups are generated in this process resulting in more active units for alkaline to attack. It has been reported that 50% of delignification by using alkaline pretreatment can be reached on monocotyledons and agriculture residues [62-63]. The removal of lignin results in a loose cell wall structure that increases the accessibility of chemicals for further fiber processing. Substantial increase of digestibility has been reported with alkaline pretreatment [64].

2.1.3.2.3 Oxidative processes: biodegradation and ozonolysis

Biodegradation of lignocellulosic biomass is a method of pretreatment that carries the purpose of lignin degradation in order to reduce the recalcitrance of cell wall. Lignin degradation enzymes are characterized by lignin peroxidase (Lip), manganese peroxidase (MnP), versatile peroxidase (VP) and laccase. These enzymes have been found in various types of white rot fungus. Bio-pretreatment has its advantages of low energy requirement, however, most of the processes require more than 4 weeks to finish the pretreatment [65-67]. A general description of the lignin biodegradation mechanism can be concluded in three steps. The first step is the oxidation of lignin oxidases by oxidants (O_2 or H_2O_2) that lignin oxidases are converted to their oxidized forms. Second the oxidation of mediators through the oxidized lignin oxidases, which is a necessary step for MnP, VP, and laccase but not LiP. The third step is the oxidation of lignin by oxidized

mediators. Lignin biodegradation is naturally being conducted under aerobic conditions since the process requires oxygen and hydrogen peroxide which is produced through the oxidation of glucose and glyoxal with oxygen [31-32].

The redox potential of lignin oxidases follow the decreasing order of LiP, MnP to laccase, which determines the LiP catalyzed oxidation can occur both on free phenolic hydroxyl groups and aryl ether bonds, but laccase can only catalyze the oxidation on free phenolic hydroxyl groups. Studies have used lignin analogues to study the lignin depolymerization scheme with oxidases. It has been found that the cleavage can happen on several linkages such as C_α-C_β bond, alkyl-aryl bond and aryl-ether bond [68]. Figure 2.13 shows the reaction scheme of lignin depolymerization with lignin oxidases.

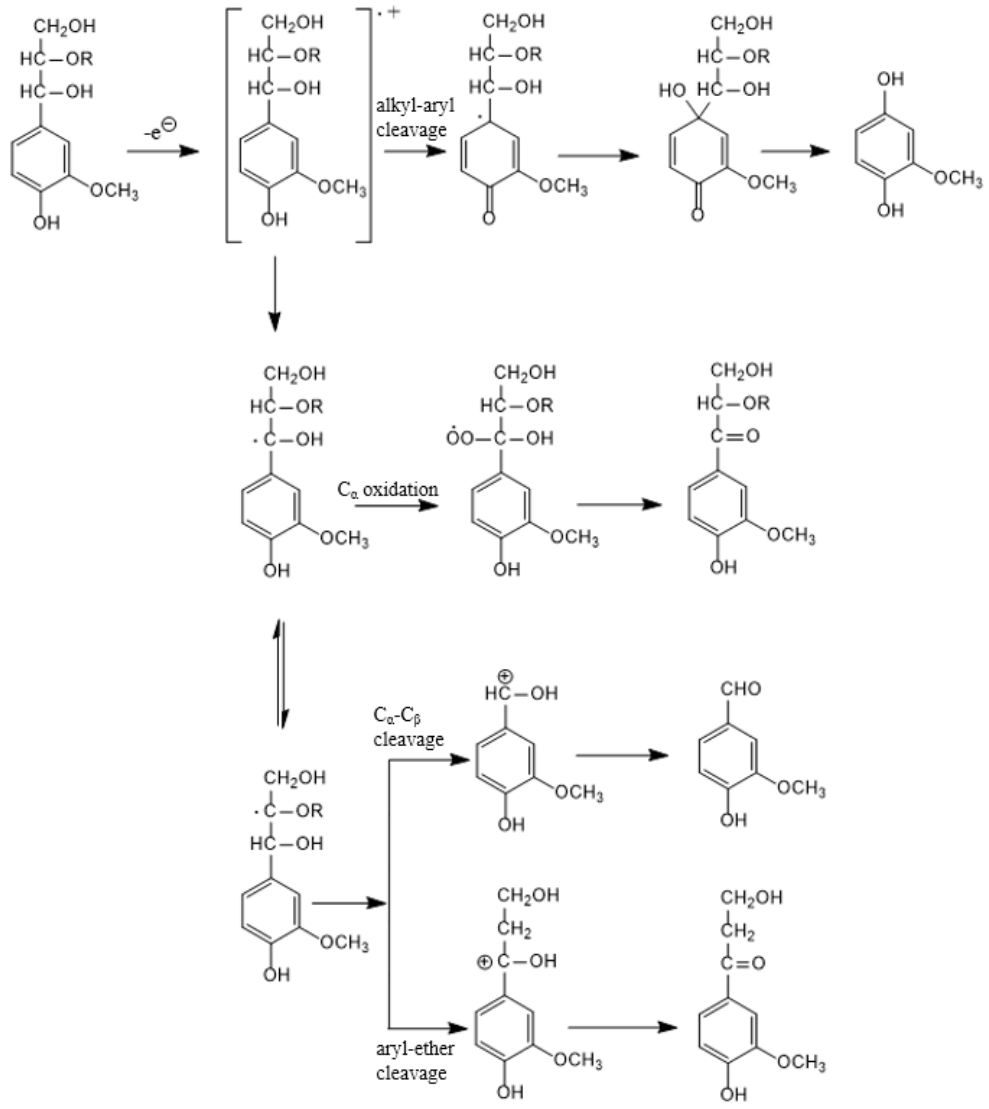

Figure 2.13. Reaction scheme of oxidative biodegradation of lignin [69-72].

Ozonolysis is another oxidative degradation process of lignin that uses ozone as oxidant. Ozonolysis is a chemical pretreatment process without any involvement of enzymes. The process is usually conducted in a fixed bed reactor under room conditions. The lignin degradation scheme of ozonolysis is slightly different from the lignin biodegradation scheme with the potential opening on the aromatic ring as shown in Figure 2.14. Lignin degradation products after ozonolysis include both aliphatic and aromatic chemicals such as caproic, levulinic, p-hydroxybenzoic, vanillic,

azelaic, malonic acids and aldehydes such as p-hydroxybenzaldehyde, vanillin, and hydroquinone [73]. The presence of aliphatic chemicals further proves higher degree of oxidation occurring during ozonolysis that breaks down the aromatic ring structure. Most studies of ozonolysis were applied on agriculture residues such as wheat straw and sugarcane bagasse. The biomass after ozonolysis shows a substantial decrease in the lignin content and increase in the enzymatic hydrolysis yield [74].

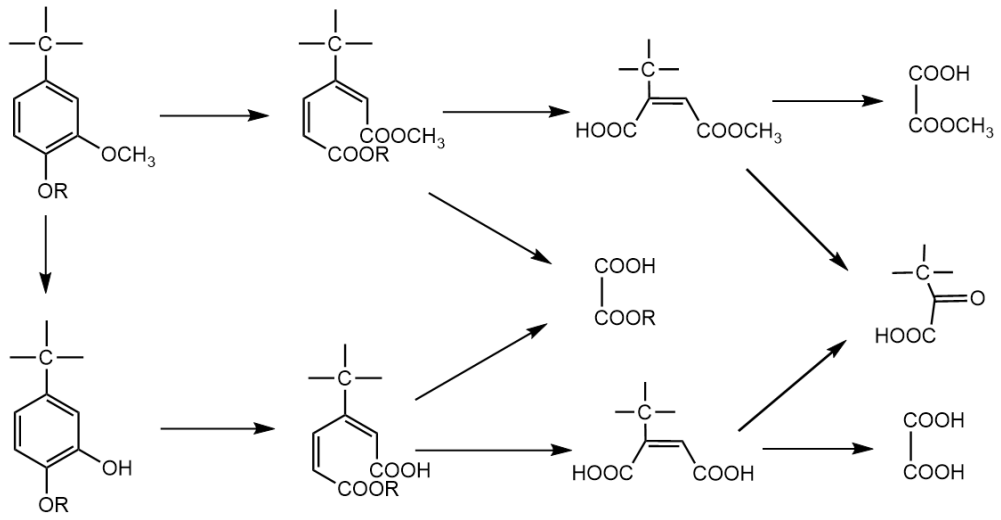

Figure 2.14. The oxidative reaction scheme of aromatic ring cleavage occurs during ozonolysis [75-76].

2.1.4 Lignin isolation and recovery

The techniques of isolating and recovering lignin from native biomass and industrial black liquor will be introduced in this session. These techniques carry different purposes that are lignin qualitative analysis, lignin quantitative analysis, and lignin applications for example. How lignin is isolated from native lignocellulosic species or from industrial black liquor streams will be introduced separately.

2.1.4.1 Lignin isolation from wood

Lignin isolation has been studied since the early last century. The primary goal at that time is to understand the structural and chemical properties of lignin. In this case, the ideal method should be selective to separate lignin from other plant constituents while keeps lignin chemically unmodified with a quantitative recovery. Method was first proposed by Brauns in 1939 by using organic solvents for lignin extraction [77]. The method is further improved by Björkman in 1956 by applying a preliminary grinding step before extraction [78]. The lignin separated from the modified method is referred as milled wood lignin (MWL) which is still acknowledged as the standard method to isolate lignin for structural analysis. On the other hand, the procedure of MWL preparation is tedious and lignin loss is substantial in the process. In this case, the MWL method is not suitable for lignin quantitative analysis. A two-step acid hydrolysis is usually applied to obtain the acid-insoluble lignin or Klason lignin content in a plant. This method uses two sequential acid hydrolysis steps with concentrated and diluted acid respectively in order to dissolve other wood constituents besides lignin [79]. Quantitatively speaking, Klason lignin method can preserve and isolate most lignin from lignocellulosic species. On the other hand, it has been reported that there are lignin structural changes during the Klason lignin procedure, which suggests that Klason lignin cannot represent the native lignin structure for qualitative analysis.

2.1.4.2 Lignin recovery from black liquor

As introduced previously, black liquor contains a significant amount of lignin and it is the major source of industrial lignin. Black liquor used to be discharged as a waste stream in pulp mills, which is no longer allowed with concerns of environmental issues since 1950s. The current process in pulping mills is to evaporate the black liquor for the production of steam. The lignin separated is further used as fuel [80]. This process is efficient as steam is necessary for paper making and lignin has a high heating value (26 MJ/kg-dry matter). However, since Kraft lignin is

sulfur-containing, its incineration causes problems of air pollution. Other lignin applications have emerged recently with the development of the biorefinery field. Some applications include using lignin as antioxidant, adhesive and adsorbent [81-83]. Those new lignin applications are promising since lignin is extremely cheap and easy to be separated from black liquor through acid precipitation. This project used acid precipitation to obtain Kraft lignin samples from black liquor. The detailed method will be introduced in the later chapter.

2.1.5 Lignin characterizations

Lignin characterization is always a popular and controversial topic due to its structural complexity. In the early 20th century, lignin characterization has been started first with wet chemistry methods, which determined the phenylpropenyl basis of the lignin structure. With the development of spectrometer technology, the lignin structure has been revealed in detail. In this session, three typical spectroscopy methods, UV, FTIR and NMR, will be introduced and how they determine the building units and interunit linkages in lignin.

2.1.5.1 Ultraviolet (UV)

Lignin shows a strong absorption of UV lignin due to its aromatic structure. In general, the major adsorption of benzene rings of lignin occurs at 205 nm while weak adsorption due to $\pi \rightarrow \pi^*$ transition and benzene ring vibration occurs 274-285 nm [84-85]. The UV method is extensively applied in lignin quantification. Kline et al. developed the method of quantifying the lignin content in biomass by first dissolving biomass in ionic liquid and monitoring its adsorption at 440 nm [86]. Aulin-Erdtman et al. applied UV spectroscopy to determine the *p*-hydroxyphenol, guaiacyl and sinapyl type as well as the phenolic group content in lignin [87-88]. The UV technology is also used in the pulping industries to determine the delignification efficiency. The lignosulfonate content is determined in the black liquor [89].

2.1.5.2 Fourier transform infrared spectroscopy (FTIR)

Due to the limited solubility of lignin in most solvents, IR spectroscopy, which does not require samples to be dissolved, is known as the simplest method for lignin characterization. Besides, only small amount of lignin (1-2 mg) is required for an IR experiment [90]. FTIR is capable in characterizing most linkages and functional groups in lignin. Generally speaking, the lignin absorption band ranges from 3450-1030 cm^{-1}. Table 2.2 summarized the band locations of most lignin functional groups and linkages in an FTIR spectra. It was also found that the band locations are slightly different between hardwood and softwood lignins [91].

Table 2.4 IR adsorption bands assignment of lignin [91-92]

Linkages/Functional groups	Location (cm^{-1})
OH stretching	3450-3400
OH-stretch in methyl and methylene groups	2940-2820
C-H stretching in CH_3 and CH_2	2940-2920
C=O stretching (noncojugated)	1715-1710
C=O stretching (conjugated to benzene ring)	1675-1660
Benzene ring vibration	1605-1600
C-O stretching in syringyl	1330-1325
C-O stretching in guaiacyl	1275-1270

2.1.5.3 Nuclear magnetic resonance (NMR) spectroscopy

NMR has become one of the most important methods in today's analytical chemistry. The high selectivity and resolution of NMR have contributed significantly in elucidating the detailed lignin structure. In an NMR analysis, lignin samples are usually required to be acetylated for a higher solubility. The NMR application in lignin structure characterization has been started with proton spectroscopy (^{1}H NMR). Based on model chemicals, ^{1}H NMR is capable in characterizing most functional groups in lignin such as hydroxyl, methoxyl, vinyl, formyl etc. [93-94]. However, due to the short range of chemical shift (12 ppm), signal overlapping in ^{1}H NMR has been observed. Also, some important linkages in lignin such as 5-5' linkage do not contain hydrogen, which cannot be characterized by ^{1}H NMR. ^{13}C NMR with a wider chemical shift range and higher

resolution has been applied to overcome these problems [95]. Hydrogen-free linkages and groups can also be characterized by ^{13}C NMR. The modern technology of 2D NMR combined the proton and carbon spectrum, which provides an even better resolution and more distinguishable peaks [96]. Table 2.3 and 2.4 give the lignin proton and carbon chemical shifts respectively.

Table 2.5 Proton chemical shifts of acetylated spruce MWL [97].

Assignment	Chemical shift (ppm)
Aliphatic acetate	1.95-2.13
β-β' linkage	3.08
Methoxyl protons	3.76-3.81
β-O-4 linkage	4.60
β-5 linkage	5.49
Aromatic and vinyl protons	6.01-6.06
Aromatics ortho to C=O	7.53
Formyl protons	9.64-9.86

Table 2.6 Carbon shifts assignment of nonacetylated lignin [98].

Assignment	Chemical shift (ppm)
C-3/C-5, etherified S	152.5
C-3, etherified G	149.7
C-3, non-etherified G	148.4
C-4, etherified G	146.8
C-4, non-etherified G	145.8
C-4, etherified 5-5'	145.0
C-4, non-etherified 5-5'	143.3
C-4, etherified S	138.2
C-1, etherified S/G	134.6

C-1, non-etherified S/G	133.4
C-5, etherified 5-5’	132.4
C-1, non-etherified 5-5’	131.1
C-β, Ar-CH=CH-CHO	129.3
C-α/C-β, Ar-CH=CH-CH_2OH	128.0
C-2/C-6, in H unit	128.1
C-5, non-etherified 5-5’	125.9
C-5, in G unit	115.1, 114.7
C-2/C-6, in S unit	104.3
C-β, in G type β-O-4	84.6
C- α, in G type β-O-4	71.8
C-β, in β-β’	53.9
C-β, in β-5’	53.4

2.2 Heavy metal pollution

Heavy metals naturally exist in the earth crust. There is no exact definition of heavy metals, but it is usually referred to metals with a specific density highly than 5 g/cm^3 [99]. Due to the toxic nature of most heavy metals, they are regarded as pollutants in the environment. In this session, the pollution sources of heavy metals, their health impact, and treatment methods will be introduced.

2.2.1 Pollution sources

In nature, most heavy metals exist in ores as sulfides such as arsenic, lead, zinc, cobalt, silver, and nickel; or oxides such as selenium and antimony. Some heavy metals can exist both as sulfide and oxide such as gold and copper [100]. The pollution of heavy metals can be a spontaneous process, for example, the heavy metal leach-out from ores to the underground water; the transportation of heavy metal containing gravels through wind and flood. Although these processes

can occur naturally, the heavy metal pollution is significantly accelerated through anthropogenic mining activities. In the mining processes, the exposure of ores as well as their disruption in the structure intensify the efflorescence and heavy metal leach-out, which results in the pollution not only in the underground water but in the whole aqua system as well as the air. And since ore recovery cannot reach 100%, the emission of heavy metal pollutants from the sites can be persistent even after the mining activity was ceased [101].

Some industrial processes rely on heavy metals as raw materials, which intensified the risks heavy metal contamination. For example, copper, zinc, nickel, silver and gold are widely used in electroplating, while the wastewater generated in the process contains these heavy metals at high concentration [102]. Cadmium usually coexists in ores with zinc oxide and lead oxide which is released during zinc and lead refinery. Some industrial applications of cadmium are known as PVC stabilizer and battery material [103]. Lead is previously used as an additive in petroleum and as a coloring material in paintings. These two applications have been banned now in most countries due to the awareness of the lead hazardous [104]. However, since the vast usage of the two applications in the early years and the stability of lead in the environment, lead pollution is still one of the most prominent environmental risks nowadays. Besides, lead is used in ammunition. Lead-acid battery is still the most commonly used type of battery in today's automobiles. Not only can the pollution occur during the battery production, it also posts the threat to the domestic water system especially in developing countries without proper battery recycling regulations or enforcement. In some pharmaceutical companies, mercury is used in the production of diuretics and teeth filling materials [105]. Mercury is also a common material used in metering equipment such as thermometers, barometers, and blood pressure meters. Heavy metals with their original ore types are summarized in Table 2.7 with their typical applications that are still not banned by

the government. These applications with their industrial manufacturing result in heavy metal contaminated water and air, which are known as the sources of heavy metal pollution from anthropogenic behaviors.

Table 2.7. The natural forms of heavy metals and their major applications nowadays.

Element name	Type of ores	Current major applications
Cadmium	Greenockite, CdS Smithsonite, coexist with zinc[106]	Electroplating, cadmium-nickel battery, LED screens, control rod in nuclear fission[103]
Lead	Galena, PbS[107]	Lead-acid battery, piping, radiation shielding[104]
Mercury	Cinnabar, HgS[108]	Pharmaceutical, chlorine production, measuring meters[105]
Copper	Chalcopyrite, $CuFeS_2$ Chalcocite, CuS_2 Cuprite, Cu_2O[109]	Electroplating, wiring, currency, alloys (brass, bronze)[110]
Nickel	Limonite, coexist with iron Garnierite, NiO[111]	Electroplating, stainless steels, cadmium-nickel battery, hydrogenation catalyst[112]
Zinc	Smithsonite, $ZnCO_3$ Wurtzite, ZnS[106]	Galvanizing, alloys (brass, bronze), zinc-carbon battery
Arsenic	Arsenopyrite, FeAsS[113]	Pesticide, alloys (gallium arsenide)[113]
Silver	Argentite, AgS[114]	Jewelry, currency

2.2.2 Health effects

Most heavy metals are toxic to human beings because of their binding to functional proteins that cause protein coagulation. For example, lead has a high binding affinity towards the sulfhydryl groups of proteins, which leads to enzyme inhibitions that can cause inhibition of hemoglobin synthesis [115]. Long-term exposure to lead can cause anemia. Other poisoning effects include kidney dysfunction, irritability, and the poisoning of the nerve system. It has also been reported that children between 9 months and 6 years old are most affected by lead poisoning due to their low body weight and faster lead adsorbing rate comparing to adults [116]. Children's intellective development is affected by lead due to its impacts on the grey matters development in the brain [117]. Since the effect occurs in the intellective developing period, such symptom will not appear

on adults. Studies have been performed on the carcinogenic effect of lead. The evidence that links lead to cancer is still weak. Lead has been classified as a possible human carcinogen by IARC [118].

Arsenic also causes the coagulation of protein that mainly impacts on the production of adenosine triphosphate (ATP) during respiration [119]. Another toxicity mechanism of arsenic is its cause of oxidative stress. Inorganic arsenic is highly toxic that can cause damage to the gastrointestinal and nerve systems. Inorganic arsenic has been classified as group 1 human carcinogen that can cause cancers in lungs, kidneys, bladder, and skin [120]. Methylated form of arsenic inhibits DNA repairing process while produces reactive oxygen species that cause cell death [121].

Both inorganic and organic forms mercury can cause chronic poisoning to the nerve system with typical symptoms as tremor, restlessness, anxiety, insomnia, and depression. Some physiological symptoms include numbness in the hands and feet, visual and auditory failure [98]. The infamous Minamata catastrophe happened in Japan is one example of organic mercury poisoning. The discharge of dimethylmercury and methylmercury chloride from a local fertilizer industry to the nearby sea leads to the mercury contamination in the seafood in the area. Over 12,000 people were affected by the Minamata disease (the disease caused by organic mercury poisoning) and 1,246 people died in the catastrophe [122].

Other heavy metals such cadmium, chromium and nickel has been classified as group 1 carcinogens [123]. Zinc poisoning has very similar signs with lead poisoning. The toxicity of zinc is relatively low, but excessive ingestion of zinc can still cause vomiting, bloody urine, liver failure, etc. [124].

2.2.3 Current pollution status

The overall status of heavy metal pollution in a worldwide basis is under improvement due to the regulations enforced by the governments. Using Pb as an example, the Pb application in antiknocking agent was banned in US since 1980s [125]. The application of Pb as petroleum additive was first banned in Germany in 1976, and then banned in Europe and China in succession [126-127]. The substitution of Pb in other products such as paint, tire, lubricating oil and grease also contributed to the lead control [128-130]. Huber et al. analyzed the historical trends of Pb and Zn concentrations in the environment and found declines in both elements [131]. A comparison of heavy metal concentrations between developed areas and developing areas was also performed in their study. The Pb concentrations in Europe, North America, and Asia was given as 30 μg/L, 15 μg/L, and 50 μg/L, respectively. Cu concentration in North America was reported at 30 μg/L and 60 μg/L in Aisa and Europe. Zn concentration in Asia reached 620 μg/L which is three times higher than Europe and North America. There are couple reasons for the different pollution status between the developed and developing areas. The heavy metal regulations in developing countries were enacted about 20 years later than the developed countries. For example, the first law of environmental protection in China was enacted in 1986, but relevant regulations about heavy metal discharge was not emphasized until 1997, which is 25 years later than the USEPA Clean Water Act [132-133]. Another reason is the distribution of manufacturers. Major emprises prefers third-world manufacturing due to the low cost of laboring and raw materials, as well as the loose environmental regulations. Meanwhile, third-world relies on manufacturing export for economic growth. The combination leads to a heavy load of manufacturing and environmental burden placed in the third-world area. Besides, the enforcement of environmental regulations is another problem in some developing countries. Studies have reported that illegal heavy metal discharges are still

occurring [134-135]. The immature battery and electronic waste recycling system in developing countries also causes pollution from the domestic wastes [136].

2.3. Heavy metal remediation technologies

Due to the awareness of the hazardous natures of heavy metals, their discharges have been highly restricted with environmental policies. Industrially, multiple technologies have been developed in the treatment of heavy metal contaminated wastewater, with the purpose of reduce the heavy metal content in the effluent as well as heavy metal recycling and reuse. Various treatment technologies such as chemical precipitation, coagulation, ion exchange, and adsorption have been applied individually or combined in the treatment process. Different technologies have their own advantages and limitations which will be introduced in this session of review.

2.3.1 Chemical precipitation

The treatment with chemical precipitation is one of the earliest technology that applied for wastewater remediation from heavy metals. The principle of the technology mainly considered the low solubility of the hydroxide and sulfide forms of heavy metals [137-138]. The conceptual mechanism of a bivalent heavy metal cation precipitation can be generalized as Eqn (c) and (d).

$$M^{2+} + 2OH^{-} \leftrightarrow M(OH)_2 \downarrow \quad \text{(c)}$$

$$M^{2+} + S^{2-} \leftrightarrow MS \downarrow \quad \text{(d)}$$

For heavy metal hydroxide precipitation, lime and calcium hydroxide are usually chosen as the base chemical considering the low price. Lime precipitation was employed in treating zinc, cadmium, and manganese with concentration ranges from 450-1085 ppm. The removal is efficient to reduce the final heavy metal concentration below 5 ppm, but which still exceeded the US EPA regulation (1 ppm) [139-140]. This suggested a post treatment after hydroxide precipitation may be required for certain heavy metal species. It should also be noticed that different heavy metals

have their optimum precipitation pH. When pH is higher than the optimum level, their hydroxide forms will become soluble again [141]. Figure 2.15 presents the relation of heavy metal hydroxides solubility against pH. The ambient solubility of heavy metal hydroxides challenges the treatment efficiency and the accuracy of the process control. Table 2.8 summarized the optimum precipitation pH for heavy metals.

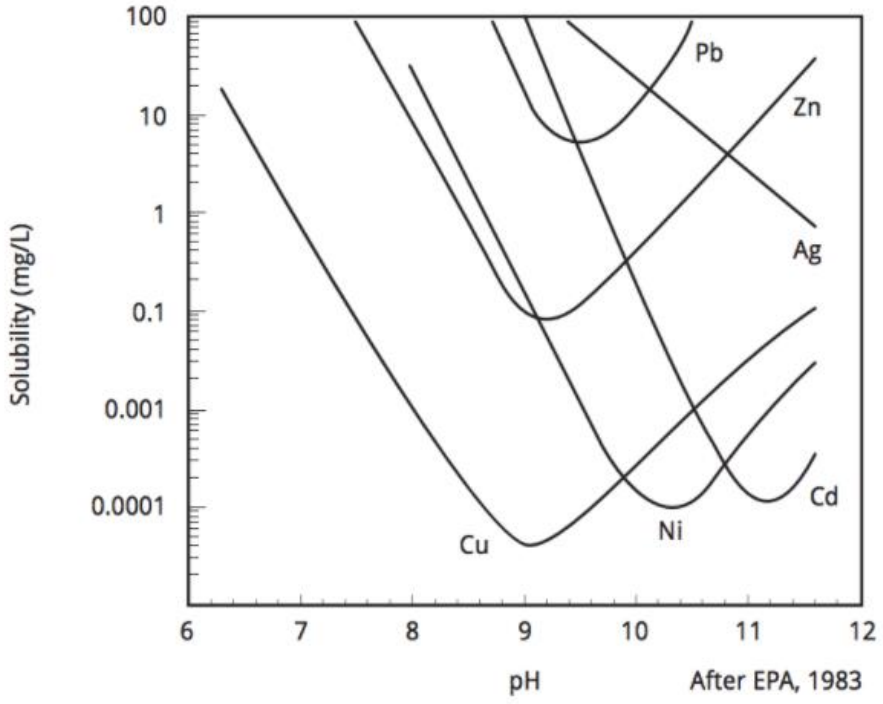

Figure 2.15. The solubility of heavy metal species at varying pH. The hydroxide forms of heavy metals will become soluble when exceeded the optimum precipitation pH [142].

Table 2.8. The environmental pH when heavy metals start to precipitate and when the precipitation reaches maximum [143-147].

Heavy metal species	Optimum precipitation pH range
Cu (II)	9-9.5
Ni(II)	10-11

Cd(II)	11-11.2
Zn(II)	9-9.5
Pb(II)	9-10
Cr(IV)	10-11

Studies have performed with sodium sulfide in the treatment of different heavy metal species including cadmium, zinc, copper, lead, arsenic, and selenium. It has been reported that the removal of all the studied heavy metal species can all reach above 90%, where the removal of Cd, Zn, and Cu can reach as high as 99%, within the range of 0.05-0.1 ppm after treatment [148]. The results also showed the removal ratio with sulfide is significantly higher than the hydroxide precipitation [149].

In general, the advantages of chemical precipitation lie on the simplicity and easiness for operation with acceptable amount of removal. On the other hand, the method requires the consumption of significant amount of chemicals. Heavy metal containing sludge will be generated after the process which may result in secondary pollution. Other characteristics such as slow precipitation and poor settling are also considered as the drawbacks of the precipitation process [150-151].

2.3.2 Flocculation

The treatment of heavy metal pollutant with coagulation has been employed industrially in countries such as Thailand and China [139,152]. The principle of flocculation is through the interaction between colloidal particles with coagulant, which results in the coagulation of target particles to a larger size in order to be removed from the liquid phase [153-154]. The mechanism of coagulation is shown as Figure 2.16.

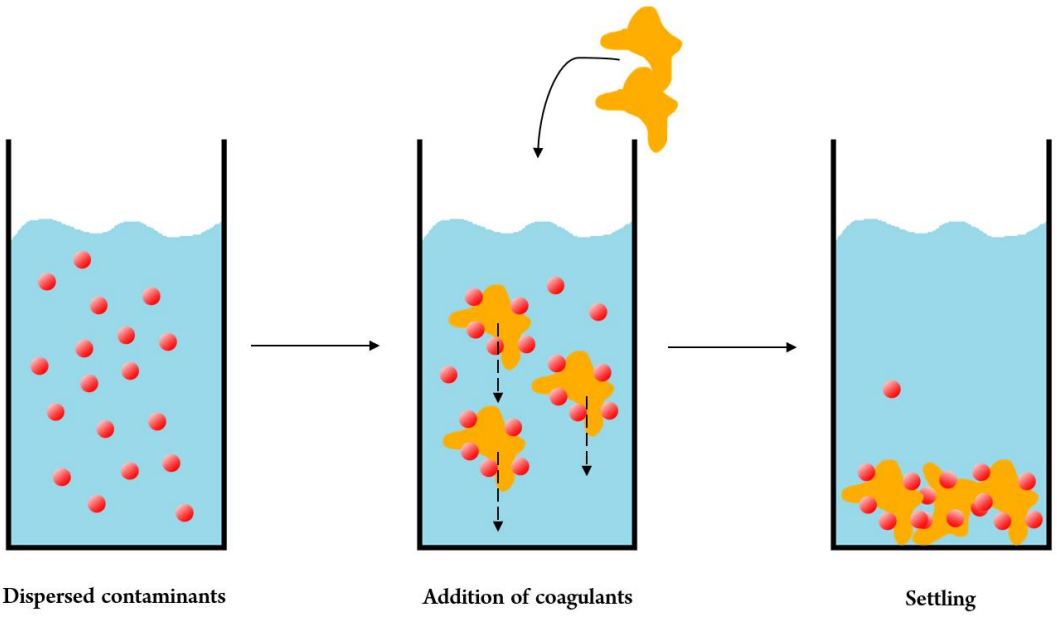

Figure 2.16. The mechanism of flocculation. Coagulant is added to interact and bind with floating impurities in the solution that generates bulk particles named floccules. The floccules are easier to be settled and removed from the liquid phase.

The process is usually conducted at pH ranging from 11.0 to 11.5 which was found to be the most effective in removing heavy metals through flocculation [155]. Li et al. studied the flocculation in the treatment of Cu(II) with poly ferric sulphate and polyacrylamide as flocculants and diethyl-dithiocarbamate (DDTC) as trapping agent. Their results showed almost complete removal of Cu(II) contaminants (>95% removal) [152]. The study also suggested that electrophilic groups such as thio groups and amine groups are functional to bind with heavy metal cations.

Compared to the chemical precipitation process, flocculation usually results in larger removal of heavy metals, improved settling, and improved sludge stability. However, the process still requires a large consumption of chemicals and more expensive chemicals. Sludge generation is another problem faced. The stability of the coagulants makes the recovery process difficult. On

the other hand, the process will be preferential in the treatment of municipal wastewater with low heavy metal content.

2.3.3 Ion exchange chromatography

Chromatography is another widely applied technology in the purpose of separation and purification, which can also be used for heavy metal treatment. During the chromatography process, liquid solution (mobile phase) is passed through the solid resin (stationary phase), while the chemical component is removed from the solution and retained in the stationary phase (Figure 2.17). When treating heavy metal contaminants, acidic resin is usually employed which is capable of capturing heavy metal cations while releasing protons to the mobile phase. The general mechanism can be expressed as Eqn (e) [156].

$$nR^- - H^+ + M^{n+} \leftrightarrow nR^- - M^{n+} + nH^+ \quad \text{(e)}$$

The process itself is reversible, which provides the potential to recover and reuse heavy metals and prevents the secondary pollution issues [157]. About 10 different types of acidic resins have been studied and reported for their heavy metal removal abilities. The results showed almost complete removal (99.5%-100%) of Zn(II), Cr(III), and Cr(IV) after treatment [158-162]. Lin et al. performed the isotherm study on the synthetic acid resin and found the ion-exchange capacity towards chromium was as high as 92.1 mg/g [160]. The high removal rate of ion exchange resins makes it an effective method in the treatment of streams with low pollution levels. On the other hand, the process requires high capital and operational costs due to expensiveness of the ion exchange resins as well as the requirement of prior treatment to eliminate solid particles in the stream [163].

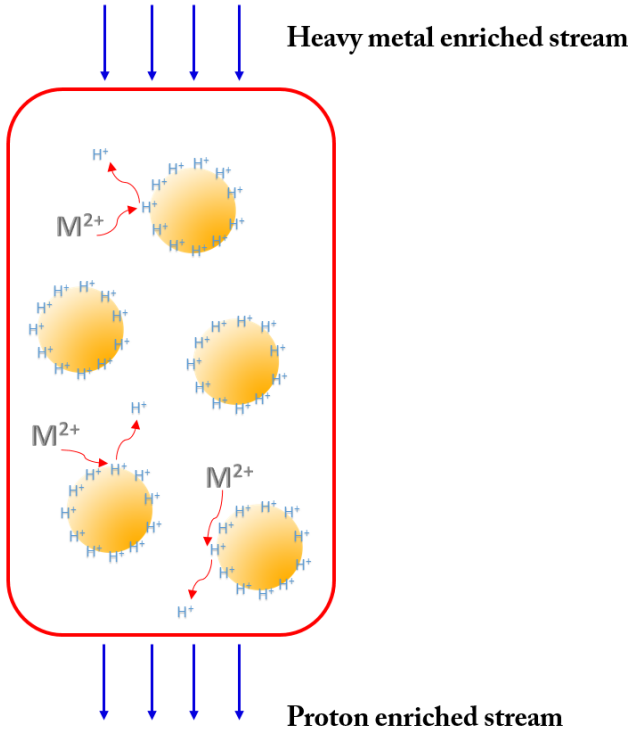

Figure 2.17. The process ion exchange chromatography in the treatment of heavy metal contaminants.

2.3.4 Bioremediation

Bioremediation is the method to clean up heavy metal contaminated water or soil by using bacteria or algae to fix heavy metal ions either extracellularly or intracellularly. The advantages of bioremediation over traditional physicochemical methods lie on its versatility in treating both contaminated water and soil, low cost, effectiveness in treating low metal contamination, and zero generation of secondary contaminant (sludge) [164-165]. During cell metabolism, the reduction of heavy metals can occur with the oxidation of organic alcohols and aromatic compounds. The reduction of heavy metal ions to lower valent or to their elemental form can significantly reduce the toxicity and solubility of some heavy metals such as chromium and selenium [166-167]. The precipitation of heavy metals can occur due to the ionic binding between metal ions with organic

acids which are secreted by microorganisms especially under anaerobic conditions. It has also been reported that sulfate-reducing bacteria is effective in convert heavy metals to their sulfide form, which significantly reduces the solubility of mobility of heavy metal contaminants [168]. In algae cells, heavy metals can be actively adsorbed into the cytoplasm. Metal ion binding groups such as OH^-, SH^-, COO^-, PO_4^{3-}, NO_3^-, RNH_2^-, RS^-, and RO^- most presented in the vacuole, which makes vacuole an important organelle in heavy metal remediation [169]. The above remediation mechanisms are restricted to living cells. Dead cells are also effective in heavy metal remediation due to the presence of metal binding groups on the cell wall, which provides the potential of using bioremediation in treating heavy metals at high concentration [170].

2.4 Adsorption

Adsorption is the process that species including atoms, ions, molecules, or particles get attached to a solid surface. In this process, the adsorbed species are also called adsorbates, while the adsorption surface is provided by the adsorbent. The bindings between adsorbate and adsorbent can either through chemical forces (ionic bindings, covalent bindings) or physical forces (van der Waals forces). Based on the binding mechanisms, the process can be further characterized as chemisorption and physisorption, respectively. The adsorption process is widely applied in industrial separations and purifications, which the process itself is also the key step for heterogeneous catalysis. As adsorption was employed in this thesis research, a detailed introduction of the adsorption theories and a review for the previous studies about heavy metal adsorption on lignin will be given in this session.

2.4.1 Adsorption theories

Adsorption is originally studied for the attachment of gas molecules on solid surface. The adsorption system can be described by the layer model (Figure 2.18) as three regions (I, II, and III). It was considered that the adsorbate cannot penetrate the solid surface. Layer II represents the

decrease of adsorbate concentration progressively with increase of distance from the adsorbent surface. Layer III is the bulk phase. Thermodynamically speaking, at adsorption equilibrium state, the chemical potential between the adsorbed phase and the bulk phase should be the same, which gives,

$$\mu_\sigma = \mu_g \tag{f}$$

Eqn(f) is further derived to the isosteric heat of adsorption equation given as,

$$\ln\frac{p^n}{p^\infty} = \frac{u^n - u^\infty}{RT} - \frac{1}{R}(s^n - s^\infty) \tag{g}$$

where p^n, u^n, and s^n stand for the pressure, enthalpy, and entropy of the adsorbed layer, and ∞ denotes the bulk phase. Ideal adsorbed solution theory (IAST) was developed in explaining the adsorption of mixed adsorbates at equilibrium in the analogous of Raoult's law.

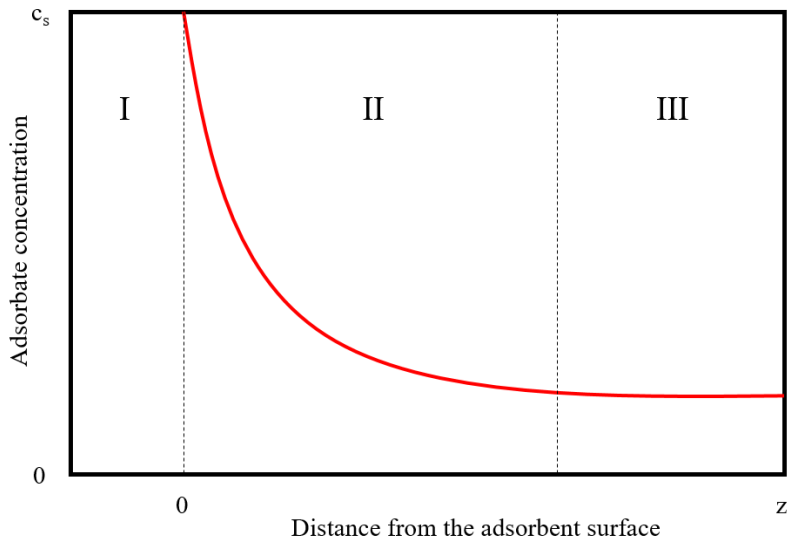

Figure 2.18 Adsorption layer model.

There have been multiple adsorption theories developed in the past to describe the process of adsorption while providing mechanisms for mathematical modeling. The most popular and

referred one is the Langmuir adsorption, and the simplest one in use is the Freundlich adsorption isotherm. While Langmuir adsorption model is considered theoretical, Freundlich adsorption isotherm is empirical. Other models include BET, Elovich, Bangham, pseudo order etc. have their own merits in describing the adsorption process.

In this session, some mechanistic based adsorption theories including Langmuir adsorption, BET adsorption, and Cooperative adsorption will be introduced. While introductions about empirical adsorption models such as Freundlich equation and pseudo first order/second order adsorption will not be given due to their lack of mechanistic background and confined application area. However, one cannot underestimate the importance of empirical adsorption models because their own advantages in the simplicity of mathematical forms and easiness to be applied especially to industrial processes.

2.4.1.1 Langmuir adsorption

Adsorption commonly refers to an inhomogeneous process with three elementary steps: (1) diffusion of an adsorbate "A" from bulk solution to the external surface of the adsorbent; (2) adsorbate diffusion from external surface through internal pores, approaching the "active center" σ of the adsorbent; (3) the attachment of adsorbates to the adsorbent through the interactions between "A" and "σ". In this process, the first and second steps are mass transfer steps and step (3) is the occurrence of adsorption. Different theories have been proposed for the third step where Langmuir adsorption is one of the most famous theory describing the adsorption on an ideal surface. In Langmuir adsorption theory, it is suggested a homogeneous adsorbent surface without surface energy flocculation, the binding between active site and adsorbate follows one to one stoichiometry, and there are no interactions between adsorbates and adjacent sites [171]. When

considering the adsorption process as a reaction between adsorbates and active sites, with the above assumptions, the process can be written as Eqn (f).

$$\mathrm{A} + \sigma \underset{k_-}{\overset{k_+}{\leftrightarrow}} \sigma \cdot \mathrm{A} \tag{f}$$

where σ·A stands for the adsorbate-adsorbent complex, K_A is the equilibrium constant which can be given as $\frac{k_+}{k_-}$.

In an adsorption process, the equilibrium level is an important property to be characterized. According to Eqn (f), the coverage of the adsorbent at equilibrium can be written as Eqn (g).

$$\theta_A = \frac{[\sigma \cdot \mathrm{A}]}{C_{\sigma,0}} = \frac{K_A C_A}{1 + K_A C_A} \tag{g}$$

Where θ_A stands for the ratio of the active sites that are occupied by the adsorbate. In this equation, the equilibrium constant is related to the forward and backward rate constants, which can be written as,

$$K_A = \frac{k_+}{k_-} = \frac{k_{+,0}}{k_{-,0}} e^{-\frac{E_+ - E_-}{RT}} = \frac{k_{+,0}}{k_{-,0}} e^{-\frac{\Delta H_{ad}}{RT}} \tag{h}$$

From Eqn (h), one can see that the adsorption equilibrium constant is related to the heat of adsorption (ΔH_{ad}) which is dependent on the adsorbate and adsorbent properties, and the adsorption temperature. In this case, when a specific adsorption process is conducted at a constant temperature, the surface coverage is only related to the adsorbate concentration. The Eqn (g) is also known as the Langmuir isotherm model. Figure 2.19 shows a plot of Langmuir isotherm. One can see when increasing the adsorbate concentration, the adsorbent becomes more saturated approaching its adsorption capacity.

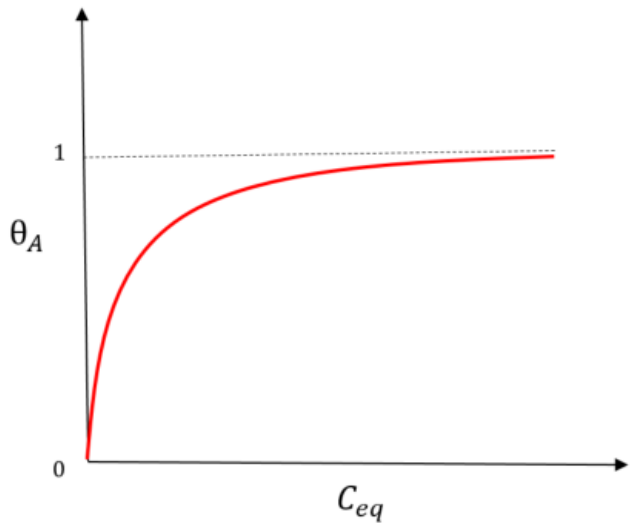

Figure 2.19. An example of Langmuir isotherm plot. The surface coverage levels off after the increase of adsorbate concentration indicating the saturation of the adsorbent surface.

The kinetics of adsorption follows naturally with the collision theory. The adsorption can only occur when adsorbate A molecule striking the solid surface. The collision frequency is given by

$$Z_{cT}(A, surface) = N_{AV} C_A \sqrt{\frac{RT}{2\pi M_A}} \tag{i}$$

Therefore the rate of Equation (f) is proportional to the collision frequency. Based on Equation (i) the rate of adsorption can be expressed as elementary reaction and the net rate is given by

$$\mathrm{r}_1 = k_A C_A[\sigma] - k_{-A}[\sigma \cdot A] = k_+ \frac{C_A C_{\sigma,0}}{1+K_A C_A} - k_- \frac{K_A C_A C_{\sigma,0}}{1+K_A C_A} \tag{j}$$

Which is known as the kinetics equation for the Langmuir adsorption theory. The Langmuir adsorption theory is adequate in explaining some adsorption processes occurring on simple adsorbent such as activated carbon, but examples of deviating from the Langmuir model is abundant suggesting non-ideal adsorption processes. The reason of false obedience and the modeling of non-ideal adsorption processes will be introduced in the later sessions.

2.4.1.2 BET theory

In 1938, Stephen Brunauer, Paul Hugh Emmett, and Edward Teller proposed the BET adsorption theory in order to explain some non-ideal gas adsorption processes. They first proposed the multilayer adsorption concept suggesting that after the first layer adsorption on the solid surface, gas molecules can pile upon each other through van der Waals forces resulting in multilayer adsorption (Figure 2.20) [172]. Based on the concept of multilayer adsorption, the binding and piling of multiple adsorbate molecules on one active site is possible. Beside the change from single layer to multilayer adsorption, BET theory applied the assumptions of Langmuir theory in each layer and suggested there can be infinite layers of adsorption.

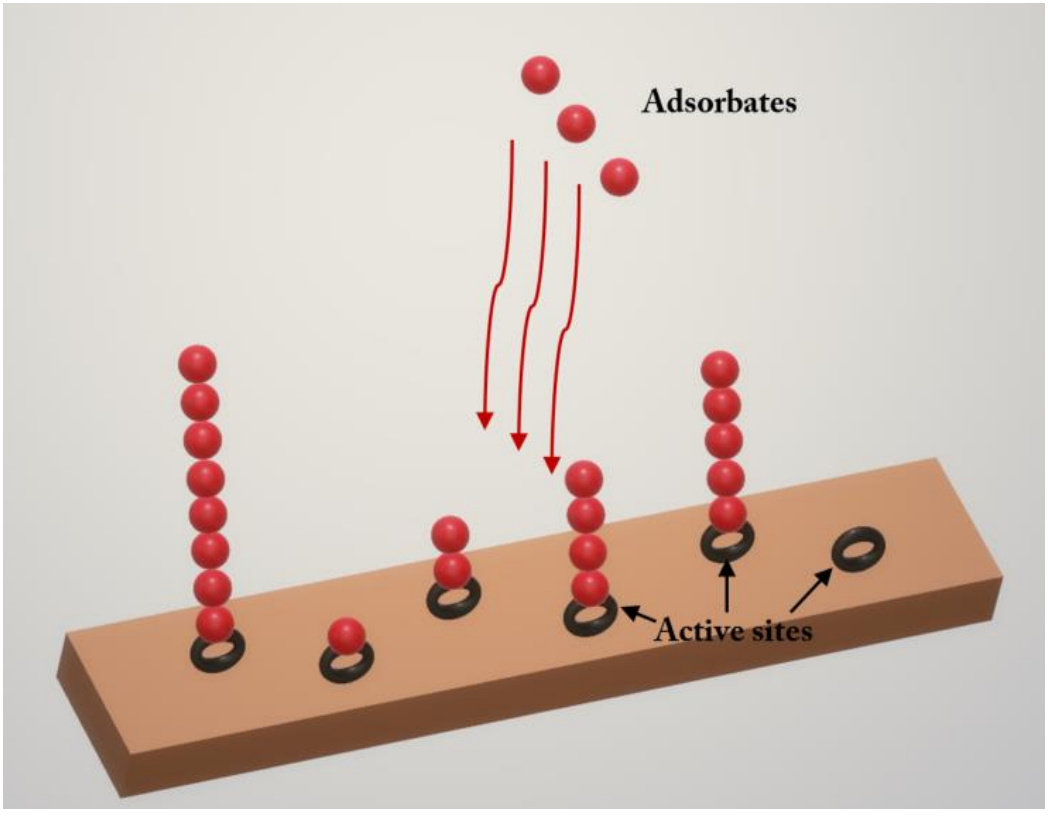

Figure 2.20. BET adsorption surface model. Beside the first-layer adsorption between active site and adsorbate, adsorbate molecules can pile on through physisorption resulting in multilayer adsorption.

In a multilayer adsorption process, the Eqn (f) needs to be rewritten as,

$$A + \sigma \cdot A_{i-1} \underset{k_{-i}}{\overset{k_i}{\rightleftarrows}} \sigma \cdot A_i \qquad 1 \leq i \leq N \tag{k}$$

In this scheme, denotation i represents the adsorption occurring on the i[th] layer, N is the total number of layers of adsorbate that can be piled, k_i and k_{-i} stands for the adsorption and desorption rate constants for the i[th] layer. According to the binding scheme proposed in the BET theory, the adsorption occurred from the second layer are all through the physical forces between the adsorbate molecules, so the binding affinities should be the same.

$$K_1 = \frac{k_1}{k_{-1}} \tag{m}$$

$$K_i = \frac{1}{c} K_1 \qquad i \geq 2 \tag{n}$$

When defining $\frac{1}{c} K_1 = \frac{p_A}{p_A^0}$, the overall adsorbed amount n_{SA} can be calculated as,

$$n_{SA} = \frac{n_{\sigma 1} c \frac{p_A}{p_A^0}}{\left(1 - \frac{p_A}{p_A^0}\right)\left[1 - (1-c)\frac{p_A}{p_A^0}\right]} \tag{o}$$

Which is known as the BET isotherm. Or its linear form,

$$\frac{\frac{p_A}{p_A^0}}{n_{SA}\left(1 - \frac{p_A}{p_A^0}\right)} = \frac{1}{n_{\sigma 1} c} + \frac{c-1}{n_{\sigma 1} c} \frac{p_A}{p_A^0} \tag{p}$$

Figure 2.21 gives an example of BET isotherm plot. The BET isotherm also provided the method in characterizing the surface area of an adsorbent. The BET surface area is defined based on the monolayer capacity [173]. It is calculated as the monolayer capacity multiplied by the Avogadro constant (L) and the average area occupied by a single molecule (ϕ), which is given as Eqn (q).

$$\mathrm{a(BET)} = n_{\sigma 1} \mathrm{L} \phi \qquad \text{(q)}$$

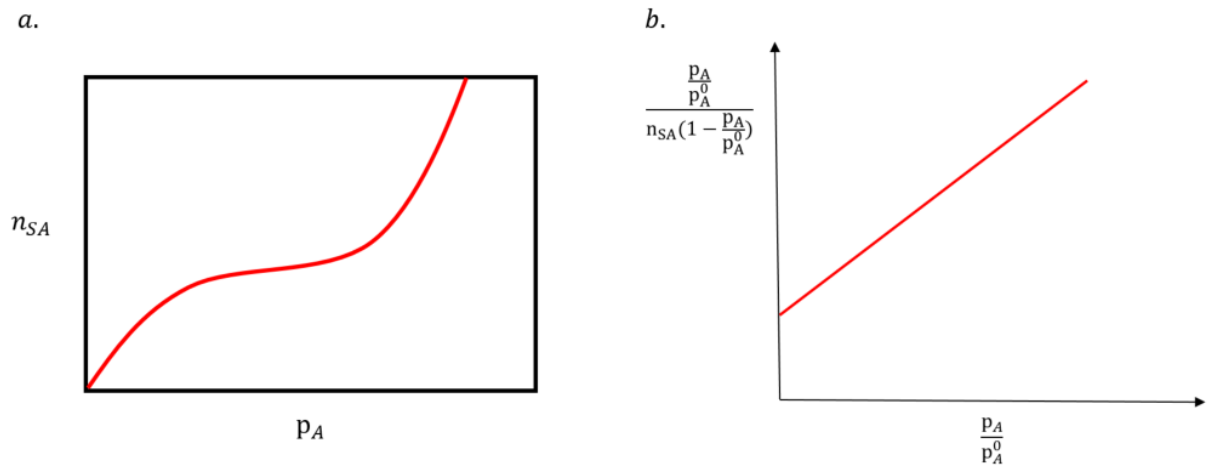

Figure 2.21. (a) BET isotherm plot; (b) linear BET isotherm plot.

By looking at the adsorption process from a multilayer point of view, BET theory has been successful in explaining many gaseous adsorption phenomenon. On the other hand, it is not plausible to apply the theory to liquid adsorptions. Neither is it applicable to a surface reaction process as a catalyst is only effective when chemicals are attached.

2.4.1.3 Cooperative adsorption

Cooperative adsorption theory is a novel adsorption theory that was recently proposed by our research group. The theory considered the existence of multiple active sites on the adsorbent surface with different interactive energies and the interactions between adsorbates and active sites. It also inherited the BET theory considered the potential piling on the adsorbent surface [174]. In this case, the new theory eliminated the assumptions from the Langmuir adsorption theory and looked into the adsorption process through a more particle view.

Surface idealization of cooperative adsorption has been described by Liu [175]. Instead of looking at the individual active sites on an adsorbent surface, adjacent active sites are grouped into active centers and the composition of active centers are the same from each other (Figure 2.22).

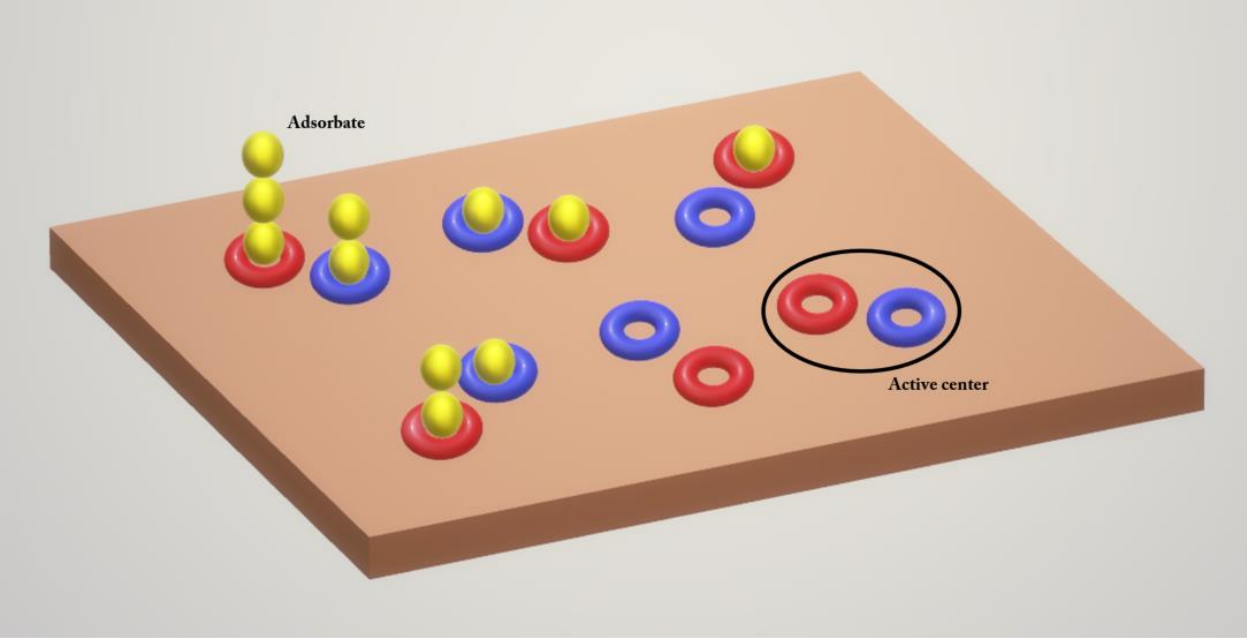

Figure 2.22. An example of non-ideal surface adsorption with two different active sites. The two adjacent distinct active sites are grouped as active centers. Both surface adsorption and intermolecular physisorption are considered in the cooperative adsorption scheme.

In this case, a non-ideal adsorbent surface with different active sites was idealized to a uniformed surface with only active centers. Apparent multilayer adsorption is an excellent model to translate cooperative adsorption behaviors mathematically [176]. When an adsorbate molecules approaches the solid surface, it always prefers to first cover those active sites with the highest interaction energy. In a multilayer point of view, those adsorbates can be regarded as the first layer. Meanwhile if another adsorbate molecule approached the location where the highest energy site was occupied, the molecule will then attached to a site with lower interaction energy (the second

layer). In this case, adsorbates are covering the active sites in a sequential manner, which is important in mathematical modeling. By grouping the sites with different energy levels, we can regard each group as an active center and the cooperative adsorption behavior can be treated as an apparent multilayer adsorption [177]. Figure 2.23 illustrated such adsorption behaviors with surface idealization.

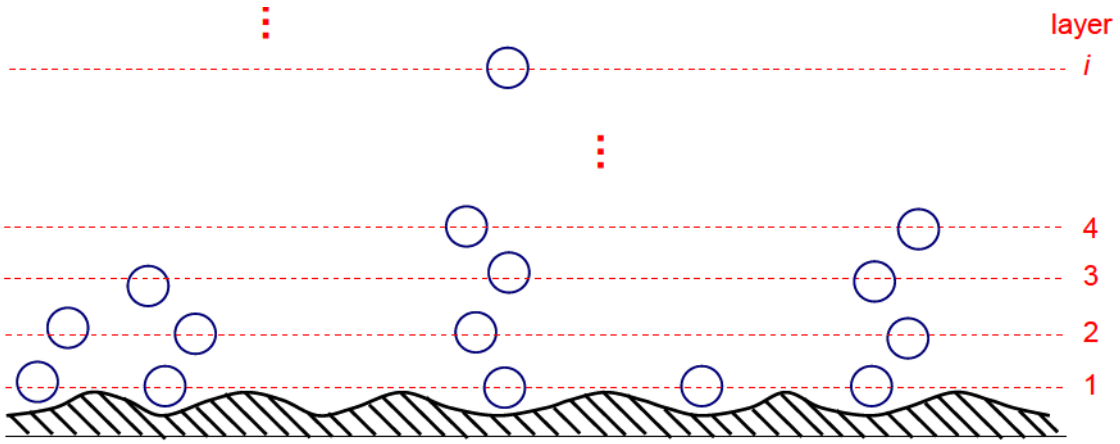

Figure 2.23. Cooperative adsorption in a multilayer point of view.

The mathematic model of cooperative adsorption isotherm behaviors has been studied in (Liu, 2015ab). For the adsorption of a single species A, the adsorption isotherm on the "i"th layer can be modeled as

$$\mathrm{A} + \sigma \cdot L_{i-1} \underset{k_{-i}}{\overset{k_i}{\rightleftarrows}} \sigma \cdot L_{i-1}A \qquad \text{(r)}$$

where L_{i-1} stands for the $i-1$ layer of adsorbates adsorbed on the active center.

Theoretically speaking, the affinity for active sites can be different when the adsorption is occurring on the solid surface. As an example that an adsorbent has two different active sites, first

two “layers” are different from rest of the layers are physisorption with identical affinities. In this case, the equilibrium constant of each “layer” can be written as,

$$K_1 = K_A \tag{s}$$

$$K_2 = c_1 K_A \tag{t}$$

$$K_\mathrm{i} = c_2 K_A \ (\mathrm{i} \geq 3) \tag{u}$$

The cooperative adsorption isotherms of the specified case are proposed as following:

$$C_{SA} = C_\sigma K_A C_A \frac{1+\frac{c_1}{c_2}\left[\frac{1-(1+N-Nc_2K_AC_A)(c_2K_AC_A)^N}{(1-c_2K_AC_A)^2}\right]}{1+K_AC_A+c_1K_A^2C_A^2\frac{1-(c_2K_AC_A)^{N-1}}{1-c_2K_AC_A}} \tag{v}$$

where C_σ is the concentration of active center groups and N is the site amount in each group. So the maximum amount of adsorbate that can be adsorbed onto the surface can be characterized as:

$$C_{SA\infty} = NC_\sigma \tag{w}$$

The cooperative adsorption theory is capable of providing better explanations of the adsorption mechanisms as well as the surface reactions [178]. Owing to the theory has a robust mechanistic support and a wide application range, itself is a more mature adsorption theory.

2.4.2 Heavy metal adsorbents

Heavy metals can be adsorbed by various kinds of materials. Activated carbon as the most common adsorbent was prepared from different sources and found to be effective in removing Ni(II), Hg(II), Zn(II), Co(II), Cd(II), Cu(II), Pb(II), Cr(III), and Cr(IV) [179-182]. Nowadays, more researches have been focused on the finding of cheap and effective heavy metal adsorbents such as zeolite and chitosan [183-184]. Natural zeolites has been studied in the removal of Cu(II), Co(II), Zn(II), and Mn(II). The adsorption was studied with Langmuir isotherm model and the

adsorption capacity was found to be 141.12 mmol/kg, 244.13 mmol/kg, 133.85 mmol/kg, and 76.78 mmol/kg, respectively [183]. Chitosan from various sources were evaluated with its adsorption capacities towards Cd(II), Cr(III), Cr(IV), Hg(II), and Pb(II) [184]. Some high adsorption capacities reported are 796 mg Pb/g, 1123 mg Hg/g, 92 mg Cr/g, and 558 mg Cd/g [185-188]. Chitosan composites such as chitosan/ceramic alumina, chitosan/perlite, chitosan/magnetite, chitosan/cellulose, chitosan/sand, chitosan/polyvinyl alcohol etc. were evaluated on overall 14 different heavy metals and the adsorption capacities varies from the lowest 6.75 mg Fe(III)/g (Chitosan/nano-hydroxyapatite) to the highest 719.39 mg Cu(II)/g (chitosan/clinoptilolite) [189-191].

Besides zeolite and chitosan, agricultural wastes as even cheaper materials were studied for their abilities in removing heavy metal contaminants. Over 20 materials were investigated including tea waste, coffee waste, hazelnut shells, cotton, corncob, rice hull, bark, orange peels, sugarcane bagasse etc. [192]. Agricultural waste is able to remove heavy metals because their chemical components such as cellulose, hemicelluloses, and lignin are effective in adsorbing heavy metal cations. On the other hand, the adsorption capacities of agricultural wastes reported ranges from 0.4-119 mg/g, which is substantially lower than that of zeolite and chitosan [192-193].

2.4.3 Heavy metal adsorption on lignin

Till now, there are about 16 published literatures reported the study of heavy metal adsorption on isolated lignin samples. In this session, we will review the different lignin sources and their adsorption capacities, the adsorption scheme, as well as the effect of temperature and pH on the process.

2.4.3.1 Lignin as heavy metal adsorbent

The use of lignin as a heavy metal adsorbent has been investigated on various heavy metal species including Pb(II), Cu(II), Cd(II), Zn(II), Ni(II), Cr(VI), Cr(III), and Ca(II). Basically, all

the studied lignin were obtained from pulp mills through precipitation from the black liquor [194-195]. There were studies that isolated lignin directly from wood species. Demirbas [196] isolated lignin from beech and polar through alkali glycerol delignication. The lignin used by Parajuli et al. was separated from the Japanese cedar trees powder [197].

Guo et al. [15] studied the adsorption capacity of Kraft lignin isolated from black liquor. Their results showed the lignin affinity with heavy metal ions follow the order of Pb(II)>Cu(II)>Cd(II)>Zn(II)>Ni(II). They reported the adsorption capacities with an initial metal concentration of 0.8 mM are 0.3 mmol/g, 0.27 mmol/g, 0.16 mmol/g, 0.13 mmol/g and 0.10 mmol/g respectively. On the other hand, Celik and Demirbas reported the adsorption capacity of their Kraft lignin sample in the order of Pb(II)> Zn(II)> Cd(II) [194]. The different order of adsorption capacities suggested that the lignin adsorption capacity may vary depending on its origin. Šćiban and Klasnja [195] invested the adsorption of Cr(VI), Cd(II), Cu(II) and Zn(II) on Kraft lignin. The result showed Cr(VI) has the highest affinity to the lignin. The stronger interaction between chromium ion and lignin is potentially because of the higher electrical charge of Cr(VI) than other metal ions.

Lignin modification has been studied in order to improve its heavy metal removal efficiency. Parajuli et al. studied the reaction of lignin with catechol in the synthesis of lignocatechol gel and observed an excellent removal of Pb(II) [197]. Peternele et al. investigated the adsorption of Cd(II) and Pb(II) onto caboxymethylated lignin and reported the adsorption capacities at 0.519 mmol/g and 0.338 mmol/g respectively [198]. Liu et al. [199] modified bagasse lignin through ammonification. Lignin was depolymerized through H_2O_2 oxidation while formaldehyde and diethylenetriamine were added to react with the depolymerized lignin. The modified lignin contains amine as an additional functional group. The Pb(II) adsorption capacity of the modified

lignin was tested to be 49.85 mg/g-lignin in the optimum condition. Ge et al. [200] performed amino and sulfonic bi-functionalization to their lignin sample and reported their modified lignin adsorption capacities at 0.71 mmol Cu(II)/g and 0.26 mmol Pb(II)/g. In Table 2.9, we summarized the current studies about this topic with their raw materials and adsorption capacities.

Table 2.9. Adsoption capacities of lignin from different origins.

	Adsorption capacities (mg/g)							Ref.
Raw materials	Pb(II)	Cu(II)	Ni(II)	Cd(II)	Cr(III)	Cr(VI)	Zn (II)	
Bi-functionalized lignin	53.8	45.4	-	-	-	-	-	[200]
Carboxymethylated lignin	80.3	-	-	37.9	-	-	-	[198]
Kraft lignin	62.1	17.3	5.9	17.9	-	-	8.2	[15]
Kraft lignin	-	3.4	-	8.2	-	11.1	1.8	[195]
Kraft lignin	-	-	-	-	18.0	-	-	[201]
Kraft lignin	-	87.7	-	136.6	-	-	-	[202]

2.4.3.2 Adsorption schemes and modeling

Studies have reported that ion-exchange is responsible when heavy metal cations are adsorbed on lignin. Christ et al. studied the adsorption of Sr and Cd on Ca-loaded Kraft lignin sample [203]. They observed a stoichiometric balance between the adsorbed heavy metals and the detached Ca. However the study cannot conclude that this process is only ion-exchanging as their lignin samples were pre-saturated with calcium. It was also suggested that the process cannot be explained with a mechanism. Multiples schemes of ion-exchanging, surface adsorption, and complexing can be involved in the process [204]. Right now, most studies applied Langmuir and Freundlich adsorption isotherms in modeling the equilibrium behaviors of the lignin adsorption process with acceptable agreements [195-202]. However, neither Langmuir nor Freundlich model is capable of explaining the process from a mechanistic point of view. The kinetics of the process was mostly

explained with the pseudo second order model. But this model is empirical and insufficient in characterizing the process. In general, there is still lack of an adequate explaining and modeling of this process mechanistically.

2.4.3.3 The effect of pH and temperature

pH has been found to be an important factor that impacts on the lignin adsorption capacity. This is because for some lignin functional groups, phenolic hydroxyl groups for example, a deprotonation step is necessary for surface ionization in order to bind with heavy metal cations. This further proves that ion-exchange mechanism is responsible in the heavy metal adsorption on lignin. Guo et al. [15] reported their lignin samples did not possess any heavy metal adsorption ability when pH is below 2.5. Wu et al. [201] studied Cr(III) adsorption with or without another heavy metal and reported some adsorption ability at low pH ($pH \leq 2$). Their result showed almost a 100% Cr(III) removal efficiency when pH was raised above 4.5. Parajuli et al. [197] observed similar pH effects on their synthetic lignin gels and observed some adsorption ability of Pb(II) at low pH and no adsorption ability of Cd(II), Zn(II), Co(II), Ni(II), La(III), Al(III), and Fe(III). All three studies observed an "s" dependency of heavy metal removal versus pH. The results from Parajuli and Wu suggested an alternative adsorption mechanism beside ion-exchange. The different results reported by Guo et al. at low pH suggests that adsorption properties of lignin may vary between species. Guo et al. modeled the effect of pH by considering the deprotonation and binding on two ion-exchange groups. The model achieved satisfactory agreement to the experimental data, but the model simplified the deprotonation and binding as one step, which reduces its reliability from a mechanistic point of view. Also, the model will be limited by the lignin species if a secondary binding scheme is not considered.

The effect of temperature has been studied by Mohan et al. [17]. They found the lignin adsorption capacities on Cu(II) and Cd(II) are both increased with higher temperature. Three different temperatures were studied at 10°C, 25°C and 40°C. The adsorption capacity Cu(II) was found to be 68.63 mg/g, 87.05 mg/g and 94.68 mg/g, while Cd(II) at 59.58 mg/g, 137.14 mg/g and 175.36 mg/g respectively. They concluded that the temperature has a higher impact on the forward adsorption process than the reverse desorption process. On the other hand, adsorption is usually an exothermic process. The phenomenon they observed is more plausible to be explained as the deprotonation step is favored by higher temperature. In all, there is still lack of a systematic study about the process from both pH and temperature aspects. A model with robust mechanistic background in explaining and predicting the lignin adsorption properties is desired.

Chapter 3

The Effect of Hot-water Treatment on the Heavy Metal Adsorption Affinity of Klason Lignin

3.1 Introduction

Lignin is an effective material in removing heavy metal cations. Every year, more than 500 thousands metric tonnes of lignin are produced from the paper pulp industries [14]. A couple of studies have been conducted upon the heavy metal adsorption by Kraft lignin that concluded Kraft lignin is effective in removing Pb(II), Cd(II) and Cu(II) from wastewater streams [15-17]. With the concept of sustainability and renewability, studies of producing renewable fuels, chemicals, and materials such as ethanol, butanol, furfural, hydroxymethylfurfural (HMF) etc. with lignocellulosic biomass has been going on [18]. Recently, attributed to the development in the field, lignocellulosic biorefinery has been industrialized. In 2014, 750 million liters of lignocellulosic bioethanol has been produced in the US, while the production capacity is anticipated to be two to three folds by 2020 [205]. In China, industries have been developed to use agriculture residues, wheat straw, rice straw and corn stover for examples, in producing lignocellulosic biofuels. The production of bioethanol and biodiesel in China have reached 1.02 million tons and 50,000 tons in 2010 and the Chinese government aims to produce 3.0 million tons of bioethanol from non-grain crops by 2020 [206]. On the other hand, challenges are faced in the second generation of biorefinery since the production costs are two to three times more expensive than the petroleum refinery [19-20]. In this case, the utilization of the byproduct, lignin, from the biorefinery process becomes important in order to expand the profit margin. The ethanol production indicates about 0.47 million tons of lignin was produced from the lignocellulosic plant in 2014 US by assuming the cellulose and lignin contents at 50% and 20%, respectively. Meanwhile, considering the fast development of the lignocellulosic biorefinery field, it is expected the lignocellulosic biorefinery industries will become another major producer of lignin in the coming years. However, the studies about lignin applications after biorefinery are limited and the use lignin from the biorefinery process as a biosorbent has not been evaluated yet.

The adsorption affinity of lignin is dependent on its functional groups. Previous studies about heavy metal ion adsorption on lignin have concluded that ion exchanging process is responsible [203]. Native lignin from higher plants contains phenolic and aliphatic hydroxyl groups that are functional in adsorbing heavy metal ions. Carboxyl group as another functional group is expected in gramineaes lignin originating from ferulic acid [21].

In lignocellulosic biorefinery processes, different lignin reactions can occur depending on the processing conditions, which can impact the lignin functional groups and further the lignin adsorption affinity. Hot water treatment is a typical biomass pretreatment technology which is conducted on biomass at high temperature (≥160°C) in a sealed vessel with liquid water [207-211]. At such conditions, the cleavage of acetyl groups first occurs on acetylated hemicelluloses such as glucomannan, glucuronoxylan and arabinoxylan [212]. The deacetylation process results in free acetyl groups, which increases the acidity of the environment. The pH of the process ranges from 2-4 depending on the type of biomass as well as the treatment temperature [213]. Previous studies have reported the lignin structural changes after hot water treatment and pointed out that both lignin depolymerization and condensation reactions can occur under high temperature, acidic conditions [53,56].

Hot water treatment is also the most common biomass pretreatment technology applied in the Department of Paper and Bioprocess Engineering, SUNY-ESF. We have evaluated hot water treatment in different scales from a 4.7 L M/K digester to a 1840 L pilot scale reactor, different biomass species including *Paulownia*, willow, and sugar maple, as well as different conditions (145 ℃ to 165 ℃, as long as 4 hours) [214-216]. In this study, hot water treatment was performed under different temperature and pH on Klason lignin isolated from *Paulownia elongate*, a fast-growing hardwood species, in order to investigate its effects on the lignin heavy metal adsorption

affinity. Synthetic wastewater samples containing 100 ppm heavy metal ions were used as a simulation of industrial wastewater. The lignin depolymerization and condensation reactions were discussed about their schemes and impacts on the lignin heavy metal adsorption affinity. FTIR analysis was performed to characterize the lignin structure. The lignin NMR spectrum was studied to compare the amount of functional groups before and after treatment.

3.2 Materials and methods

3.2.1 Adsorbent preparation

Four-year old *Paulownia elongata* wood logs were harvested at Fort Valley State University, Fort Valley, Georgia and shipped to Syracuse. The wood logs were further chipped to 2.5×2.0×0.5 cm^3 size with bark at the SUNY-ESF piolet plant located in Syracuse, NY and preserved in a cool dry environment.

The wood chips were milled to 40-mesh wood powder and oven-dried at 50°C for 12 hours before use. Klason lignin was prepared through the method described in TAPPI standard T 222 om-02. Hot water treatment was conducted at 150°C and 160°C on the obtained Klason lignin in glass tubes with sealing caps. The 1:20 g/mL solid/liquid ratio was used during the treatment. Acidified hot water treatment was carried out with 23.5 mM acetic acid solution. Lignin samples were taken every 10 minutes until 1 hour of treatment. The obtained lignin samples were washed with DI water and dried at 50°C in a vacuum oven for 12 hours.

3.2.2 Adsorption of heavy metal ions

Pb(II), Cu(II) and Cd(II) solutions were prepared with lead nitrate, copper chloride and cadmium chloride from Fisher Scientific Inc. The initial heavy metal ion concentrations were at 100 ppm. 100 mL of the prepared solutions were transferred to 250 mL flasks with the addition of 0.1 g of lignin samples. The adsorption experiments were conducted in a shaker stirring at 25°C, 150 rpm. After 3 hours of adsorption, 10 mL of the liquid samples were taken and filtered. The

heavy metal ion concentrations in the filtrates were analyzed by inductively coupled plasma optical emission spectrometry (ICP-OES, Optima 5300 DV, PerkinElmer). The adsorption affinity was determined by the metal ion concentration difference before and after the adsorption.

$$\text{Adsorption affinity} = \frac{C_{M,0} - C_{M,\mathrm{t}}}{C_L} \quad \text{(x)}$$

Where $C_{M,0}$ and $C_{M,\mathrm{t}}$ are the heavy metal concentrations before and after adsorption in mg/L, C_L is the lignin loading in g/L.

3.2.3 Adsorbent characteristics

The untreated lignin sample was analyzed by Fourier-transformed infrared spectra (FT-IR) using a PerkinElmer Frontier FT-IR/NIR spectrometer. Before the analysis, lignin sample was dried in a vacuum oven at 50°C for 12 hours. The dried lignin sample was placed under the press which is built-in to the instrument. The sample is then pressed and scanned to obtain the FT-IR spectrum.

Lignin is acetylated in 20 mL pyridine/acetate anhydrate solution (1:1 v/v) for at least 24 hours following the method described by Lundquist [217]. Sample was centrifuged and filtered afterwards. The solution was dripped onto ice cubes. The precipitant was filtered and dried in a vacuum oven at 50 °C as acetylated lignin. Acetylated lignin samples were prepared for nuclear magnetic resonance (NMR) analysis. 0.05 g of the dried acetylated lignin sample was added into 500 µL deuterated dimethyl sulfoxide (DMSO-d6) and mixed with a vortex mixer until the dissolution of all the solids. 100 µL, 0.4% w/v trimethylamine hydrochloride (TMA) internal standard was added to the solution. The mixture was then transferred into an NMR tube. The NMR experiments were performed at 30°C with a Bruker AVANCE III HD 800 MHz NMR spectrometer. The NMR method has been described in Goundalkar et al. [218] Both proton NMR

(^{1}H NMR) and heteronuclear single quantum coherence (HSQC) analysis were conducted. The obtained spectra were processed using MestReNova 6.1.1-6224.

3.3 Results and discussion

3.3.1 FTIR characterization

The FT-IR spectrum of the untreated Klason lignin sample was shown in Figure 3.1. The band shown at 3434 cm^{-1} was attributed to the stretching of the phenolic and aliphatic hydroxyl groups which are also considered as the major functional group for the metal ion adsorption. C-H stretching on the aliphatic side chain was shown at 2934 cm^{-1} and 2847 cm^{-1}. The band at 1717 cm^{-1} was designated to the nonconjugated C=O stretching. The presence of C=O groups can be two reasons: one is the presence of cinnamyl aldehyde units in the sample which is originated from the reversible catalysis of cinnamyl alcohol dehydrogenase (CAD) and the CAD downregulation [219]; or it is because of the structural modification during the isolation procedure. Three bands at 1595 cm^{-1}, 1500 cm^{-1} and 1461 cm^{-1} were assigned to the aromatic ring vibration. The absorption at 1214 cm^{-1} depicts C-O stretching from the guaiacyl units. As a hardwood species, the absorption at 1114 cm^{-1} suggests the presence of syringyl units [220]. The designations were summarized in Table 3.1.

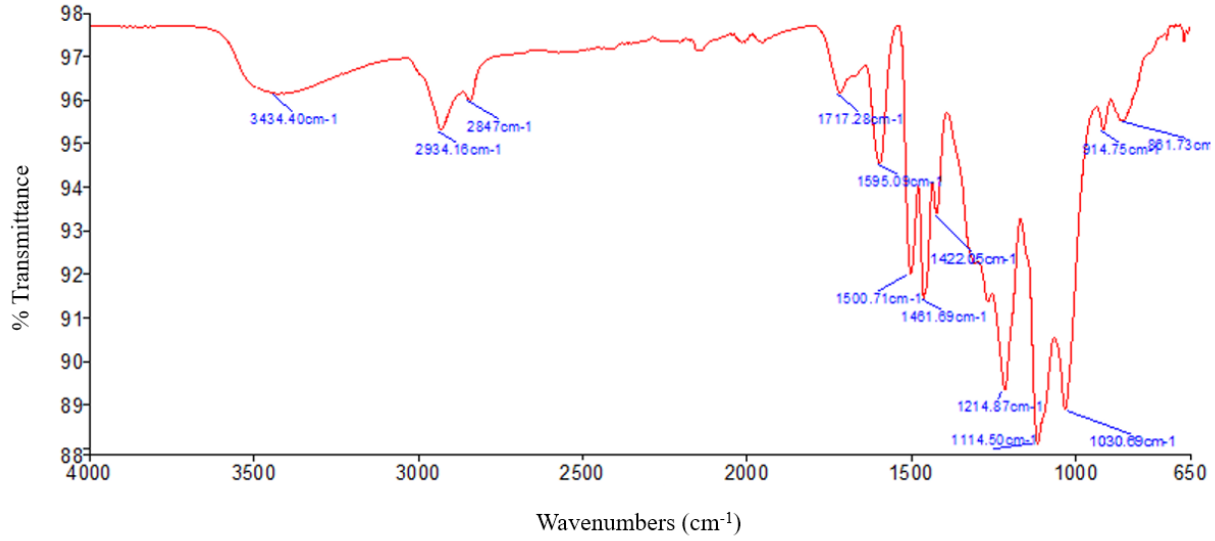

Figure 3.1. FT-IR spectra of untreated Klason lignin isolated from *Paulownia elongata*.

Table 3.1. FT-IR absorption bands designations [15,24].

Band assignment	Wavenumber (cm^{-1})
-OH stretching	3434
C-H stretching (aliphatic chain)	2934, 2847
C=O stretching (nonconjugated)	1717
Aromatic ring vibration	1595, 1500, 1461
C-O stretching in guaiacyl	1214
C-H inplane deformation in syringyl	1114

3.3.2 Effect of hot water treatment on the adsorption affinity

The starting pH of the hot water treatment were measured at 6.50 and 3.30 with water and acetic acid media; respectively. After 60 minutes of treatment, the pH values in the media decreased. The water treatment groups at 150°C and 160°C have the pH decreased to 2.79 and 2.65; respectively, while the acetic acid group decreased to 2.61. The decrease in pH is due to the deprotonation of the functional groups in lignin molecules. The deprotonation of the lignin

functional groups also created an acidic environment for adsorption (pH<4.0). Due to the acidity and low substrate concentration, heavy metals were fully soluble. Temperature also plays a critical role in the adsorption equilibrium. In this study, the adsorption temperature was maintained at 25°C as a reference point and the heavy metal concentrations at the end point were measured in order to evaluate the adsorption affinity of the lignin samples.

The results of the Pb(II) adsorption affinity test of the Klason lignin samples before and after treatment are shown in Figure 3.2. The Pb(II) adsorption affinity of untreated Klason lignin sample was at 8.11 mg/g-sample with 8.11% Pb(II) removal. At the beginning of the hot water treatment, a slight increase of the adsorption affinity was observed in all three groups. The highest adsorption affinity was reached after 20 minutes of water treatment at 160°C with 11.5% of increase. Samples that were pretreated for longer than 20 minutes exhibited a substantial decrease in the Pb(II) adsorption affinity. With 60 minutes of treatment, more than 40% of the Pb(II) adsorption affinity was lost in all three groups. It was also observed that effectiveness of the lignin samples dropped faster in the groups with higher treatment temperature and acidity. The lignin samples with the highest (160°C, 20 min, water pretreated) and the lowest (160°C, 60 min, acetic acid pretreated) effectiveness together with the untreated sample were further tested with Cu(II) and Cd(II) solutions. The adsorbed Cu(II) and Cd(II) on the untreated lignin sample were at 2.25 mg/g-sample and 1.42 mg/g-sample. The same trend of the effectiveness change was observed on Cu(II) and Cd(II) adsorption as shown in Figure 3.3.

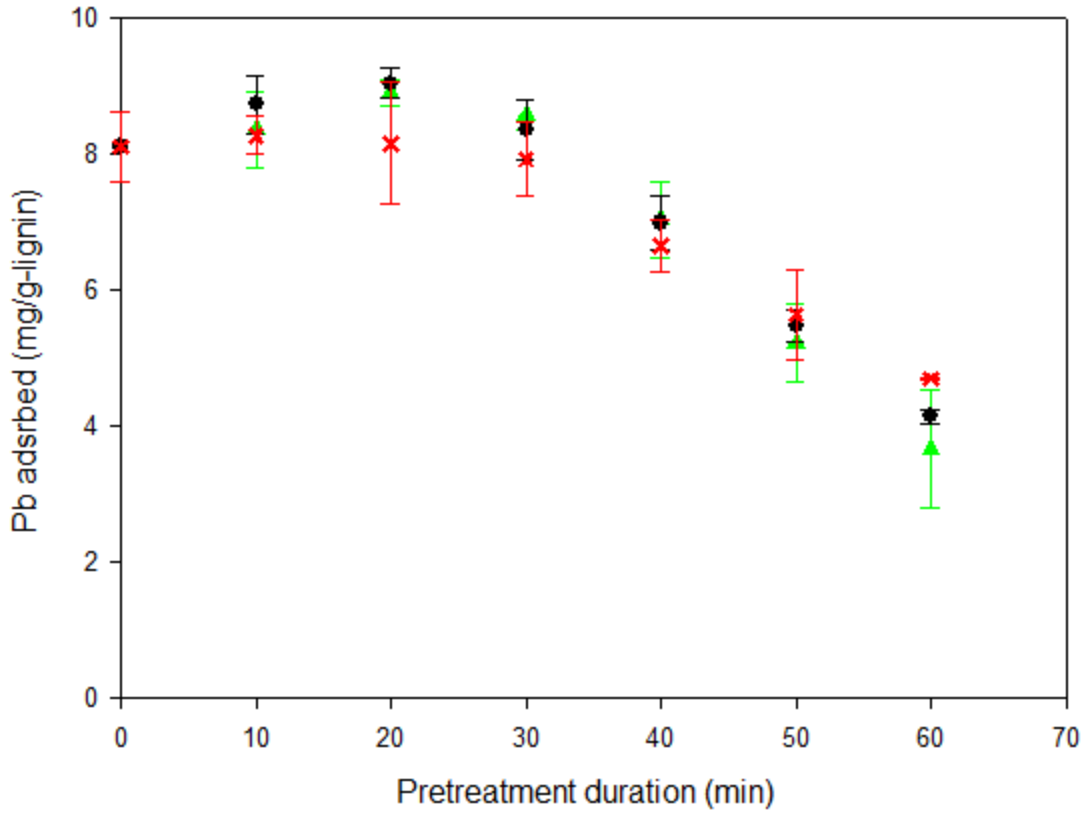

Figure 3.2. Adsorption capacities of untreated and pretreated lignin samples with initial Pb(II) concentration of 100 ppm. ▲: pretreated at 160°C with 23.5 mM acetic acid solution; ●: pretreated at 160°C with water; ×: pretreated at 150°C with water. Each data point has been duplicated with the result range displayed in the figure. Data point is averaged from the range.

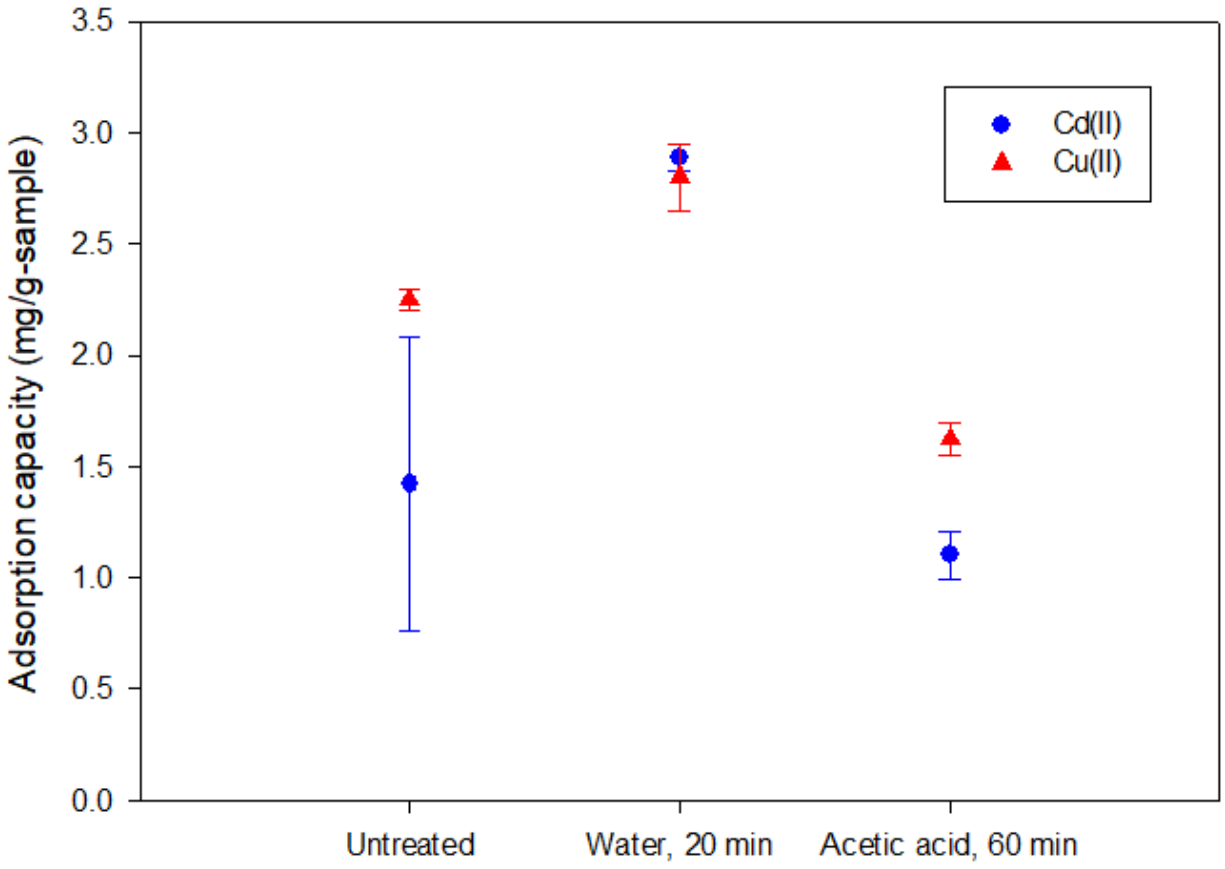

Figure 3.3. Adsorption capacities of Cu(II) and Cd(II) tested on lignin samples pretreated at 160°C with different durations and mediums. Each data point has been duplicated with the result range displayed in the figure. Data point is averaged from the range.

The adsorption of heavy metals on lignin is an ion exchange process that the hydroxyl groups on lignin can deprotonate and adsorb a heavy metal cation through ionic binding. The process of heavy metal ions uptake by lignin can be generalized as Eqn (y) [221].

$$\text{R-OH} + \text{M}^{2+} \rightarrow \text{R-OM}^{+} + \text{H}^{+} \qquad \text{(y)}$$

From the native lignin structure, one can infer that free phenolic groups, as well as aliphatic hydroxyl groups, are the major functional groups that are responsible for the heavy metal ions adsorption. The affinity change after treatment can be explained by the lignin reactions occurred

during hot water treatment which impacts the amount and effectiveness of the functional groups. Hot water treatment provides an acidic, high temperature environment which causes both lignin depolymerization and condensation to happen. The aryl ether bonds in lignin such as α-O-4 and β-O-4 linkages can be cleaved under acidic environment as shown in Figure 2.11. Lignin depolymerization results in more free phenolic hydroxyl groups, which increases the lignin adsorption affinity, which interprets the slight increase of the adsorption affinity with short treatment duration. On the other hand, due to the formation of carbon cation on C_α after the cleavage of aryl ether bonds, lignin repolymerization can occur between C_α and C_6. Condensation results in the formation of C-C bond with high stability as shown in Figure 2.12. Based on the scheme in Figure 2.12, lignin condensation consumes the aliphatic hydroxyl groups on C_α that reduces the amount of the functional groups. Meanwhile, lignin molecular weight is increased after condensation, which does not favor the deprotonation from the functional groups. Li et al. have studied the intensity of lignin depolymerization and condensation reactions by monitoring the molecular weight after hot water treatment [211]. They reported that lignin reactions are dominated by condensation when hot water treatment was performed in high severity (S_0=3.2-4.5). This explains the decrease of adsorption affinity after long treatment. Comparing to Kraft lignin, it has been reported that Kraft lignin exhibited the adsorption affinity of Pb(II) at 62 mg/g-lignin, which is 7.6 times higher than the Klason lignin sample [15]. Besides the differences in biomass sources and operation conditions (initial Pb(II) concentration, adsorption temperature), one major reason is that the lignin aryl-ether bonds are cleaved during Kraft cooking and bleaching, which favors lignin as an adsorbent.

3.3.3 Functional group determination

NMR analysis was conducted in order to quantify the hydroxyl groups in the lignin samples. A characteristic HSQC, as shown in Figure 3.4, was performed to locate the chemical shifts of the

acetylated hydroxyl groups. The three methyl groups in TMA gave the signal at 2.74/44.48 ppm ($^{1}H/^{13}C$). Two strong signals at 2.26/20.68 ppm and 2.01/20.96 ppm were assigned to the aromatic acetate and aliphatic acetate respectively [217]. In HSQC spectrum, no other signals was observed with ^{1}H shift between 2.4-1.8 ppm. Proton NMR, as shown in Figure 3.5 was applied to quantify the functional groups in the samples based on the integral of the acetylated –OH groups. The amount of –OH groups was calculated by Eqn (z).

$$n_{-OH}(mmol/g) = \frac{n_{TMA} \times 3 \times Integral}{m_{sample}} \quad (z)$$

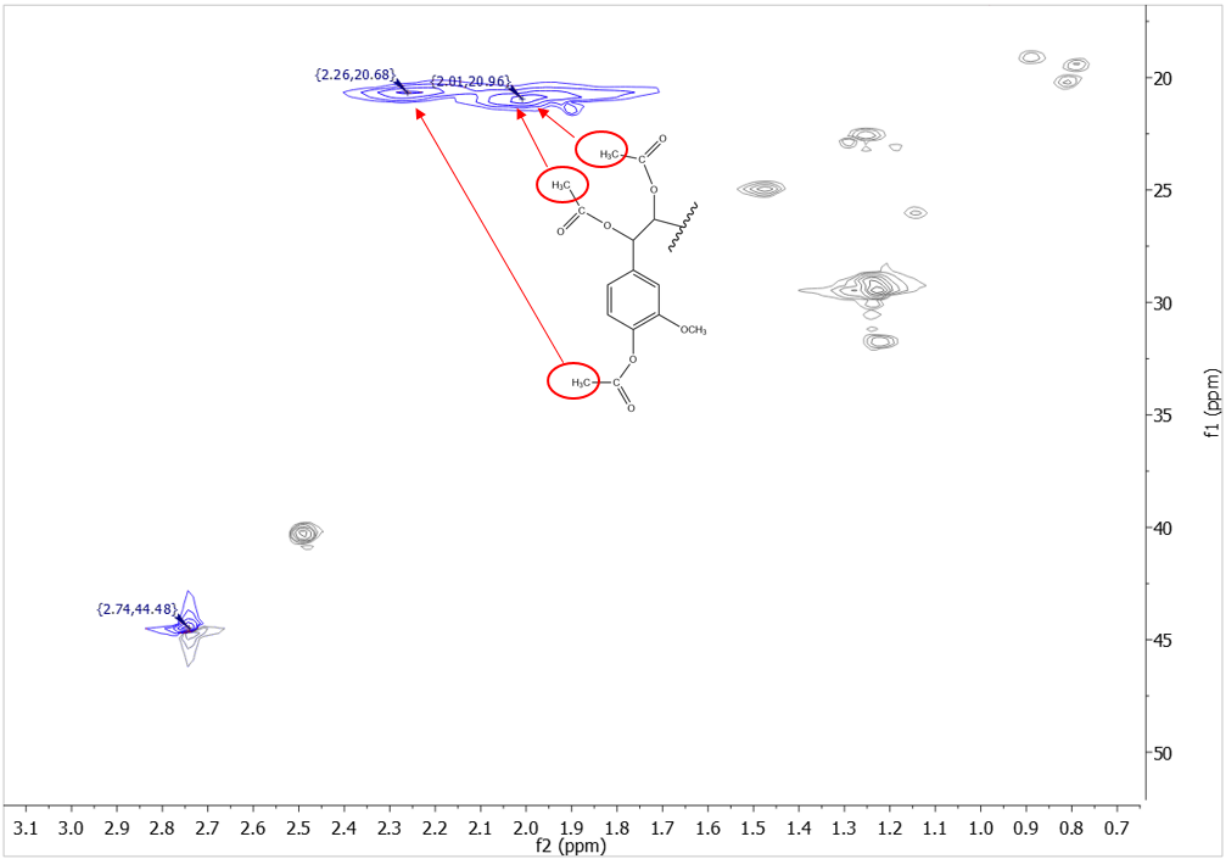

Figure 3.4. HSQC characterization of acetylated phenolic and aliphatic hydroxyl groups with an acetylated guaicyl unit model.

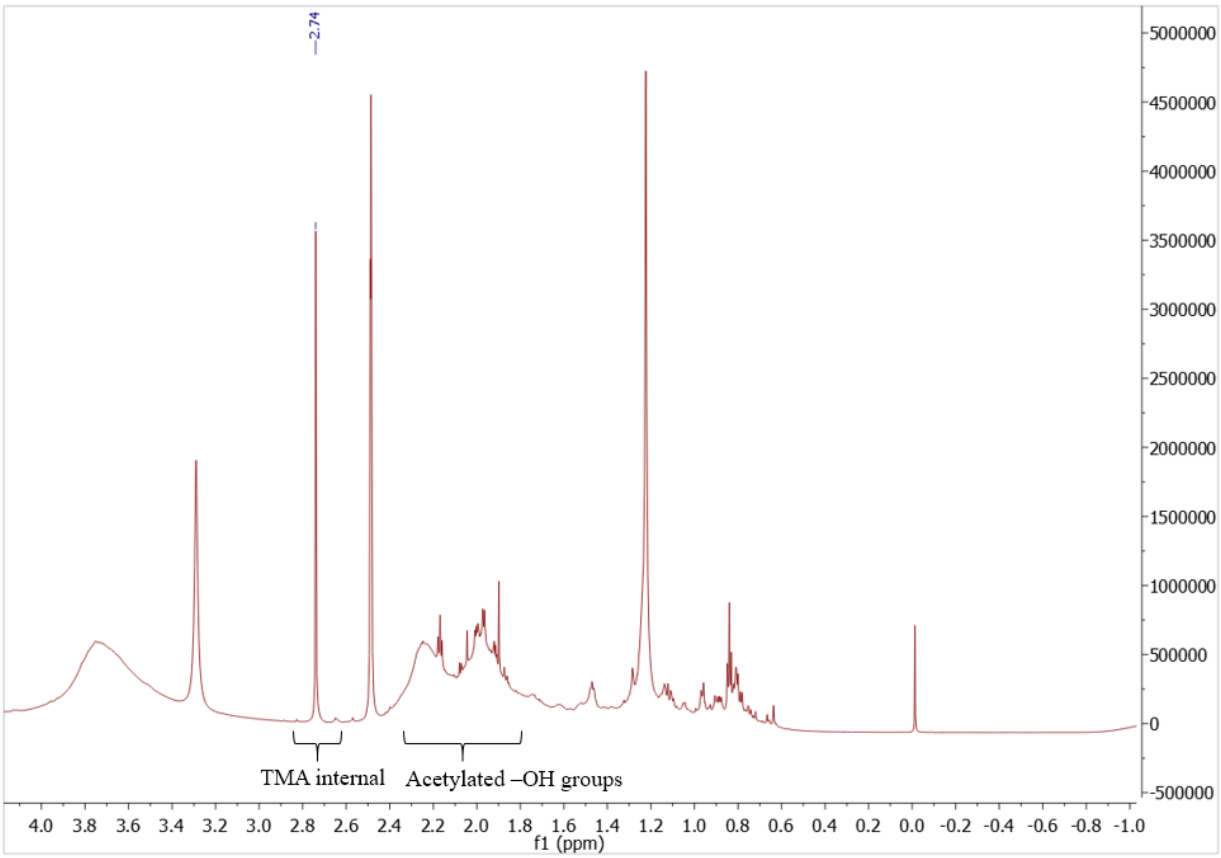

Figure 3.5. Proton NMR used in quantification the content of heavy metal adsorption functional groups in samples with TMA as internal standard. Each sample has been duplicated.

The results showed that the –OH contents in untreated lignin sample, sample pretreated at 160°C for 20 minutes with water and sample pretreated at 160°C for 60 minutes with acetic acid were at 4.45 mmol/g, 4.50 mmol/g and 4.09 mmol/g; respectively. The changes in the –OH contents were speculated to be the result of the lignin depolymerization and condensation reactions occurred during the hot water treatment. The difference of –OH content between the untreated sample and the sample pretreated at 160°C for 60 minutes with acetic acid further indicates a condensation dominant lignin reaction scheme at late stage of hot water treatment.

3.4 Conclusions

Klason lignin lignin isolated from *Paulownia elongata* exhibited the ability in removing heavy metal ions in the order of Pb(II)>Cd(II)>Cu(II). The adsorption affinity was impacted after hot water treatment. Sample with the highest adsorption affinity was obtained after 20 minutes treatment at 160°C with water while the lowest was after 60 minutes treatment at 160°C with acetic acid. During hot water treatment, two types of lignin reactions can occur as depolymerization and condensation. Depolymerization cleaves the aryl-ether structure in lignin that gives more functional groups for heavy metal adsorption. On the other hand, condensation which reduces the –OH content while forming bulk lignin molecule is not favored. NMR quantification of –OH content suggested a condensation dominant lignin reaction scheme with long duration of hot water treatment at low pH. For the future application of lignin from a biorefinery process, if a long duration of high temperature, acidic treatment has been conducted on the biomass, the leftover lignin is no longer suggested to be used as a heavy metal adsorbent. On the other hand, short duration of acidic treatment favors the adsorption affinity, although short-time hot water treatment of biomass is usually not sufficient for carbohydrate utilization. Other treatment technologies such as alkaline treatments were expected to favor the adsorption affinity since Kraft lignin exhibits a much higher adsorption affinity because of the cleavage of aryl-ether bonds during the Kraft pulping process.

Chapter 4

Cooperative Adsorption of Heavy Metal Cations on Lignin

4.1. Introduction

Heavy metals have been long noticed as major pollutants due to their toxic nature, in particular to humans. Cadmium, nickel, and chromium have been classified as human carcinogens by the Internation Agency for Research on Cancer (IARC) [3]. Lead exhibits high affinity to the sulfhydryl groups which leads to its high toxicity to structural proteins and enzymes [115]. Since heavy metals are highly accumulative in human bodies, the harm can be caused at any levels of concentration [222]. Typical symptoms of heavy metal poisoning include memory loss, organ failure, anemia etc. Study about lead poisoning also pointed out that children are more affected by heavy metals due to their low body weight and a faster adsorbing rate comparing to adults [116]. The discharge of heavy metals to the environment is highly related to human activities. To date, our modern industries are still heavily dependent on heavy metals in producing many necessities such as batteries, pigments, electroplates, pesticides, and leathers [2]. Mining activities also accelerate the exposure and leach-out of heavy metals to the aqua system [223-225].

Municipal, agriculture and industrial wastewater can all contain heavy metal pollutants. Some heavy metal ions such as Pb^{2+}, Ni^{2+}, Cd^{2+}, Cu^{2+} and Zn^{2+} are relatively difficult to be removed from wastewater streams due to the amphotericity of their hydroxide forms. For example, lead cation can generally be precipitated as lead hydroxide at pH between 8 and 8.5. However, when pH is raised above 9.5, the hydroxide becomes soluble again [10]. Other heavy metals exhibit different optimum precipitation pH, copper at 8.1, and cadmium at 11.0, for example [11]. The moderate solubility of heavy metal hydroxides makes pH adjustment ineffective especially in streams with multiple heavy metal pollutants. Some conventional treatment technologies for heavy metals are chemical precipitation, membrane filtration, and electrochemical methods [12]. However, these technologies either require large capital investments or high operational costs [2].

Regardless of the enacted heavy metal discharge regulations, some industries, especially small industries in developing countries, are not treating their wastewater properly due to economic reasons. One replacement of the costly conventional treatment technology is adsorption. The advantage of adsorption lies in its low treatment time, low energy input as well as the recyclability of adsorbent and heavy metals [226-229]. There has been an increase in studies on heavy metal treatment using low-cost adsorbent. Some low-cost adsorbents such as zeolite, agriculture waste, clay, biochar and fly ash have been reported to be effective in adsorbing heavy metals [230-239].

Kraft lignin has also been found to be an effective adsorbent for heavy metals. The advantage of lignin comparing to other materials lies in its vast availability. Every year, more than 500 thousand metric tonnes of lignin are produced from the paper pulp industries [14]. The results of previous studies have shown lignin presents adsorption capacity towards bivalent heavy metal cations [15-16]. Crist et al. studied ionic stoichiometry with calcium loaded lignin and concluded that ion-exchanging is responsible for the adsorption process [203]. Considering the chemical structure of lignin, native lignin contains phenolic hydroxyl groups (PhOH) which are able to deprotonate and adsorb heavy metal ions. For Kraft lignin, carboxyl groups (-COOH) are presented due to the oxidative bleaching process, which can also ion-exchange with heavy metal ions [240]. On the other hand, the process cannot be absolutely considered as ion-exchanging, as heavy metals cations can potentially complexing with electrophilic groups presented in Kraft lignin.

Early studies have used Langmuir, Freundlich or pseudo second order model in simulating the process [15,192]. However, these models fail to illustrate the lignin adsorption process from a mechanistic point of view. For example, the process deviates from the Langmuir adsorption theory because lignin contains multiple functional groups with different interactive energies towards heavy metal cations. Also, a multivalent heavy metal cation can bind with more than one ion-

exchanging groups indicating a situation that one adsorbate can bind with multi active site. Freundlich or pseudo second order models are more empirical. Recent study also questioned the accuracy of pseudo second order model in simulating adsorption kinetics [241]. In this study, 1-n cooperative theory was proposed with its mathematic model. The new theory has considered the existence of multiple active sites on the adsorbent surface and the cooperativity of multiple functional groups to one adsorbate molecule. We performed adsorption with three heavy metal ions (Pb^{2+}, Cd^{2+}, and Ni^{2+}). The initial heavy metal concentration ranges from 50-200 ppm, pH<7, as a simulation of industrial heavy metal contaminated wastewater. The theory has been found successful in simulating the adsorption results under different pH and temperature. The proposed theory also provides guidelines for Kraft lignin industrial applications and future studies with non-ideal adsorbent surfaces.

4.2. Materials and Methods

4.2.1. Adsorbent preparation

Concentrated black liquor was generously provided by International Paper Inc. The concentrated black liquor was in gel state that was first dissolved by adding deionized water. 37 wt% hydrochloric acid was then added dropwise to the black liquor solution until pH dropped between 2 to 3. The solution was filtered. The obtained solid was washed three times for 24 hours with DI water at 1g : 400mL solid-liquid ratio. The washed solid was then dried in a vacuum oven at 50°C for 24 hours and milled to pass a 30 mesh sieve. The obtained solid was used as the adsorbent in the following experiments.

4.2.2. Adsorbent characterization

Lignin samples were acetylated based on the procedure described in the previous chapter 3.2.3. 0.05 g of the dried acetylated lignin sample was added into 500 µL deuterated dimethyl sulfoxide (DMSO-d6) and mixed with a vortex mixer until the dissolution of all the solids. 100 µL, 0.4%

w/v trimethylamine hydrochloride (TMA) internal standard was added to the solution. The mixture was then transferred to an NMR tube. The NMR experiments were performed at 30°C with a Bruker AVANCE III HD 800 MHz NMR spectrometer. The NMR method has been described in Goundalkar et al. and Liu et al. [218,242]. Both carbon NMR (13C NMR) and heteronuclear single quantum coherence (HSQC) analysis were conducted. The obtained spectra were processed using MestReNova 6.1.1-6224.

4.2.3. Effect of pH and temperature

The effect of pH was investigated by first preparing three 1 L solutions which contain 50 ppm, 100 ppm and 200 ppm Pb(II) with lead nitrate. 100 ppm Cd(II) and Ni(II) containing solutions were prepared with cadmium chloride and nickel chloride hexahydrate. 1 g of lignin samples were introduced to each of solutions. The mixtures were stirred intensively at 500 rpm on a stirring plate to reach a homogenous environment. 0.5 M NaOH solution was then added to the solution-lignin mixture dropwise. After each increment of pH, 30 mL solution together with lignin was withdrawn from the system. The mixture was transferred to a 50 mL centrifuge tube and shaken at 25°C, 150 rpm for 24 hours. Afterwards, the solution was filtered and acidified with HNO_3 for metal ion analysis. The pH was maintained below 7 during the process in order to prevent metal ions precipitation.

The effect of temperature was investigated with 100 ppm Pb(II) solutions under 25°C, 40°C and 55°C with the same experimental strategy demonstrated above. The heavy metal concentrations in the filtrates were analyzed by inductively coupled plasma optical emission spectrometry (ICP-OES, Optima 5300 DV, PerkinElmer). Each data point has been duplicated and averaged in use.

4.2.4. 1-n cooperative adsorption theory

Previous studies about cooperative adsorption theory has concluded any deviations from Langmuir adsorption as the inconsistency of the solid surface and the interaction between adsorbates. It has been successful in using an apparent multilayer point of view to model the different energy levels on a solid surface. The cooperativity concept was introduced to describe the interaction between adsorbates. Successful applications of the cooperative adsorption model have been achieved in explaining both adsorption and catalysis [117-118].

On the other hand, previous investigations about cooperative adsorption have been focused on the 1-1 case that one adsorbate molecule can only interact with one active site. However, heavy metal cation adsorption on Kraft lignin involves a multivalent binding process that interaction between one adsorbate and multiple sites is expected, which requires a further development of the cooperative adsorption theory to fit the 1-n scenario (Figure 4.1). In Figure 1, *K* stands for the binding affinity constant. When an adsorbate has been previously bound with an active site, its affinity towards other active sites will be altered due to the conformation change, which is represented with a cooperativity coefficient "c". The value of "c" larger or smaller than 1 indicates a positive or negative cooperativity. Consider random bindings of an adsorbate A to n active sites on an adsorbent surface named σ_1 to σ_n, the binding of the ith site can be written as Eqn (aa).

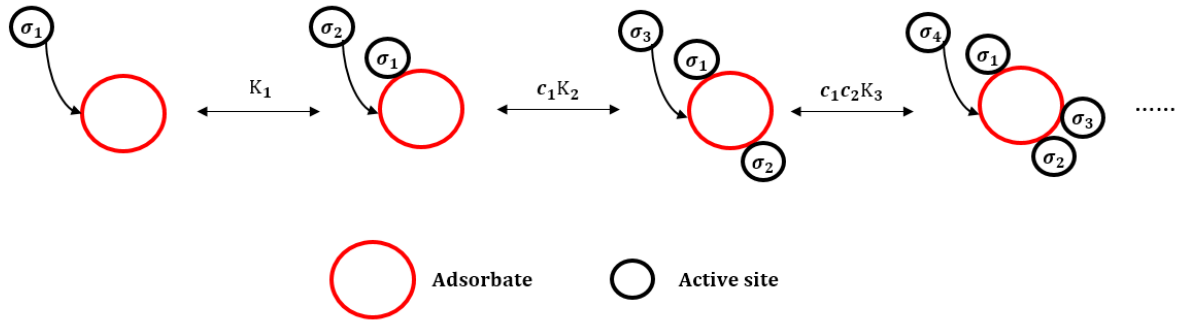

Figure 4.1. Cooperative binding of one adsorbate to multiple active sites.

$$\sigma_{ai} + \sigma_{a1}\sigma_{a2} \dots \sigma_{a(i-1)}A \xleftrightarrow{\prod_{j=1}^{i-1} c_{aj}K_{ai}} \sigma_{a1}\sigma_{a2} \dots \sigma_{ai}A \quad \text{(aa)}$$

Here σ_{ai} can be any active sites from σ_1 to σ_n. Based on Eqn (aa), the equilibrium concentration of A bound with i sites can be written as,

$$[\sigma_{a1}\sigma_{a2} \dots \sigma_{ai}A] = \prod_{j=1}^{i-1} c_{aj}^{i-j} K_{aj} [\sigma_{aj}] K_{ai} [\sigma_{ai}] C_A \quad \text{(ab)}$$

Eqn (ab) can be used for the overall amount of adsorbed adsorbate as C_{SA}.

$$C_{SA} = \sum_{i=1}^{n} [\sigma_{a1}\sigma_{a2} \dots \sigma_{ai}A] \quad \text{(ac)}$$

This 1-n cooperative theory will be later applied to model the adsorption behaviors of Kraft lignin.

4.3. Results and Discussion

4.3.1. Adsorbent characterization

NMR analysis was conducted in order to characterize the functional groups that are responsible for Pb(II) removal. HSQC and ^{13}C NMR spectra are shown in Figure 4.2 and 4.3 respectively. In Figure 2, the signal at 2.74/44.48 ppm (^{1}H/^{13}C) was attributed by TMA which was used as a shift reference. Two strong signals at 2.24/20.78 ppm and 1.94/21.03 ppm were assigned to the aromatic acetate and aliphatic acetate respectively, which were originated from aliphatic and phenolic hydroxyl groups [217]. In ^{13}C NMR spectrum, the solvent DMSO-d6 gave its signal at 39.99 ppm. The chemical shifts between 172.38 ppm and 168.55 ppm were designated to the carboxyl groups in the Kraft lignin structure [243]. During the adsorption process, both hydroxyl groups and carboxyl groups are functional groups that can deprotonate and ion exchange with Pb(II) cations in the solution. However, since the experiments were carried out under acidic environment, the adsorption on aliphatic hydroxyl groups was neglected while only PhOH and –COOH were considered as the ion-exchange functional groups in our case.

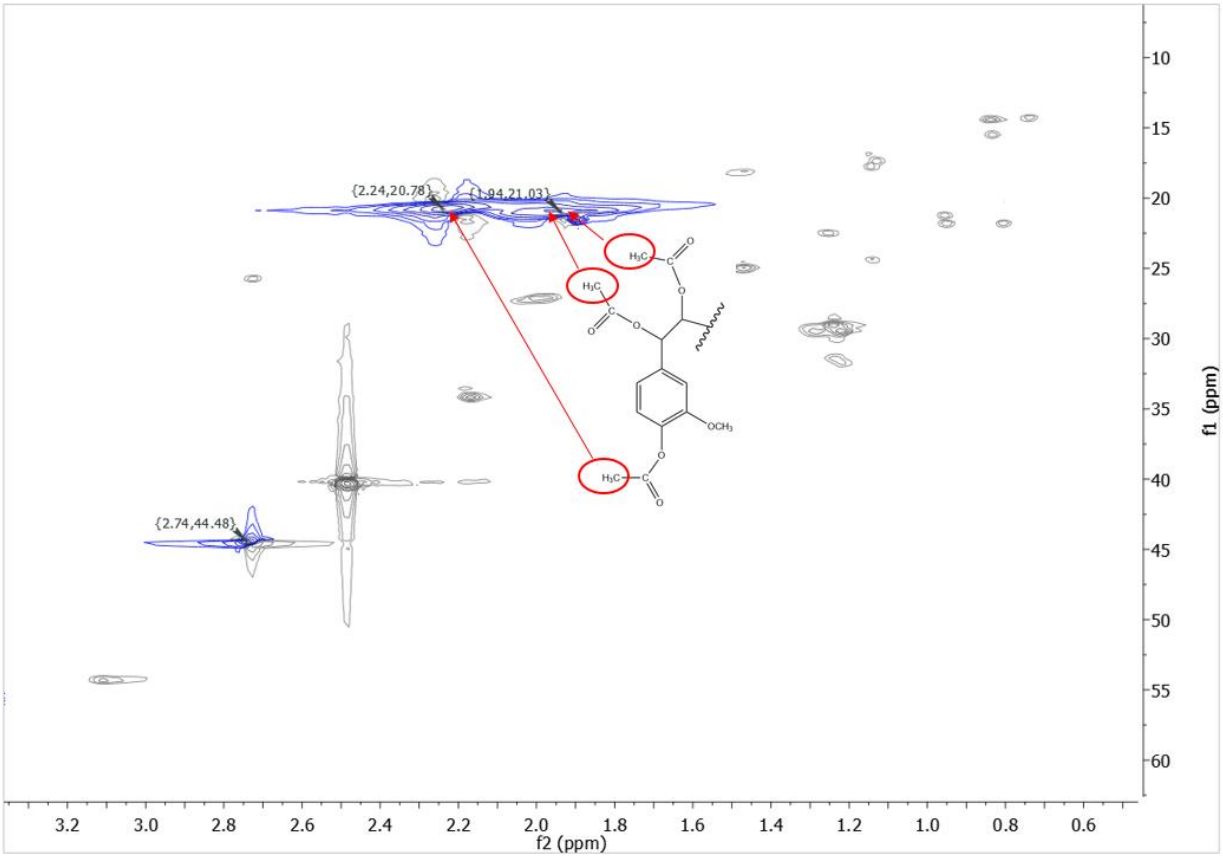

Figure 4.2. HSQC characterization of acetylated phenolic and aliphatic hydroxyl groups with an acetylated guaicyl unit model.

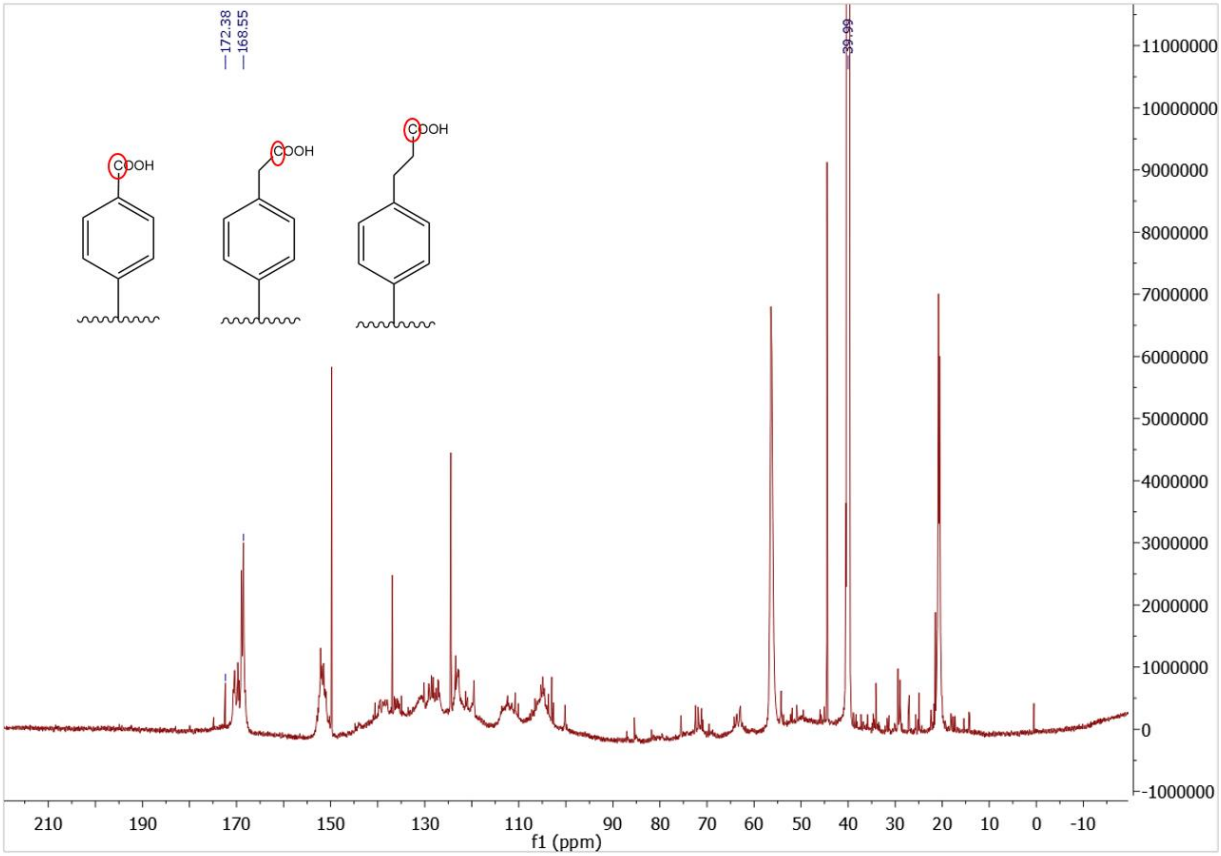

Figure 4.3. Characterization of carboxyl groups in acetylated Kraft lignin sample with ^{13}C NMR.

4.3.2. Langmuir adsorption model

The impact of environmental pH on the adsorption capacity was observed as shown in Figure 4.4. This is because the pH controls the deprotonation step of the ion-exchanging functional groups which generates negatively charged functional groups for ionic bonding with heavy metal cations. In this case, the deprotonation step should be prior to the adsorption step. The Langmuir adsorption model suggests the uniformity of the adsorbent surface, which leads to the mechanisms shown as Eqns (ad) and (ae),

$$\sigma \overset{K_H}{\leftrightarrow} \sigma^- + H^+ \quad \text{(ad)}$$

$$\sigma^- + M^{2+} \overset{K}{\leftrightarrow} \sigma \bullet M^+ \quad \text{(ae)}$$

where σ is the ion-exchanging active sites on the lignin surface, M stands for the heavy metal ions in the solution, $\sigma \cdot M^+$ stands for the adsorbed heavy metal ions. According to the mechanisms, the overall heavy metal balance can be written as Eqn (af),

$$[M^{2+}]_0 = [M^{2+}] + [\sigma \cdot M^+] \quad \text{(af)}$$

where at equilibrium states, the adsorbed heavy metal ions can be written as,

$$[\sigma \cdot M^+] = KK_H[\sigma]_0[M^{2+}]/(K_H + [H^+] + KK_H[M^{2+}]) \quad \text{(ag)}$$

The heavy metal concentration at equilibrium can be obtained combining Eqns (f) and (g), where $[\sigma]_0$ stands for the overall amount of active sites on the lignin surface. One can tell that at certain temperature, the equilibrium metal ion concentration is only related to the environmental pH.

Pb(II) adsorption data were obtained for the simulation with Langmuir adsorption model. The results were shown in Figure 4.4 that significant deviations from the experimental data were observed. Such deviation results from the inappropriate assumption of Kraft lignin surface as an ideal surface with a single type of active site. However, two types of ion-exchanging functional groups, PhOH and –COOH, have been characterized by NMR and their interaction with heavy metal ions can be different. The secondary decrease of the Pb(II) concentration with the increase of pH also suggested the existence of two ion-exchanging functional groups with two distinct deprotonation processes. Such trend cannot be simulated with Langmuir adsorption model.

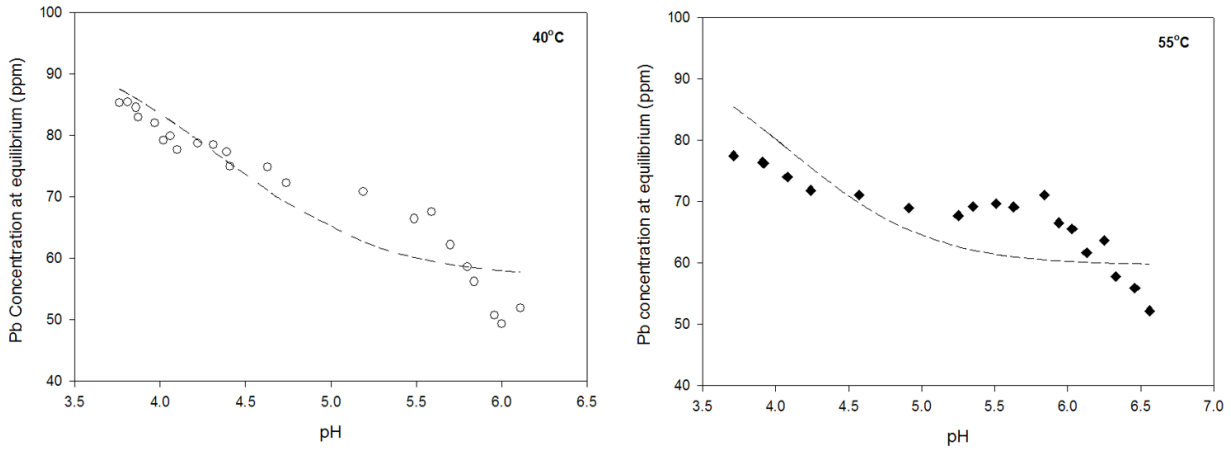

Figure 4.4. Simulation of Pb(II) adsorption experimental data performed at 40°C and 55°C with Langmuir adsorption model derived as Eqns (ac) and (ad). The parameters were given in Table 4.1.

Table 4.1. Simulation parameters for Langmuir adsorption model. σ_0 is the overall amount active site which is consistent at different temperatures.

Temperature	40°C	55°C
K (mM^{-1})	108.70	31.96
K_H (mM)	0.0011	0.0058
σ_0 (mM)	0.20	

4.3.3. Cooperative adsorption on Kraft lignin

4.3.3.1. Cooperative adsorption model

The complex nature of lignin surface lies in the existence of multiple functional groups. It was considered that the deviation from the simple Langmuir isotherm is contributed by two parts. First is the different interactive energies among functional groups. Second is the affinity change on the

secondary binding due to the prior bound. Since the hydroxide complexes of Pb(II), Cd(II), and Ni(II) are formed at pH above 8.0 according to previous studies [10-11], the heavy metal cations are considered to be only existed in their bivalent cation forms under our pH range. Based on the mechanism, the bivalent metal ions adsorption at equilibrium can be characterized by two possibilities: 1) only one positive charge is neutralized by one ion-exchange groups; 2) two positive charges are neutralized either through ion-exchanging or complexing, which leads to overall eight binding states.

When a heavy metal cation approaches the lignin surface, it will first interact with the nearest functional groups and get adsorbed. A single functional group is considered as an active site will be saturated by one heavy metal cation. An active site on the lignin surface can further be classified based on the nature of the surface: PhOH groups (σ_1), –COOH groups (σ_2), and electrophilic groups (σ_3). A bivalent heavy metal cation can either be captured by one or two functional group. Similar mechanisms has been reported by Ali et al. in the study of Cu(II) adsorption onto peanut hull [244]. To simplify the mathematical model later, we considered when a heavy metal cation is complexed with electrophilic groups, there will not be further adsorption to occur. All schemes of binding are shown in Figure 4.5.

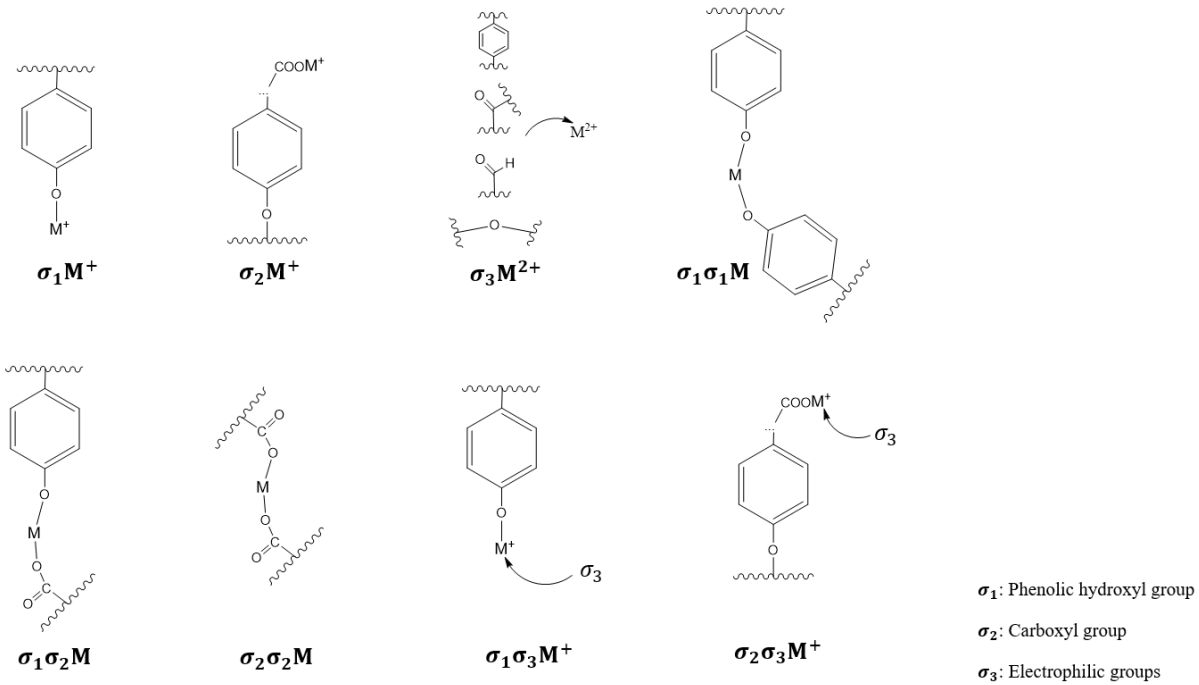

Figure 4.5. The eight metal ion adsorption states on Kraft lignin surface. Denotations 1 is used for PhOH groups, 2 for –COOH groups, 3 for electrophilic groups including aldehyde group, acetone group, ether bond, and aromatic ring. An active site is defined as a single functional groups. *p*-hydroxyphenyl (H) unit was chosen for demonstration purpose.

In order to model the process from a mechanistic point of view, one needs to consider the deprotonation process, the different affinities between each active sites towards heavy metals, as well as the cooperativity among the sites. Figure 4.6a, Eqns (1-2) shows the deprotonation processes of the two ion-exchanging sites. In the mechanism, $K_{\mathrm{H},1}$ stands for the equilibrium constant for PhOH deprotonation, while $K_{\mathrm{H},2}$ is the equilibrium constant for –COOH deprotonation. The followed adsorption processes are shown in Figure 4.6b and 4.6c, Eqns (3-11), where K_1, K_2 and K_3 are the binding affinity constants for phenolic hydroxyl groups, carboxyl groups and electrophilic groups, respectively. The parameters, c_1 and c_2, are cooperative coefficients from the PhOH and –COOH, respectively.

a.

$$\sigma_1 \overset{K_{H,1}}{\longleftrightarrow} \sigma_1^- + H^+ \quad (1)$$

$$\sigma_2 \overset{K_{H,2}}{\longleftrightarrow} \sigma_2^- + H^+ \quad (2)$$

b.

$$\sigma_1^- + M^{2+} \overset{K_1}{\longleftrightarrow} \sigma_1 M^+ \quad (3)$$

$$\sigma_2^- + M^{2+} \overset{K_2}{\longleftrightarrow} \sigma_2 M^+ \quad (4)$$

$$\sigma_3 + M^{2+} \overset{K_3}{\longleftrightarrow} \sigma_3 M^{2+} \quad (5)$$

c.

$$\sigma_1^- + \sigma_1 M^+ \overset{c_1 K_1}{\longleftrightarrow} \sigma_1 \sigma_1 M \quad (6)$$

$$\sigma_2^- + \sigma_1 M^+ \overset{c_1 K_2}{\longleftrightarrow} \sigma_1 \sigma_2 M \quad (7)$$

$$\sigma_3 + \sigma_1 M^+ \overset{c_1 K_3}{\longleftrightarrow} \sigma_1 \sigma_3 M^+ \quad (8)$$

$$\sigma_1^- + \sigma_2 M^+ \overset{c_2 K_1}{\longleftrightarrow} \sigma_1 \sigma_1 M \quad (9)$$

$$\sigma_2^- + \sigma_2 M^+ \overset{c_2 K_2}{\longleftrightarrow} \sigma_1 \sigma_2 M \quad (10)$$

$$\sigma_3 + \sigma_2 M^+ \overset{c_1 K_3}{\longleftrightarrow} \sigma_2 \sigma_3 M^+ \quad (11)$$

Figure 4.6. (a) The deprotonation processes for the two ion-exchanging sites. (b) Metal ion adsorption processes on the sites in 1-1 stoichiometry. (c) Secondary cooperative binding of the site-metal ion complex.

By following the mechanisms described in Figure 5. The overall lead balance can be written as Eqn (12),

$$[M^{2+}]_0 = [M^{2+}](1 + \sum_{i=1}^{2} \frac{K_{\mathrm{H,i}} K_{\mathrm{i}} [\sigma_{\mathrm{i}}]}{[H^+]} + K_3[\sigma_3] + \sum_{i=1,j=1}^{2,2} \frac{c_{\mathrm{i}} K_{\mathrm{H,i}} K_{\mathrm{H,j}} K_{\mathrm{i}} K_{\mathrm{j}} [\sigma_{\mathrm{i}}][\sigma_{\mathrm{j}}]}{[H^+]^2} + \sum_{i=1}^{2} \frac{c_{\mathrm{i}} K_{\mathrm{H,i}} K_{\mathrm{i}} [\sigma_{\mathrm{i}}][\sigma_3]}{[H^+]}) \quad (12)$$

Site balances of PhOH and –COOH groups leads to

$$[\sigma_{\mathrm{i}}]_0 = [\sigma_{\mathrm{i}}][1 + \frac{K_{\mathrm{H,i}}}{[H^+]} + \frac{K_{\mathrm{H,i}} K_{\mathrm{i}} [M^{2+}]}{[H^+]} + \frac{c_i K_{H,i}^2 K_i^2 [\sigma_{\mathrm{i}}][M^{2+}]}{[H^+]^2} + (c_1 + c_2) \frac{K_{\mathrm{H,1}} K_{\mathrm{H,2}} K_1 K_2 [\sigma_2][M^{2+}]}{[H^+]^2} + \frac{c_i K_{\mathrm{H,i}} K_{\mathrm{i}} K_3 [\sigma_3][M^{2+}]}{[H^+]}] \quad (13)$$

Site balances of electrophilic groups leads to

$$[\sigma_3]_0 = [\sigma_3](1 + K_3[M^{2+}] + \frac{c_1 K_{\mathrm{H,1}} K_1 K_3 [\sigma_1][M^{2+}]}{[H^+]} + \frac{c_2 K_{\mathrm{H,2}} K_2 K_3 [\sigma_2][M^{2+}]}{[H^+]}) \quad (14)$$

Combining Eqns (12), (13) and (14), one can obtain the metal cation concentration at equilibrium that only related to the pH and temperature of the environment.

4.3.3.2 Simulation

Figure 4.7 and 4.8 shows the effect of pH on the lignin adsorption capacity towards Pb(II), Cd(II) and Ni(II) at 25°C. Based on Eqns (1-2), pH can significant influence the deprotonation equilibrium of the functional group. With the increase of pH, more functional groups are deprotonated, which generates more active sites to interact with heavy metal cation through ionic binding. This mechanism was well expressed in the Pb(II) and Cd(II) adsorption that the equilibrium concentration decreased with the increased pH. However, Ni(II) adsorption was only slightly influenced mainly because of the weak cooperativity of –COOH group and weak interaction with PhOH groups (low c_2 and K_1 value). The cooperative coefficients, c_1 and c_2, larger than 1 indicate the positive cooperativity that there is a tendency for a secondary binding to reach an electron-neutral state. Also, it can be concluded that the Kraft lignin sample has a higher capacity in adsorbing Pb(II) than Cd(II) and Ni(II) based on the obtained K_1, K_2, and K_3 values. The experimental data were simulated with the model proposed in Eqns (12-14). The K_H and σ_0 values were fixed during the simulation due to the consistency of the temperature and the adsorbent used. The parameters in the model were given in Table 4.2.

The deprotonation equilibrium constants $K_{H,1} < K_{H,2}$ indicates an easier deprotonation process of carboxyl groups than phenolic hydroxyl groups in the Kraft lignin. The low values of $K_{H,1}$ and $K_{H,2}$ suggested that the release of active sites is likely to be controlled by the deprotonation process. The previous study has applied Mannich reaction to induce ammine groups to the lignin surface and found a substantial increase in the adsorption capacity [245]. Although the mechanism was not provided at that time, we can now speculate it is due to the alkalinity of amine groups that favors the deprotonation process. The binding affinity constants indicate a stronger interaction of heavy metal cations with PhOH groups than -COOH groups. Weak interactions between heavy metal cations and electrophilic groups (low K_3 values) were also observed.

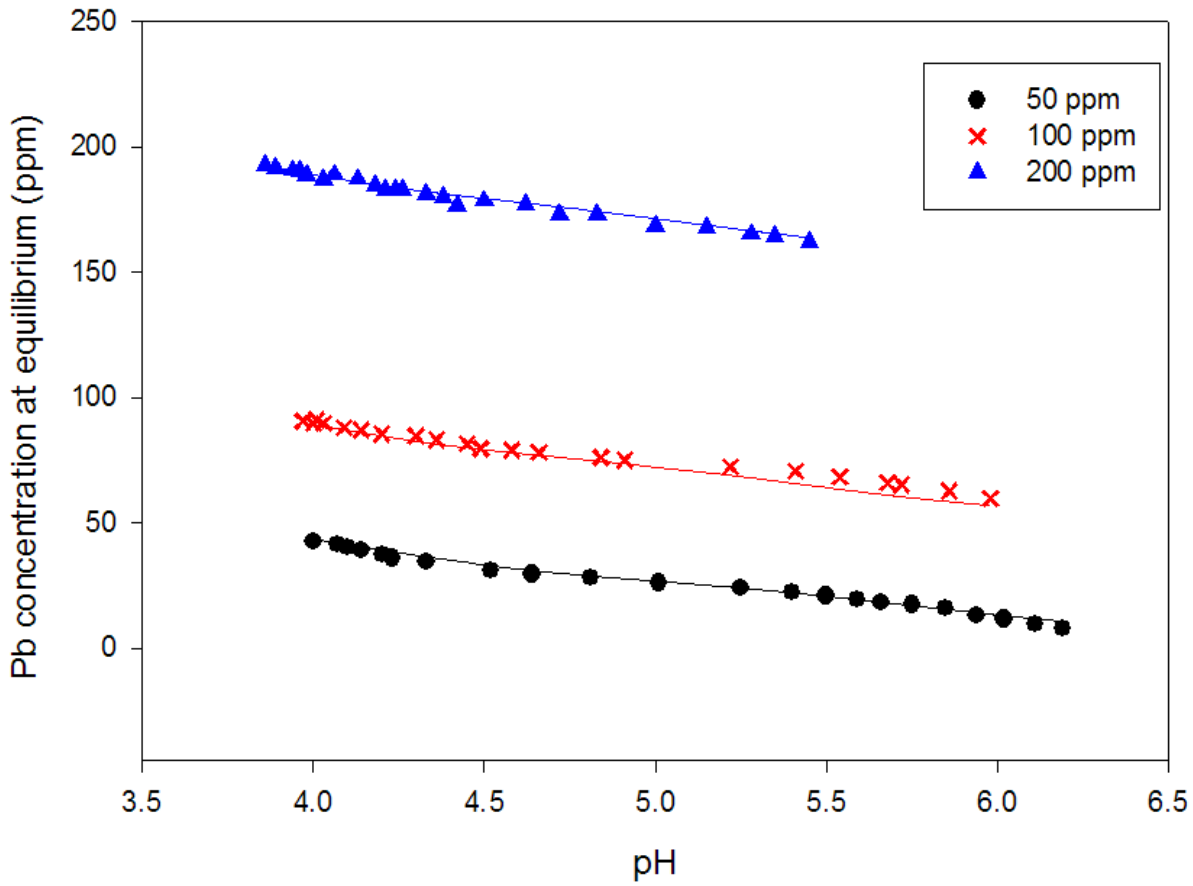

Figure 4.7. The equilibrium Pb(II) concentration measured after adsorption for 24 hours at 25°C. Three groups with different initial Pb(II) concentration were investigated at 50 ppm (●), 100 ppm (×) and 200 ppm (▲). Solid lines are simulated by Eqns (12-14) with the parameters shown in Table 2. The experiment was duplicated with an average standard deviation at 0.81 ppm.

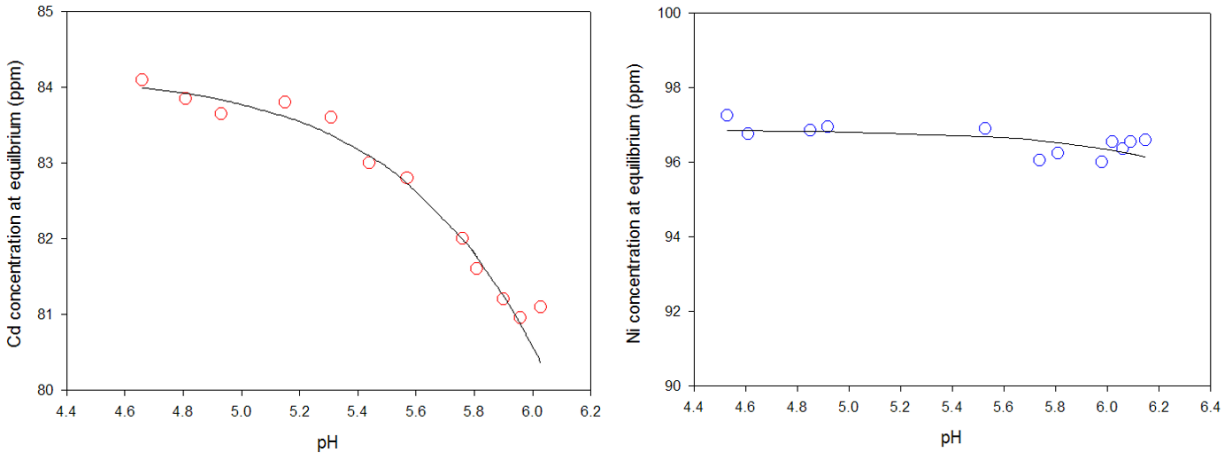

Figure 4.8. The equilibrium Cd(II) and Ni(II) concentration measured after adsorption for 24 hours at 25°C. Solid lines are simulated by Eqns (12-14) with the parameters shown in Table 2. The experiment was duplicated with an average standard deviation at 1.36 ppm.

Table 4.2. Parameter values of Eqns (12-14) at 25°C for Pb(II), Cd(II) and Ni(II). K_H and σ_0 stand for the deprotonation constants and the overall amount of each active sites, respectively, which are consistent for different adsorption species.

Species	Pb(II)	Cd(II)	Ni(II)
$K_1(mM^{-1})$	1.43×10^{13}	3.96×10^{11}	3.44
$K_2(mM^{-1})$	540	4.05×10^{-7}	1.63
$K_3(mM^{-1})$	0	1.03×10^{-2}	9.21×10^{-3}
c_1	4.05	1.25	1.02
c_2	1.27×10^{4}	1.15×10^{4}	1.12
$K_{H,1}(mM)$	4.85×10^{-16}		
$K_{H,2}(mM)$	2.50×10^{-6}		
$\sigma_{1,0}(mM)$	0.254		
$\sigma_{2,0}(mM)$	0.117		
$\sigma_{3,0}(mM)$	2.03		

The results showed that Kraft lignin can be a more effective adsorbent in removing Pb(II) than other heavy metal ions, with adsorption capacity close to 50 mg/g at elevated pH. This indicates a potential industrial application of Kraft lignin in the treatment of Pb(II) contaminated wastewater. In this case, the adsorption of Pb(II) was further investigated at two other different temperatures at 40°C and 55°C as shown in Figure 4.9. The data were modeled with Eqns (12-14). The deprotonation and binding affinity constants at different temperatures were restricted with Van't Hoff equation as Eqn (15).

$$\frac{d\ln K_{eq}}{dT} = \frac{\Delta H^{\ominus}}{RT^2} \tag{15}$$

Corporative coefficients were treated as constants over temperatures. A significant improvement of the agreement was achieved compared to the Langmuir adsorption model. Comparing binding affinity constants at 25°C, 40°C and 55°C, the changes in the deprotonation constants are more significant than the binding affinity constants, suggesting temperature will affect more on the deprotonation steps.

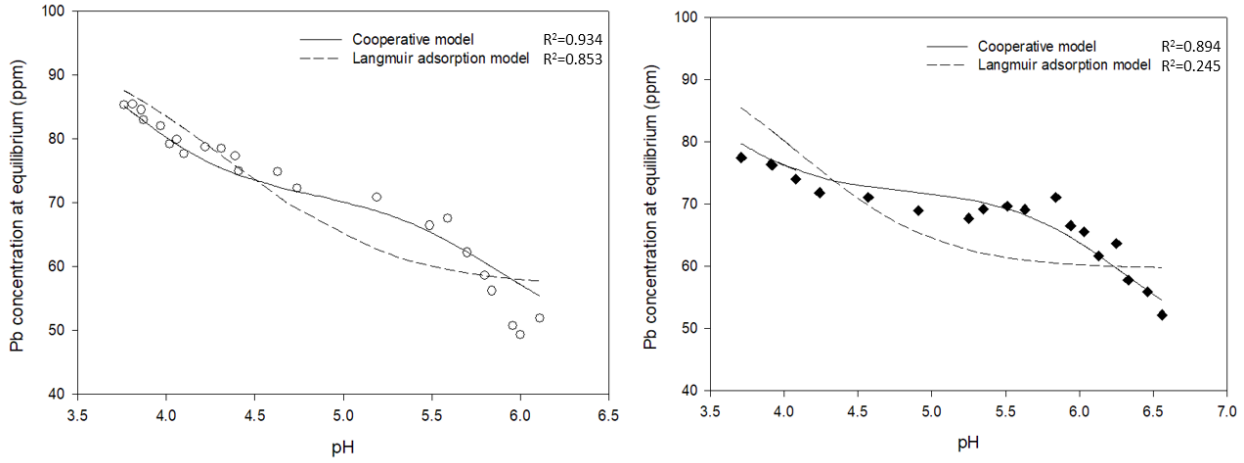

Figure 4.9. The equilibrium Pb(II) concentration measured after adsorption for 24 hours at 40°C (○) and 55°C (♦). Solid lines were fitted with Eqns (12-14) with the parameters shown in Table 4.3. The experiment was duplicated with an average standard deviation at 2.4 ppm.

Table 4.3. Parameter values of Eqns (12-14) at 40°C, and 55°C. σ_0 remains consistent with what obtained in Table 4.2.

Temperature	40°C	55°C	ΔH (kJ/mol)
$K_{H,1}$(mM)	1.80×10^{-16}	7.23×10^{-17}	-51.1
$K_{H,2}$(mM)	1.02×10^{-5}	3.63×10^{-5}	72.5
K_1(mM^{-1})	1.42×10^{13}	1.42×10^{13}	-0.18
K_2(mM^{-1})	536	532	-0.42
K_3(mM^{-1})	0	0	-

The adsorption isotherm plot of Pb(II) adsorption at 25°C is given in Figure 4.10. The surface saturation is calculated based on Eqn (16) and (17) and the parameters from Table 4.2.

$$\theta_A = \frac{([\sigma_{1,0}]-[\sigma_1]-[\sigma_1^-])+([\sigma_{2,0}]-[\sigma_2]-[\sigma_2^-])}{[\sigma_{1,0}]+[\sigma_{2,0}]} \quad (16)$$

$$q = \sum_{i=1}^{3}[\sigma_i M] + \sum_{i=1,j=1}^{2,3}[\sigma_i \sigma_j M] \quad (17)$$

One can further tell how pH impacts on the adsorption capacity. The isotherm indicates that our lignin sample can be close to saturation (θ_A=0.971) at neutral pH at low Pb(II) equilibrium level (5 ppm). This also explains why we did not observe much differences in the adsorbed Pb(II) amount at closed to neutral pH in our experiment with different initial Pb(II) concentrations. The shape of the isotherm curves are very similar to the Langmuir isotherm. That is why previous

studies managed to applied Langmuir isotherm to a single experimental condition with satisfactory agreement, when the pH and temperature effects were not further investigated.

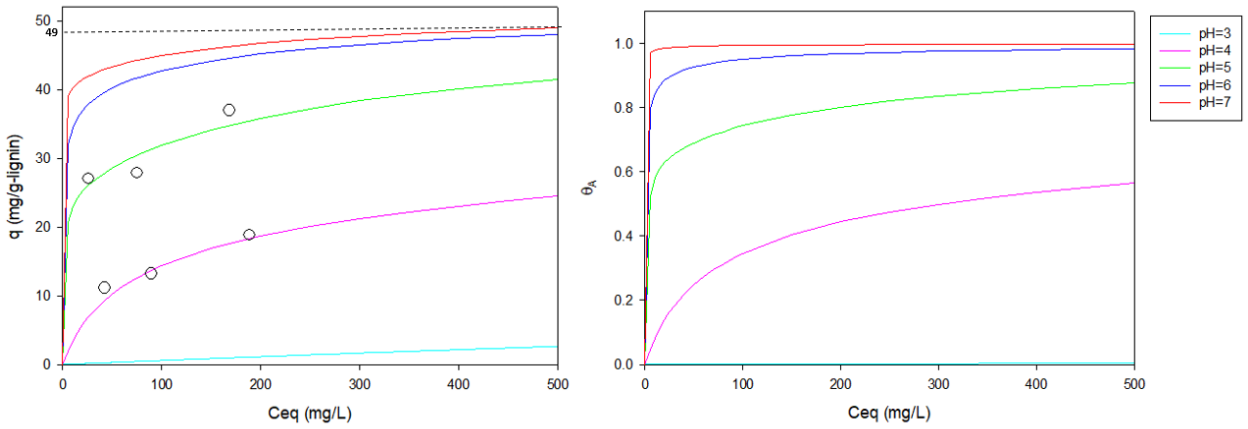

Figure 4.10. Pb(II) adsorption isotherm plot at 25°C at varying pH. The curves are obtained based on Eqn (12-14,16) and Table 4.2. The adsorbed amount still increases when saturation is reached due to the reformation between the "1-1" and "1-2" binding states. Data points are experimental values at integral pHs.

4.4. Conclusions

A surface characterization of Kraft lignin found the existence of multiple functional groups in the adsorption process including phenolic hydroxyl groups, carboxyl groups, and electrophilic groups. Due to the different interaction between functional groups and adsorbates, and the cooperativity among functional groups, deviations from the Langmuir adsorption model were observed. A cooperative adsorption theory describing a single adsorbate interacting with multiple sites was developed. Kraft lignin showed a higher adsorption capacity of Pb(II) than Cd(II) and Ni(II). The positive cooperativity or stronger affinity for the neutralizing the second electron vacancy was observed indicating the tendency for the system to reach an electron-neutral state. The low values of $K_{H,1}$ and $K_{H,2}$ (deprotonation equilibrium constants for PhOH and –COOH)

suggested the release of ion-exchanging sites was controlled by the environmental pH. Change of temperature affects more on the deprotonation step than the binding step. The developed 1-n cooperative theory can explain the heavy metal ion interactions with lignin very well. The new theory also has the potential to be applied to other multivalent interactions including adsorption, flocculation, chelation, and filtration.

Chapter 5
Conclusions

Klason lignin isolated from *paulownia* wood powder and Kraft lignin were evaluated as heavy metal adsorbents. In this study, a review of the lignin origin and structure was first given, which painted a picture about what lignin is and why it can adsorb heavy metal cations. The lignin isolation and recovery methods was then introduced and later applied to this study. The pollution sources of heavy metals and their heavy effects were then introduced. Most heavy metals including Pb, Cu, Ni, Co, Cd, Cr, Hg, Zn etc. are accumulative in biological systems and toxic to human beings. The current heavy metal pollution status was then reviewed both in the developed areas and developing areas. It was concluded that the late execution of environmental policy and the high density of traditional industries are the two major reasons resulting in the intensive heavy metal pollution status in the developing areas. Several heavy metal treatment technologies such as chemical precipitation, flocculation, ion exchange chromatography, and bioremediation were introduced about their working mechanism with their pros and cons. Adsorption, as the technology employed in this study, was then introduced with Langmuir, BET, and cooperative adsorption theories. Previous studies of using lignin as heavy metal adsorbent was also reviewed with their findings. Some deficiencies of this area of research were also pointed out such as the lack of mechanistic study and study of lignin from different origins, which motivated the studies performed in this thesis.

To investigate how hot water treatment, a typical biorefinery process will impact on the lignin adsorption affinities, *Paulownia elongata* Klason lignin was tested for its heavy metal adsorption affinities with Pb(II), Cu(II) and Cd(II). Hot water treatment was conducted on the lignin with both water and dilute acetic acid solution. Samples with both increased and decreased adsorption capacity were observed after the treatment, while samples with long duration of treatment encountered a substantial loss in the adsorption ability. Depolymerization and condensation lignin

reaction schemes under acidic environment were summarized and applied to explain the capacity changes. NMR analysis was performed to quantify the functional groups in the lignin samples. Changes in the amount of functional groups were found in the samples after pretreatment. The results suggested that hot water treatment can either increase or decrease the adsorption affinity of lignin depending on the treatment severity. Lignin byproducts after treated under acidic and high temperature environment with long duration is no longer suggested to be used as a heavy metal adsorbent.

The adsorption of heavy metal cations, Pb(II), Cd(II) and Ni(II), on Kraft lignin was then evaluated mechanistically in this study. The Pb(II) adsorption affinity of Kraft lignin was found to follow an "S" dependency on the environmental pH, indicating a non-ideal adsorption process. NMR characterization revealed two ion-exchanging functional groups as phenolic hydroxyl and carboxyl groups in the Kraft lignin structure. Other electrophilic groups such as aldehyde group, acetone group, ether bond, and aromatic ring are also considered as functional groups which can complex with heavy metal cations. Due to the existence of multiple functional groups and their cooperative interactions with one adsorbate molecule, deviations were observed when applying the Langmuir adsorption model. "1-n cooperative adsorption theory" was developed to explain the surface interaction when an adsorbate can bind with multiple active sites. A cooperative coefficient was introduced representing the cooperativity among active sites in capturing an adsorbate. The simulation achieved significant improvement comparing to the Langmuir model. The cooperativity was discovered in the system with the tendency to reach an electron-neutral state. The developed theory provides guidelines for Kraft lignin applications as adsorbent, as well as for complicated multi-valent surface interactions in processes such as adsorption, flocculation, chelation, and filtration.

Combined the results of the study, couple directions that can be developed further was proposed. Lignin modification through depolymerization, nanocrystallization, amination, and sulfonation can potentially enhance its adsorption capacity. A kinetic and mass transfer study will be necessary to develop the process from batch to continuous. The effect of pH on the lignin adsorption capacity indicates the process can be easily reversed. A desorption study will be preferred prove lignin as a “green” adsorbent with recycling capability.

Chapter 6
Future Studies

Comparing the adsorption affinities of Klason lignin and Kraft lignin, we observed a substantial differences between the two lignin samples. This can be explained by the lignin depolymerization schemes during the Kraft pulping and bleaching process. Also based on the results obtained in Figure 3.2 and 3.3, one can conclude that deploymerization favors the lignin as an adsorbent. In this case, it is proposed that lignin chemical modification through alkaline or oxidative depolymerization with the potential to enhance its adsorption capacity. Other modifications such as lignin nanocrystallization, amination, and sulfonation are also expected to be able to functionalize lignin as an adsorbent.

Based on the research on the pH effect on the adsorption process. It is suggested that a pH control at neutral level is desired. The acceptable adsorption capacity (49 mg Pb(II)/g-Kraft lignin based on the isotherm at pH=7) suggested a potential future application of Kraft lignin as a Pb(II) adsorbent. The huge capacity differences at varying pH levels (Figure 2.10) suggested an easy desorption process through pH adjustment. A desorption study is necessary to be continued in this project to achieve heavy metal recycling and adsorbent regeneration.

From the reaction engineering point of view, the process now has been studied in a batch system. A future development to a continuous PFR reactor with kinetics and mass transfer studies will be desired. The novel “1-n cooperative adsorption theory” needs a further development to obtain a more universal mathematical form. The theory itself also requires a further dissemination by applying to other multivalent processes.

References

1. Järup L, Hazards of heavy metal contamination. Br Med Bull 68:167-182 (2003).

2. Ngah WW, Hanafiah MAKM, Removal of heavy metal ions from wastewater by chemically modified plant wastes as adsorbents: a review. Bioresour Technol 99:3935-3948 (2008).

3. Fairbrother A, Wenstel R, Sappington K, Wood W, Framework for metals risk assessment. Ecotox Environ Saf 68:145-227 (2007).

4. Sytar O, Kumar A, Latowski D, Kuczynska P, Strzałka K, Prasad MNV, Heavy metal-induced oxidative damage, defense reactions, and detoxification mechanisms in plants. Acta Physiol Plant 35:985-999 (2013).

5. U.S. EPA, 2017. National Primary Drinking Water Regulations.

6. Gao Z, Su C, Treatment of tannery wastewater. Beijing: Chemical Engineering Publisher; 2001.

7. Ucun H, Bayhana YK, Kaya Y, Cakici A, Algur OF, Biosorption of lead (II) from aqueous solution by cone biomass of Pinus sylvestris. Desalination 154:233-238 (2003).

8. Khan S, Ahmad I, Shah MT, Rehman S, Khaliq A, Use of constructed wetland for the removal of heavy metals from industrial wastewater. J Environ Manage 90:3451-3457 (2009).

9. Liu G, Yu Y, Hou J, Xue W, Liu X, Liu Y, Wang W, Alsaedi A, Hayat T, Liu Z, An ecological risk assessment of heavy metal pollution of the agricultural ecosystem near a lead-acid battery factory. Ecol Indic 47:210-218 (2014).

10. Sitko, R.; Turek, E.; Zawisza, B.; Malicka, E.; Talik, E.; Heimann, J.; Gagor, A.; Feist, B.; Wrzalik, R. Adsorption of divalent metal ions from aqueous solutions using graphene oxide. Dalton Trans. 2013, 42, 5682-5689.

11. U.S. EPA. Summary Report: Control and Treatment Technology for the Metal Finishing Industry: Sulfide Precipitation; 1980.

12. Fu, F.; Wang, Q. Removal of heavy metal ions from wastewaters: a review. J. Environ. Manage. 2011, 92, 407-418.

13. Ahmed MJK, Ahmaruzzaman M, A review on potential usage of industrial waste materials for binding heavy metal ions from aqueous solutions. J Water Process Eng 10:39-47 (2016).

14. Gosselink RJA, De Jong E, Guran B, Abächerli A, Co-ordination network for lignin—standardisation, production and applications adapted to market requirements (EUROLIGNIN). Ind Crops Prod 20:121-129 (2004).

15. Guo X, Zhang S, Shan XQ, Adsorption of metal ions on lignin. J Hazard Mater 151:134-142 (2008).

16. Celik A, Demirbaş A, Removal of heavy metal ions from aqueous solutions via adsorption onto modified lignin from pulping wastes. Energy Sources 27:1167-1177 (2005).

17. Mohan D, Pittman CU, Steele PH, Single, binary and multi-component adsorption of copper and cadmium from aqueous solutions on Kraft lignin—a biosorbent. J Colloid Interface Sci 297:489-504 (2006).

18. Ximenes E, Farinas CS, Kim Y, Ladisch MR, Hydrothermal Pretreatment of Lignocellulosic Biomass for Bioethanol Production, in Production of Bioethanol and High Added-Value Compounds of Second and Third Generation Biomass, ed by Ruiz HA, Trajano HL and Thomsen MH, Springer International Publishing, Switzerland, pp 181-205 (2017).

19. Torres AI, Ashrat MT, Chatuverdi T, Schmidt JE, Stephanopoulos G, Process Modeling and Economic Assessment Within Framework of Biorefinery Processes, in Production of Bioethanol

and High Added-Value Compounds of Second and Third Generation Biomass, ed by Ruiz HA, Trajano HL and Thomsen MH, Springer International Publishing, Switzerland, pp 207-236 (2017).

20. Balan V, Current challenges in commercially producing biofuels from lignocellulosic biomass. ISRN Biotechnol 2014, 31 pages (2014).

21. Sjöström, E., 1993. Wood chemistry: fundamentals and applications. Gulf Professional Publishing.

22. Adler, E. (1977). Lignin chemistry—past, present and future. *Wood science and technology*, *11*(3), 169-218.

23. Baucher, M., Monties, B., Montagu, M. V., & Boerjan, W. (1998). Biosynthesis and genetic engineering of lignin. *Critical reviews in plant sciences*, *17*(2), 125-197.

24. Calvo-Flores, F. G., & Dobado, J. A. (2015). *Lignin and lignans as renewable raw materials: chemistry, technology and applications*. John Wiley & Sons.

25. Campbell, M. M., Sainsbury, M., & Searle, P. A. (1993). The biosynthesis and synthesis of shikimic acid, chorismic acid, and related compounds. *Synthesis*, *1993*(02), 179-193.

26. Lewis, N. G., Davin, L. B., & Sarkanen, S. (1998). Lignin and lignan biosynthesis: distinctions and reconciliations.

27. Pascual, M. B., El-Azaz, J., Fernando, N., Cañas, R. A., Avila, C., & Cánovas, F. M. (2016). Biosynthesis and metabolic fate of phenylalanine in conifers. Frontiers in Plant Science, 7.

28. Boerjan, W., Ralph, J., & Baucher, M. (2003). Lignin biosynthesis. *Annual review of plant biology*, *54*(1), 519-546.

29. Steeves, V., Förster, H., Pommer, U., & Savidge, R. (2001). Coniferyl alcohol metabolism in conifers—I. Glucosidic turnover of cinnamyl aldehydes by UDPG: coniferyl alcohol glucosyltransferase from pine cambium. *Phytochemistry*, *57*(7), 1085-1093.

30. Lim, E. K., Li, Y., Parr, A., Jackson, R., Ashford, D. A., & Bowles, D. J. (2001). Identification of glucosyltransferase genes involved in sinapate metabolism and lignin synthesis in Arabidopsis. Journal of Biological Chemistry, 276(6), 4344-4349.

31. Wong, C. M., Wong, K. H., & Chen, X. D. (2008). Glucose oxidase: natural occurrence, function, properties and industrial applications. Applied microbiology and biotechnology, 78(6), 927-938.

32. Carpenter, S., Merkler, D., Miller, D., Mehta, N., & Consalvo, A. (2007). U.S. Patent Application No. 11/654,211.

33. Christensen, J. H., Baucher, M., O'Connell, A., Van Montagu, M., & Boerjan, W. (2000). Control of lignin biosynthesis. In Molecular biology of woody plants (pp. 227-267). Springer Netherlands.

34. Gross, G. G. (2008). From lignins to tannins: Forty years of enzyme studies on the biosynthesis of phenolic compounds. *Phytochemistry*, *69*(18), 3018-3031.

35. Holmgren, A., Brunow, G., Henriksson, G., Zhang, L., & Ralph, J. (2006). Non-enzymatic reduction of quinone methides during oxidative coupling of monolignols: implications for the origin of benzyl structures in lignins. Organic & biomolecular chemistry, 4(18), 3456-3461.

36. Davin, L. B., & Lewis, N. G. (2000). Dirigent proteins and dirigent sites explain the mystery of specificity of radical precursor coupling in lignan and lignin biosynthesis. *Plant Physiology*, *123*(2), 453-462.

37. Umezawa, T. (2003). Diversity in lignan biosynthesis. *Phytochemistry Reviews*, *2*(3), 371-390.

38. Rodrigues Pinto, P. C., Borges da Silva, E. A., & Rodrigues, A. E. (2010). Insights into oxidative conversion of lignin to high-added-value phenolic aldehydes. *Industrial & Engineering Chemistry Research*, *50*(2), 741-748.

39. Lange, H., Decina, S., & Crestini, C. (2013). Oxidative upgrade of lignin–Recent routes reviewed. European Polymer Journal, 49(6), 1151-1173.

40. Rubin, E.M., 2008. Genomics of cellulosic biofuels. Nature, 454(7206), pp.841-845.

41. Pettersen, R.C., 1984. The chemical composition of wood. The chemistry of solid wood, 207, pp.57-126.

42. Christensen, T., 1982. A mathematical model of the kraft pulping process.

43. Sixta, H. and Schild, G., 2009. A new generation kraft process. Lenzinger Berichte, 87(1), pp.26-37.

44. Gierer, J., 1980. Chemical aspects of kraft pulping. Wood Science and Technology, 14(4), pp.241-266.

45. Gierer, J., 1985. Chemistry of delignification. Wood Science and technology, 19(4), pp.289-312.

46. Chakar, F.S. and Ragauskas, A.J., 2004. Review of current and future softwood kraft lignin process chemistry. Industrial Crops and Products, 20(2), pp.131-141.

47. van Hazendonk, J. M., Reinerik, E. J., de Waard, P., & van Dam, J. E. (1996). Structural analysis of acetylated hemicellulose polysaccharides from fibre flax (Linum usitatissimum L.). *Carbohydrate Research*, *291*, 141-154.

48. Pielhop, T., Larrazábal, G. O., & von Rohr, P. R. (2016). Autohydrolysis pretreatment of softwood–enhancement by phenolic additives and the effects of other compounds. *Green Chemistry*, *18*(19), 5239-5247.

49. Mosier, N., Wyman, C., Dale, B., Elander, R., Lee, Y. Y., Holtzapple, M., & Ladisch, M. (2005). Features of promising technologies for pretreatment of lignocellulosic biomass. *Bioresource technology*, *96*(6), 673-686.

50. Zhou, C. H., Xia, X., Lin, C. X., Tong, D. S., & Beltramini, J. (2011). Catalytic conversion of lignocellulosic biomass to fine chemicals and fuels. *Chemical Society Reviews*, *40*(11), 5588-5617.

51. Meshgini, M., & Sarkanen, K. V. (1989). Synthesis and kinetics of acid-catalyzed hydrolysis of some α-aryl ether lignin model compounds.

52. Overend, W. G., Rees, C. W., & Sequeira, J. S. (1962). 675. Reactions at position 1 of carbohydrates. Part III. The acid-catalysed hydrolysis of glycosides. *Journal of the Chemical Society (Resumed)*, 3429-3440.

53. Li J, Henriksson G, Gellerstedt G, Lignin depolymerization/repolymerization and its critical role for delignification of aspen wood by steam explosion. Bioresour Technol 98:3061-3068 (2007).

54. Borrega, M., Nieminen, K., & Sixta, H. (2011). Effects of hot water extraction in a batch reactor on the delignification of birch wood. *BioResources*, *6*(2), 1890-1903.

55. Toledano, A., Serrano, L., & Labidi, J. (2014). Improving base catalyzed lignin depolymerization by avoiding lignin repolymerization. *Fuel*, *116*, 617-624.

56. Shimada K, Hosoya S, Ikeda T, Condensation reactions of softwood and hardwood lignin model compounds under organic acid cooking conditions. J Wood Chem Technol 17:57-72 (1997).

57. Hu, F., Jung, S., & Ragauskas, A. (2012). Pseudo-lignin formation and its impact on enzymatic hydrolysis. *Bioresource technology*, *117*, 7-12.

58. Sannigrahi, P., Kim, D. H., Jung, S., & Ragauskas, A. (2011). Pseudo-lignin and pretreatment chemistry. *Energy & Environmental Science*, *4*(4), 1306-1310.

59. Alizadeh, H., Teymouri, F., Gilbert, T. I., & Dale, B. E. (2005). Pretreatment of switchgrass by ammonia fiber explosion (AFEX). *Applied biochemistry and biotechnology*, *124*(1), 1133-1141.

60. Teymouri, F., Laureano-Pérez, L., Alizadeh, H., & Dale, B. E. (2004). Ammonia fiber explosion treatment of corn stover. In *Proceedings of the Twenty-Fifth Symposium on Biotechnology for Fuels and Chemicals Held May 4–7, 2003, in Breckenridge, CO* (pp. 951-963). Humana Press.

61. Jin, Y., Jameel, H., Chang, H. M., & Phillips, R. (2010). Green liquor pretreatment of mixed hardwood for ethanol production in a repurposed kraft pulp mill. *Journal of wood chemistry and technology*, *30*(1), 86-104.

62. Isci, A., Himmelsbach, J. N., Pometto, A. L., Raman, D. R., & Anex, R. P. (2008). Aqueous ammonia soaking of switchgrass followed by simultaneous saccharification and fermentation. *Applied biochemistry and biotechnology*, *144*(1), 69-77.

63. Kim, T. H., & Lee, Y. Y. (2005). Pretreatment of corn stover by soaking in aqueous ammonia. In *Twenty-Sixth Symposium on Biotechnology for Fuels and Chemicals* (pp. 1119-1131). Humana Press.

64. Kaar, W. E., & Holtzapple, M. T. (2000). Using lime pretreatment to facilitate the enzymic hydrolysis of corn stover. *Biomass and Bioenergy*, *18*(3), 189-199.

65. Ballesteros, I., Negro, M. J., Oliva, J. M., Cabañas, A., Manzanares, P., & Ballesteros, M. (2006). Ethanol production from steam-explosion pretreated wheat straw. In *Twenty-seventh symposium on biotechnology for fuels and chemicals* (pp. 496-508). Humana Press.

66. Okano, K., Kitagawa, M., Sasaki, Y., & Watanabe, T. (2005). Conversion of Japanese red cedar (Cryptomeria japonica) into a feed for ruminants by white-rot basidiomycetes. *Animal feed science and technology*, *120*(3), 235-243.

67. Akin, D. E., Rigsby, L. L., Sethuraman, A., Morrison, W. H., Gamble, G. R., & Eriksson, K. E. (1995). Alterations in structure, chemistry, and biodegradability of grass lignocellulose treated with the white rot fungi Ceriporiopsis subvermispora and Cyathus stercoreus. *Applied and environmental microbiology*, *61*(4), 1591-1598.

68. Wong, D. W. (2009). Structure and action mechanism of ligninolytic enzymes. *Applied biochemistry and biotechnology*, *157*(2), 174-209.

69. Tuor, U., Wariishi, H., Schoemaker, H. E., & Gold, M. H. (1992). Oxidation of phenolic arylglycerol beta-aryl ether lignin model compounds by manganese peroxidase from Phanerochaete chrysosporium: oxidative cleavage of an alpha-carbonyl model compound. *Biochemistry*, *31*(21), 4986-4995.

70. Bao, W., Fukushima, Y., Jensen, K. A., Moen, M. A., & Hammel, K. E. (1994). Oxidative degradation of non-phenolic lignin during lipid peroxidation by fungal manganese peroxidase. *FEBS letters*, *354*(3), 297-300.

71. Kawai, S., Umezawa, T., & Higuchi, T. (1988). Degradation mechanisms of phenolic β-1 lignin substructure model compounds by laccase of Coriolus versicolor. *Archives of Biochemistry and Biophysics*, *262*(1), 99-110.

72. Kawai, S., Nakagawa, M., & Ohashi, H. (2002). Degradation mechanisms of a nonphenolic β-O-4 lignin model dimer by Trametes versicolor laccase in the presence of 1-hydroxybenzotriazole. Enzyme and microbial technology, 30(4), 482-489.

73. García-Cubero, M. T., González-Benito, G., Indacoechea, I., Coca, M., & Bolado, S. (2009). Effect of ozonolysis pretreatment on enzymatic digestibility of wheat and rye straw. Bioresource Technology, 100(4), 1608-1613.

74. Travaini, R., Otero, M. D. M., Coca, M., Da-Silva, R., & Bolado, S. (2013). Sugarcane bagasse ozonolysis pretreatment: effect on enzymatic digestibility and inhibitory compound formation. Bioresource technology, 133, 332-339.

75. Meza, P. R., Felissia, F. E., & Area, M. C. (2011). Reduction of the recalcitrant COD of high yield pulp mills effluents by AOP. Part 1. Combination of ozone and activated sludge. BioResources, 6(2), 1053-1068.

76. Lotfi, S., Boffito, D. C., & Patience, G. S. (2016). Gas–solid conversion of lignin to carboxylic acids. Reaction Chemistry & Engineering, 1(4), 397-408.

77. Brauns, F.E., 1939. Native Lignin1 I. Its Isolation and Methylation. Journal of the American Chemical Society, 61(8), pp.2120-2127.

78. Björkman, A., 1956. Studies on finely divided wood. Part 1. Extraction of lignin with neutral solvents. Svensk papperstidning, 59(13), pp.477-485.

79. Effland, M.J., 1977. Modified procedure to determine acid-insoluble lignin in wood and pulp. Tappi;(United States), 60(10).

80. Naqvi, M., Yan, J. and Dahlquist, E., 2010. Black liquor gasification integrated in pulp and paper mills: A critical review. Bioresource technology,101(21), pp.8001-8015.

81. Barclay, L.R.C., Xi, F. and Norris, J.Q., 1997. Antioxidant properties of phenolic lignin model compounds. Journal of wood chemistry and technology, 17(1-2), pp.73-90.

82. Khan, M.A., Ashraf, S.M. and Malhotra, V.P., 2004. Development and characterization of a wood adhesive using bagasse lignin. International Journal of Adhesion and Adhesives, 24(6), pp.485-493.

83. Carrott, P.J.M. and Carrott, M.R., 2007. Lignin–from natural adsorbent to activated carbon: a review. Bioresource technology, 98(12), pp.2301-2312.

84. Janshekar, H., Brown, C. and Fiechter, A., 1981. Determination of biodegraded lignin by ultraviolet spectrophotometry. Analytica Chimica Acta, 130(1), pp.81-91.

85. Schöing AG, Johansson G. Absorptiometric determination of acid-soluble lignin in semi-chemical bisulfite pulps and in some woods and plants. Sven Papperstidn. 1965;68(18):607–613.

86. Kline, L.M., Hayes, D.G., Womac, A.R. and Labbe, N., 2010. Simplified determination of lignin content in hard and soft woods via UV-spectrophotometric analysis of biomass dissolved in ionic liquids. BioResources, 5(3), pp.1366-1383.

87. Aulin-Erdtman G, Sanden R. Spectrographic contributions to lignin chemistry. IX. Absorption properties of some 4-hydroxyphenyl, guaiacyl, and 4-hydroxy-3,5-dimethoxyphenyl type model compounds for hardwood lignins. Acta Chem Scand. 1968;22(4):1187–209.

88. Aulin-Erdtman G, Hegbom L. Spectrographic contributions to lignin chemistry. VII. The ultraviolet absorption and ionization δε-curves of some phenols. Sven Papperstidn.1957;60: 671–681.

89. Gadda L. Delignification of Wood Fibre Cell Wall During Alkaline Pulping Processes. Institute of Wood Chemistry and Pulp and Paper Technology; 1981.

90. Lin, S.Y. and Dence, C.W. eds., 2012. Methods in lignin chemistry. Springer Science & Business Media.

91. Hon, D.N.S. and Shiraishi, N., 2000. Wood and cellulosic chemistry, revised, and expanded. CRC Press.

92. Sarkanen, K.V. and Ludwig, C.H., 1971. Lignins: occurrence, formation, structure and reactions. Lignins: occurrence, formation, structure and reactions.

93. Lundquist, K. and Stern, K., 1989. Analysis of lignins by 1H NMR spectroscopy. Nordic Pulp & Paper Research Journal, 4(3), pp.210-213.

94. Gellerstedt, G. and Gierer, J., 1971. Reactions of lignin during acidic sulphite pulping. Svensk Papperstidn.

95. Nimz, H.H., Robert, D., Faix, O. and Nemr, M., 1981. Carbon-13 NMR spectra of lignins, 8. Structural differences between lignins of hardwoods, softwoods, grasses and compression wood. Holzforschung-International Journal of the Biology, Chemistry, Physics and Technology of Wood, 35(1), pp.16-26.

96. Ede, R.M. and Kilpelainen, I., 1995. Homo-and hetero-nuclear 2D NMR techniques: Umambiguous structural probes for non-cyclic benzyl aryl ethers in soluble lignin samples. Research on chemical intermediates, 21(3), pp.313-328.

97. Lundquist, K.N.U.T., 1980. NMR studies of lignins. 4. Investigation of spruce lignin by 1H NMR spectroscopy. Acta Chem. Scand. B, 34, pp.21-26.

98. Wen, J.L., Sun, S.L., Xue, B.L. and Sun, R.C., 2013. Recent advances in characterization of lignin polymer by solution-state nuclear magnetic resonance (NMR) methodology. Materials, 6(1), pp.359-391.

99. Järup, L., 2003. Hazards of heavy metal contamination. British medical bulletin, 68(1), pp.167-182.

100. Duruibe, J.O., Ogwuegbu, M.O.C. and Egwurugwu, J.N., 2007. Heavy metal pollution and human biotoxic effects. International Journal of Physical Sciences, 2(5), pp.112-118.

101. Peplow, D., 1999. Environmental impacts of mining in Eastern Washington. University of Washington Water Center.

102. Šćiban, M., Radetić, B., Kevrešan, Ž. and Klašnja, M., 2007. Adsorption of heavy metals from electroplating wastewater by wood sawdust. Bioresource Technology, 98(2), pp.402-409.

103. Arıca, M.Y., Kacar, Y. and Genç, Ö., 2001. Entrapment of white-rot fungus Trametes versicolor in Ca-alginate beads: preparation and biosorption kinetic analysis for cadmium removal from an aqueous solution. Bioresource technology, 80(2), pp.121-129.

104. Harrison, R., 2012. Lead pollution: causes and control. Springer Science & Business Media.

105. WHO. Inorganic Mercury. Environmental Health Criteria, vol. 118. Geneva: World Health Organization, 1991.

106. Schwartz, M.O., 2000. Cadmium in zinc deposits: economic geology of a polluting element. International Geology Review, 42(5), pp.445-469.

107. Doe, B.R. and Delevaux, M.H., 1972. Source of lead in southeast Missouri galena ores. Economic Geology, 67(4), pp.409-425.

108. Covelli, S., Faganeli, J., Horvat, M. and Brambati, A., 2001. Mercury contamination of coastal sediments as the result of long-term cinnabar mining activity (Gulf of Trieste, northern Adriatic sea). Applied Geochemistry, 16(5), pp.541-558.

109. Heyes, G.W. and Trahar, W.J., 1979. Oxidation-reduction effects in the flotation of chalcocite and cuprite. International Journal of Mineral Processing, 6(3), pp.229-252.

110. Davis, J.R. ed., 2001. Copper and copper alloys. ASM international.

111. Rice, N.M. and Strong, L.W., 1974. The leaching of lateritic nickel ores in hydrochloric acid. Canadian Metallurgical Quarterly, 13(3), pp.485-493.

112. Keim, W., 1990. Nickel: an element with wide application in industrial homogeneous catalysis. Angewandte Chemie International Edition, 29(3), pp.235-244.

113. Nordstrom, D.K., 2002. Worldwide occurrences of arsenic in ground water. Science, 296(5576), pp.2143-2145.

114. Yuehua, H., Guanzhou, Q., Jun, W. and Dianzuo, W., 2002. The effect of silver-bearing catalysts on bioleaching of chalcopyrite. Hydrometallurgy, 64(2), pp.81-88.

115. H. Needleman, Lead poisoning, Annu. Rev. Med. 55 (2004) 209-222.

116. Centers for Disease Control CDC, Preventing lead poisoning in young children--United States, MMWR, Morb. Mortal. Wkly. Rep. 34 (1985) 66.

117. Udedi, S.S., 2003. From guinea worm scourge to metal toxicity in Ebonyi State. Chem Nigeria New Millenn Unfold, 2, pp.13-14.

118. Lead, I.A.R.C., 1987. lead compounds: lead and inorganic lead compounds (Group 2B) and organolead compounds (Group 3). IARC Monogr Eval Carcinog Risk Hum Suppl, 7, pp.230-232.

119. Institute of Environmental Conservation and Research INECAR (2000). Position Paper Against Mining in Rapu-Rapu, Published by INECAR, Ateneo de Naga University, Philippines

120. Arsenic, I.A.R.C., 2004. Arsenic compounds. Envrionmental Health Criteria.

121. Hartwig, A. and Schwerdtle, T., 2002. Interactions by carcinogenic metal compounds with DNA repair processes: toxicological implications. Toxicology letters, 127(1), pp.47-54.

122. Harada, M., 1995. Minamata disease: methylmercury poisoning in Japan caused by environmental pollution. Critical reviews in toxicology, 25(1), pp.1-24.

123. Kim, H.S., Kim, Y.J. and Seo, Y.R., 2015. An overview of carcinogenic heavy metal: molecular toxicity mechanism and prevention. Journal of cancer prevention, 20(4), p.232.

124. Willoughby, R.A., MacDonald, E., McSherry, B.J. and Brown, G., 1972. Lead and zinc poisoning and the interaction between Pb and Zn poisoning in the foal. Canadian Journal of Comparative Medicine, 36(4), p.348.

125. FHWA, 1999. Is Highway Runoff a Serious Problem? Office of Infrastructure R&D, Turner-Faribank Highway Research Center, McLean, VA

126. Berbee, R., Rijs, G. and De Brouwer, R., 1999. Characterization and treatment of runoff from highways in the Netherlands paved with impervious and pervious asphalt. Water Environment Research, 71(2), pp.183-190.

127. Gan, H., Zhuo, M., Li, D. and Zhou, Y., 2008. Quality characterization and impact assessment of highway runoff in urban and rural area of Guangzhou, China. Environmental Monitoring and Assessment, 140(1), pp.147-159.

128. Mosley, L.M. and Peake, B.M., 2001. Partitioning of metals (Fe, Pb, Cu, Zn) in urban run-off from the Kaikorai Valley, Dunedin, New Zealand. New Zealand journal of marine and freshwater research, 35(3), pp.615-624.

129. Davis, A.P., Shokouhian, M. and Ni, S., 2001. Loading estimates of lead, copper, cadmium, and zinc in urban runoff from specific sources. Chemosphere, 44(5), pp.997-1009.

130. Ball, J.E., Jenks, R. and Aubourg, D., 1998. An assessment of the availability of pollutant constituents on road surfaces. Science of the Total Environment, 209(2-3), pp.243-254.

131. Huber, M., Welker, A. and Helmreich, B., 2016. Critical review of heavy metal pollution of traffic area runoff: Occurrence, influencing factors, and partitioning. Science of the Total Environment, 541, pp.895-919.

132. Ji, G., Sun, T., Zhou, Q., Sui, X., Chang, S. and Li, P., 2002. Constructed subsurface flow wetland for treating heavy oil-produced water of the Liaohe Oilfield in China. Ecological Engineering, 18(4), pp.459-465.

133. Copeland, C., 1999. Clean Water Act: a summary of the law. Washington, DC: Congressional Research Service, Library of Congress.

134. Sin, S.N., Chua, H., Lo, W. and Ng, L.M., 2001. Assessment of heavy metal cations in sediments of Shing Mun River, Hong Kong. Environment international, 26(5), pp.297-301.

135. Salati, S. and Moore, F., 2010. Assessment of heavy metal concentration in the Khoshk River water and sediment, Shiraz, Southwest Iran. Environmental monitoring and assessment, 164(1), pp.677-689.

136. He, K., Sun, Z., Hu, Y., Zeng, X., Yu, Z. and Cheng, H., 2017. Comparison of soil heavy metal pollution caused by e-waste recycling activities and traditional industrial operations. Environmental Science and Pollution Research, 24(10), pp.9387-9398.

137. Tünay, O. and Kabdaşli, N.I., 1994. Hydroxide precipitation of complexed metals. *Water Research*, *28*(10), pp.2117-2124.

138. Robinson, A.K. and Sum, J.C., 1980. Sulfide precipitation of heavy metals.

139. Charerntanyarak, L., 1999. Heavy metals removal by chemical coagulation and precipitation. *Water Science and Technology*, *39*(10-11), pp.135-138.

140. US Environmental Protection Agency (EPA), Development Document for Effluent Limitations Guidelines and Standards for the Metal Finishing.

141. Zouboulis, A.I., Prochaska, C.A. and Solozhenkin, P.M., 2005. Removal of zinc from dilute aqueous solutions by galvanochemical treatment. *Journal of Chemical Technology and Biotechnology*, *80*(5), pp.553-564.

142. US. EPA, 1983 Control and treatment technology for the metal finishing industry.

143. Tzanetakis, N., Taama, W.M., Scott, K., Jachuck, R.J.J., Slade, R.S. and Varcoe, J., 2003. Comparative performance of ion exchange membranes for electrodialysis of nickel and cobalt. *Separation and Purification Technology*, *30*(2), pp.113-127.

144. Marder, L., Bernardes, A.M. and Ferreira, J.Z., 2004. Cadmium electroplating wastewater treatment using a laboratory-scale electrodialysis system. *Separation and Purification Technology*, *37*(3), pp.247-255.

145. Rana, P., Mohan, N. and Rajagopal, C., 2004. Electrochemical removal of chromium from wastewater by using carbon aerogel electrodes. *Water research*, *38*(12), pp.2811-2820.

146. Martínez, S.A., Rodríguez, M.G., Aguilar, R. and Soto, G., 2004. Removal of chromium hexavalent from rinsing chromating waters electrochemical reduction in a laboratory pilot plant. *Water Science and Technology*, *49*(1), pp.115-122.

147. Subbaiah, T., Mallick, S.C., Mishra, K.G., Sanjay, K. and Das, R.P., 2002. Electrochemical precipitation of nickel hydroxide. *Journal of power sources*, *112*(2), pp.562-569.

148. Bhattacharyya, D., Jumawan Jr, A.B. and Grieves, R.B., 1979. Separation of toxic heavy metals by sulfide precipitation. *Separation Science and Technology*, *14*(5), pp.441-452.

149. Anderson, J. and Weiss, C., Sybron Corp, 1973. *Method for precipitation of heavy metal sulfides*. U.S. Patent 3,740,331.

150. Yang, X.J., Fane, A.G. and MacNaughton, S., 2001. Removal and recovery of heavy metals from wastewaters by supported liquid membranes. *Water Science and Technology*, *43*(2), pp.341-348.

151. Bose, P., Bose, M.A. and Kumar, S., 2002. Critical evaluation of treatment strategies involving adsorption and chelation for wastewater containing copper, zinc and cyanide. *Advances in Environmental Research*, *7*(1), pp.179-195.

152. Li, Y., Zeng, X., Liu, Y., Yan, S., Hu, Z. and Ni, Y., 2003. Study on the treatment of copper-electroplating wastewater by chemical trapping and flocculation. *Separation and Purification Technology*, *31*(1), pp.91-95.

153. Wang, L.K., Hung, Y.T. and Shammas, N.K. eds., 2005. *Physicochemical treatment processes* (Vol. 3). Humana Press.

154. Semerjian, L. and Ayoub, G.M., 2003. High-pH–magnesium coagulation–flocculation in wastewater treatment. *Advances in Environmental Research*, *7*(2), pp.389-403.

155. Cheng, R.C., Liang, S., Wang, H.C. and Beuhler, M.D., 1994. Enhanced coagulation for arsenic removal. *Journal-American Water Works Association*, *86*(9), pp.79-90.

156. Rengaraj, S., Yeon, K.H. and Moon, S.H., 2001. Removal of chromium from water and wastewater by ion exchange resins. *Journal of hazardous materials*, *87*(1-3), pp.273-287.

157. Dąbrowski, A., Hubicki, Z., Podkościelny, P. and Robens, E., 2004. Selective removal of the heavy metal ions from waters and industrial wastewaters by ion-exchange method. *Chemosphere*, *56*(2), pp.91-106.

158. Rengaraj, S., Joo, C.K., Kim, Y. and Yi, J., 2003. Kinetics of removal of chromium from water and electronic process wastewater by ion exchange resins: 1200H, 1500H and IRN97H. *Journal of hazardous materials*, *102*(2-3), pp.257-275.

159. Juang, R.S., Lin, S.H. and Wang, T.Y., 2003. Removal of metal ions from the complexed solutions in fixed bed using a strong-acid ion exchange resin. *Chemosphere*, *53*(10), pp.1221-1228.

160. Lin, S.H. and Kiang, C.D., 2003. Chromic acid recovery from waste acid solution by an ion exchange process: equilibrium and column ion exchange modeling. *Chemical Engineering Journal*, *92*(1-3), pp.193-199.

161. Kabay, N., Arda, M., Saha, B. and Streat, M., 2003. Removal of Cr (VI) by solvent impregnated resins (SIR) containing aliquat 336. *Reactive and Functional Polymers*, *54*(1-3), pp.103-115.

162. Gode, F. and Pehlivan, E., 2003. A comparative study of two chelating ion-exchange resins for the removal of chromium (III) from aqueous solution. *Journal of Hazardous Materials*, *100*(1-3), pp.231-243.

163. Ahmed, S., Chughtai, S. and Keane, M.A., 1998. The removal of cadmium and lead from aqueous solution by ion exchange with Na Y zeolite. *Separation and purification technology*, *13*(1), pp.57-64.

164. Kurniawan, T.A., Chan, G.Y., Lo, W.H. and Babel, S., 2006. Physico–chemical treatment techniques for wastewater laden with heavy metals. Chemical engineering journal, 118(1), pp.83-98.

165. Malik, A., 2004. Metal bioremediation through growing cells. Environment international, 30(2), pp.261-278.

166. Garbisu, C., Ishii, T., Leighton, T. and Buchanan, B.B., 1996. Bacterial reduction of selenite to elemental selenium. Chemical Geology, 132(1-4), pp.199-204.

167. Garbisu, C., Alkorta, I., Llama, M.J. and Serra, J.L., 1998. Aerobic chromate reduction by Bacillus subtilis. Biodegradation, 9(2), pp.133-141.

168. Iwamoto, T. and Nasu, M., 2001. Current bioremediation practice and perspective. Journal of bioscience and bioengineering, 92(1), pp.1-8.

169. Perales-Vela, H.V., Pena-Castro, J.M. and Canizares-Villanueva, R.O., 2006. Heavy metal detoxification in eukaryotic microalgae. Chemosphere, 64(1), pp.1-10.

170. Zeraatkar, A.K., Ahmadzadeh, H., Talebi, A.F., Moheimani, N.R. and McHenry, M.P., 2016. Potential use of algae for heavy metal bioremediation, a critical review. Journal of environmental management, 181, pp.817-831.

171. Langmuir, I., 1918. The adsorption of gases on plane surfaces of glass, mica and platinum. *Journal of the American Chemical society*, *40*(9), pp.1361-1403.

172. Brunauer, S., Emmett, P.H. and Teller, E., 1938. Adsorption of gases in multimolecular layers. *Journal of the American chemical society*, *60*(2), pp.309-319.

173. Rouquerol, J., Rouquerol, F., Llewellyn, P., Maurin, G. and Sing, K.S., 2013. *Adsorption by powders and porous solids: principles, methodology and applications*. Academic press.

174. Liu, S., 2016. *Bioprocess Engineering: Kinetics, Sustainability, and Reactor Design*. Elsevier.

175. Liu, S., 2014. A visit on the kinetics of surface adsorption. *Journal of Bioprocess Engineering and Biorefinery*, *3*(2), pp.100-114.

176. Liu, S., 2015. A mathematical model for competitive adsorptions. *Separation and Purification Technology*, *144*, pp.80-89.

177. Liu, S., 2015. Cooperative adsorption on solid surfaces. *Journal of colloid and interface science*, *450*, pp.224-238.

178. Chen, H. and Liu, S., 2015. Cooperative adsorption based kinetics for dichlorobenzene dechlorination over Pd/Fe bimetal. *Chemical Engineering Science*, *138*, pp.510-515.

179. Kobya, M., Demirbas, E., Senturk, E. and Ince, M., 2005. Adsorption of heavy metal ions from aqueous solutions by activated carbon prepared from apricot stone. *Bioresource technology*, *96*(13), pp.1518-1521.

180. Kadirvelu, K., Thamaraiselvi, K. and Namasivayam, C., 2001. Removal of heavy metals from industrial wastewaters by adsorption onto activated carbon prepared from an agricultural solid waste. *Bioresource technology*, *76*(1), pp.63-65.

181. Corapcioglu, M.O. and Huang, C.P., 1987. The adsorption of heavy metals onto hydrous activated carbon. *Water Research*, *21*(9), pp.1031-1044.

182. Baccar, R., Bouzid, J., Feki, M. and Montiel, A., 2009. Preparation of activated carbon from Tunisian olive-waste cakes and its application for adsorption of heavy metal ions. *Journal of Hazardous Materials*, *162*(2-3), pp.1522-1529.

183. Erdem, E., Karapinar, N. and Donat, R., 2004. The removal of heavy metal cations by natural zeolites. *Journal of colloid and interface science*, *280*(2), pp.309-314.

184. Bailey, S.E., Olin, T.J., Bricka, R.M. and Adrian, D.D., 1999. A review of potentially low-cost sorbents for heavy metals. *Water research*, *33*(11), pp.2469-2479.

185. Shafaei, A., Ashtiani, F.Z. and Kaghazchi, T., 2007. Equilibrium studies of the sorption of Hg (II) ions onto chitosan. *Chemical Engineering Journal*, *133*(1-3), pp.311-316.

186. Jha, I.N., Iyengar, L. and Rao, A.P., 1988. Removal of cadmium using chitosan. *Journal of Environmental Engineering*, *114*(4), pp.962-974.

187. Udaybhaskar, P., Iyengar, L. and Rao, A.V.S., 1990. Hexavalent chromium interaction with chitosan. *Journal of Applied Polymer Science*, *39*(3), pp.739-747.

188. Masri, M.S., Reuter, F.W. and Friedman, M., 1974. Binding of metal cations by natural substances. *Journal of Applied Polymer Science*, *18*(3), pp.675-681.

189. Ngah, W.W., Teong, L.C. and Hanafiah, M.A.K.M., 2011. Adsorption of dyes and heavy metal ions by chitosan composites: A review. *Carbohydrate polymers*, *83*(4), pp.1446-1456.

190. Kousalya, G.N., Gandhi, M.R., Sundaram, C.S. and Meenakshi, S., 2010. Synthesis of nano-hydroxyapatite chitin/chitosan hybrid biocomposites for the removal of Fe (III). *Carbohydrate polymers*, *82*(3), pp.594-599.

191. Dinu, M.V. and Dragan, E.S., 2010. Evaluation of Cu2+, Co2+ and Ni2+ ions removal from aqueous solution using a novel chitosan/clinoptilolite composite: Kinetics and isotherms. *Chemical Engineering Journal*, *160*(1), pp.157-163.

192. Demirbas, A., 2008. Heavy metal adsorption onto agro-based waste materials: a review. *Journal of hazardous materials*, *157*(2-3), pp.220-229.

193. Gardea-Torresdey, J.L., De La Rosa, G. and Peralta-Videa, J.R., 2004. Use of phytofiltration technologies in the removal of heavy metals: A review. *Pure and Applied Chemistry*, *76*(4), pp.801-813.

194. Celik, A. and Demirbaş, A., 2005. Removal of heavy metal ions from aqueous solutions via adsorption onto modified lignin from pulping wastes. *Energy sources, 27*(12), pp.1167-1177.

195. Šćiban, M.B., Klašnja, M.T. and Antov, M.G., 2011. Study of the biosorption of different heavy metal ions onto Kraft lignin. *Ecological engineering*, *37*(12), pp.2092-2095.

196. Demirbas, A., 2004. Adsorption of lead and cadmium ions in aqueous solutions onto modified lignin from alkali glycerol delignication. *Journal of hazardous materials*, *109*(1-3), pp.221-226.

197. Parajuli, D., Inoue, K., Ohto, K., Oshima, T., Murota, A., Funaoka, M. and Makino, K., 2005. Adsorption of heavy metals on crosslinked lignocatechol: a modified lignin gel. *Reactive and functional polymers*, *62*(2), pp.129-139.

198. Peternele, W.S., Winkler-Hechenleitner, A.A. and Pineda, E.A.G., 1999. Adsorption of Cd (II) and Pb (II) onto functionalized formic lignin from sugar cane bagasse. *Bioresource Technology*, *68*(1), pp.95-100.

199. Zu-guang, L.I.U., Shi-xian, L. and Xiao-xue, Y.A.N., 2011. Adsorption of lead ions in effluent onto lignin amines adsorbents from modified kraft lignin. *Transactions of China Pulp and Paper*, *26*(2), p.53.

200. Ge, Y., Li, Z., Kong, Y., Song, Q. and Wang, K., 2014. Heavy metal ions retention by bi-functionalized lignin: Synthesis, applications, and adsorption mechanisms. *Journal of Industrial and Engineering Chemistry*, *20*(6), pp.4429-4436.

201. Wu, Y., Zhang, S., Guo, X. and Huang, H., 2008. Adsorption of chromium (III) on lignin. *Bioresource technology*, *99*(16), pp.7709-7715.

202. Mohan, D., Pittman Jr, C.U. and Steele, P.H., 2006. Single, binary and multi-component adsorption of copper and cadmium from aqueous solutions on Kraft lignin—a biosorbent. *Journal of colloid and interface science*, *297*(2), pp.489-504.

203. Crist, R.H., Martin, J.R. and Crist, D.R., 2002. Heavy metal uptake by lignin: comparison of biotic ligand models with an ion-exchange process. *Environmental science & technology*, *36*(7), pp.1485-1490.

204. Srivastava, S.K., Singh, A.K. and Sharma, A., 1994. Studies on the uptake of lead and zinc by lignin obtained from black liquor–a paper industry waste material. *Environmental technology*, *15*(4), pp.353-361.

205. Valdivia M, Galan JL, Laffarga J, Ramos J L, Biofuels 2020: Biorefineries based on lignocellulosic materials. Microb Biotechnol **9**:585-594 (2016).

206. Tan T, Shang F, Zhang X, Current development of biorefinery in China. Biotechnol Adv **28:**543-555 (2010).

207. Kumar P, Barrett DM, Delwiche MJ, Stroeve P, Methods for pretreatment of lignocellulosic biomass for efficient hydrolysis and biofuel production. Ind Eng Chem Res **48**:3713-3729 (2009).

208. Yan J, Joshee N, Liu S, Utilization of Hardwood in Biorefinery: A Kinetic Interpretation of Pilot-Scale Hot-Water Pretreatment of Paulownia elongata Woodchips. J Biobased Mater Bioenergy **10**:339-348 (2016).

209. Xie Y, Liu S, Purification and concentration of paulownia hot water wood extracts with nanofiltration. Sep Purif Technol **156**:848-855 (2015).

210. Yan J, Liu S, Hot water pretreatment of boreal aspen woodchips in a pilot scale digester. Energies **8**:1166-1180 (2015).

211. Wyman CE, and Yang B, Combined Severity Factor for Predicting Sugar Recovery in Acid-Catalyzed Pretreatment Followed by Enzymatic Hydrolysis, ed by Ruiz HA, Trajano HL and Thomsen MH, Springer International Publishing, Switzerland, pp 161-180 (2017).

212. Wojtasz-Mucha J, Hasani M, Theliander H, Hydrothermal pretreatment of wood by mild steam explosion and hot water extraction. Bioresour Technol **241**:120-126 (2017).

213. Pielhop T, Larrazábal GO, Studer MH, Brethauer S, Seidel CM, von Rohr PR, Lignin repolymerisation in spruce autohydrolysis pretreatment increases cellulase deactivation. Green Chem **17**:3521-3532 (2015).

214. Yan, J., Joshee, N. and Liu, S., 2016. Utilization of hardwood in biorefinery: a kinetic interpretation of pilot-scale hot-water pretreatment of Paulownia elongata woodchips. *Journal of Biobased Materials and Bioenergy*, *10*(5), pp.339-348.

215. Yan, J. and Liu, S., 2015. Hot water pretreatment of boreal aspen woodchips in a pilot scale digester. *Energies*, *8*(2), pp.1166-1180.

216. Yan, J., Joshee, N. and Liu, S., 2013. Kinetics of the hot-water extraction of paulownia elongata woodchips. *Journal of Bioprocess Engineering and Biorefinery*, *2*(1), pp.1-10.

217. Lundquist, K., 1992. Proton (1 H) NMR Spectroscopy. In *Methods in lignin chemistry* (pp. 242-249). Springer, Berlin, Heidelberg.

218. Goundalkar MJ, Corbett DB, Bujanovic BM, Comparative analysis of milled wood lignins (MWLs) isolated from sugar maple (SM) and hot-water extracted sugar maple (ESM). Energies **7**:1363-1375(2014).

219. Pomar F, Merino F, Barceló AR, O-4-Linked coniferyl and sinapyl aldehydes in lignifying cell walls are the main targets of the Wiesner (phloroglucinol-HCl) reaction. Protoplasma **220**:17-28 (2002).

220. Ibarra D, José C, Gutiérrez A, Rodríguez IM, Romero J, Martínez MJ, Martínez ÁT, Chemical characterization of residual lignins from eucalypt paper pulps. J Anal Appl Pyrolysis **74**:116-122 (2005).

221. Lalvani SB, Wiltowski TS, Murphy D, Lalvani LS, Metal removal from process water by lignin, Environ Technol **18**:1163-1168 (1997).

222. P.B. Tchounwou, C.G. Yedjou, A.K. Patlolla, D.J. Sutton, Heavy metal toxicity and the environment, Mol. Clin. Toxicol. 101 (2012) 133-164.

223. Z. Li, Z. Ma, T.J. van der Kuijp, Z. Yuan, L. Huang, A review of soil heavy metal pollution from mines in China: pollution and health risk assessment, Sci. Total Environ. 468 (2014) 843-853.

224. I. Razo, L. Carrizales, J. Castro, F. Díaz-Barriga, M. Monroy, Arsenic and heavy metal pollution of soil, water and sediments in a semi-arid climate mining area in Mexico, Water Air Soil Pollut. 152 (2004) 129-152.

225. T.C. Hutchinson, L.M. Whitby, Heavy-metal pollution in the Sudbury mining and smelting region of Canada, I. Soil and vegetation contamination by nickel, copper, and other metals, Environ. Conserv. 1 (1974) 123-132.

226. E. Repo, J.K. Warchoł, A. Bhatnagar, M. Sillanpää, Heavy metals adsorption by novel EDTA-modified chitosan–silica hybrid materials, J. Colloid Interface Sci. 358 (2011) 261-267.

227. A. Abbas, A.M. Al-Amer, T. Laoui, M.J. Al-Marri, M.S. Nasser, M. Khraisheh, M.A. Atieh. Heavy metal removal from aqueous solution by advanced carbon nanotubes: critical review of adsorption applications, Sep. Purif. Technol. 157 (2016) 141-161.

228. M.K. Uddin, A review on the adsorption of heavy metals by clay minerals, with special focus on the past decade, Chem. Eng. J. 308 (2017) 438-462.

229. J. Song, M. Liu and Y. Zhang, Ion-exchange adsorption of calcium ions from water and geothermal water with modified zeolite, AIChE J. 61 (2015) 640-654.

230. Z. Reddad, C. Gerente, Y. Andres, P. Le Cloirec, Adsorption of several metal ions onto a low-cost biosorbent: kinetic and equilibrium studies, Environ. Sci. Technol. 36 (2002) 2067-2073.

231. X. Li, H. Zhou, W. Wu, S. Wei, Y. Xu, Y. Kuang, Studies of heavy metal ion adsorption on Chitosan/Sulfydryl-functionalized graphene oxide composites, J. Colloid Interface Sci. 448 (2015) 389-397.

232. T. Chen, Y. Zhang, H. Wang, W. Lu, Z. Zhou, Y. Zhang, L. Ren, Influence of pyrolysis temperature on characteristics and heavy metal adsorptive performance of biochar derived from municipal sewage sludge, Bioresour. Technol. 164 (2014) 47-54.

233. X. Sun, B. Peng, Y. Ji, J. Chen, D. Li, Chitosan (chitin)/cellulose composite biosorbents prepared using ionic liquid for heavy metal ions adsorption, AIChE J. 55 (2009) 2062-2069.

234. R. Shawabkeh, A. Al-Harahsheh, M. Hami, A. Khlaifat, Conversion of oil shale ash into zeolite for cadmium and lead removal from wastewater, Fuel 83 (2004) 981-985.

235. A.I. Okoye, P.M. Ejikeme, O.D. Onukwuli, Lead removal from wastewater using fluted pumpkin seed shell activated carbon: Adsorption modeling and kinetics, Int. J. Environ. Sci. Technol. 7 (2010) 793-800.

236. S.A. Al-Jlil, F.D. Alsewailem, Saudi Arabian clays for lead removal in wastewater, Appl. Clay Sci. 42 (2009) 671-674.

237. V.K. Gupta, I. Ali, Removal of lead and chromium from wastewater using bagasse fly ash—a sugar industry waste, J. Colloid Interface Sci. 271 (2004) 321-328.

238. M. Huang, H. Tu, J. Chen, R. Liu, Z. Liang, L. Jiang, X. Shi, Y. Du, H. Deng, Chitosan-rectorite nanospheres embedded aminated polyacrylonitrile nanofibers via shoulder-to-shoulder electrospinning and electrospraying for enhanced heavy metal removal, Appl. Surf. Sci. 437 (2018) 294-303.

239. M. Visa, A.M. Chelaru, Hydrothermally modified fly ash for heavy metals and dyes removal in advanced wastewater treatment, Appl. Surf. Sci. 303 (2014) 14-22.

240. M.Y. Balakshin, E.A. Capanema, C.L. Chen, H.S. Gracz, Elucidation of the structures of residual and dissolved pine kraft lignins using an HMQC NMR technique, J. Agric. Food Chem. 51 (2003) 6116-6127.

241. Y. Huang, M.U. Farooq, S. Lai, X. Feng, P. Sampranpiboon, X. Wang, W. Huang. Model fitting of sorption kinetics data: Misapplications overlooked and their rectifications, AIChE J.

242. Z. Liu, L. Meng, J. Chen, Y. Cao, Z. Wang, H. Ren, The utilization of soybean straw III: Isolation and characterization of lignin from soybean straw, Biomass Bioenergy 94 (2016) 12-20.

243. K.P. Kringstad, R. Mörck, 13C-NMR spectra of kraft lignins, Holzforschung 37 (1983) 237-

244. R.M. Ali, H.A. Hamad, M.M. Hussein, G.F. Malash. Potential of using green adsorbent of heavy metal removal from aqueous solutions: adsorption kinetics, isotherm, thermodynamic, mechanism and economic analysis, Ecol. Eng. 91 (2016) 317-332.

245. Y. Ge, Q. Song, Z. Li, A Mannich base biosorbent derived from alkaline lignin for lead removal from aqueous solution, Ind. Eng. Chem. Res. 23 (2015) 228-234.

Resume

Hanchi Chen

hchen23@syr.edu

I. Work Experiences:

SUNY - ESF, Department of Paper and Bioprocess Engineering

Teaching Assistant: Bioreaction Engineering

Teaching Assistant: Differential Equations

Teaching Assistant: Numerical Method & Computer Programing

AkzonNobel, Shanghai, China **May, 2013 – Aug, 2013**

Reach Assistant

BASF (BACH), Shanghai, China **June, 2014 – Aug, 2014**

Analytical Chemist

Chinese Student and Scholar Association, SUNY-ESF **May, 2014 – May, 2015**

President

II. Education:

Bioprocess Engineering SUNY-ESF (2016-2018), Ph.D

Bioprocess Engineering SUNY-ESF (2013-2015), Master of Science

Bioprocess Engineering SUNY-ESF (2012-2013), Bachelor's degree

Chemical Engineering Sichuan University (2009-2012), Bachelor's degree

III. Research Experiences:

Joined State University of New York, College of Environmental Science and Forestry (SUNY-ESF) as transferred senior student from China at August 2012. Started to research on the biorefinery of dried distiller's grains (DDG) since December 2012 and published a peer-reviewed article titled "Conversion of distillers grain to chemicals, liquid fuel and materials" discussing the latest technologies in DDG biorefinery.

Joined the Master of Science program at SUNY-ESF at August 2013, continuing the research on DDG biorefinery. Studied the hot-water pretreatment and acid hydrolysis technologies. Used NMR in hydrolysate characterizations and sugar quantifications. Published a peer-reviewed article titled "A Kinetic Study of DDGS Hemicellulose Acid Hydrolysis and NMR Characterization of DDGS Hydrolysate", introducing a mechanistic based kinetics study of acid hydrolysis and the NMR method in sugar quantification. During the Master's period, I conducted an independent research project on non-ideal adsorption. Developed the "cooperative adsorption theory" that characterized the deviation from Langmuir adsorption as the interactions between adsorbate and active site. During the project, a peer-reviewed article titled "Cooperative adsorption based kinetics for dichlorobenzene dechlorination over Pd/Fe bimetal" was

published. The article studied the mechanism and kinetics of dichlorobenzene dechlorination over Pd/Fe bimetal with the "cooperative adsorption theory". The theory eliminated the hypothesis in Langmuir and BET models that achieved a breakthrough in the fields of non-ideal adsorption and catalysis.

I continued my PhD program at SUNY-ESF starting at January 2016. My PhD program is about adsorption of heavy metal cations from wastewater using lignin. During the program, a peer-reviewed paper titled "The effect of hot water pretreatment on the heavy metal adsorption capacity of acid insoluble lignin from *Paulownia elongata*" was published. The paper illustrated how hot-water pretreatment can alter the chemical structure of lignin and change its adsorption capacity. Discussed the possibility of using lignin from the biorefinery industry as a heavy metal adsorbent. Another research paper titled "Cooperative adsorption of heavy metals on Kraft lignin" has been drafted discussing the mechanism of the process. The paper used "cooperative adsorption theory" successfully explained the non-ideal adsorption behaviors of Kraft lignin under pH changes. This part of study has been presented in AIChE 2017 annual conference and received great feedbacks.

In summary, my major research fields are wastewater treatment, renewable energy, biorefinery, and reaction kinetics. Besides, I have personal research experiences in enzyme catalysis (glucose isomerase, glucokinase, glycogen phosphorylase), fermentation (bioethanol production with *S. cerevisiae*), and anaerobic digestion.

IV. Publications:

Published 4 peer-reviewed paper as the first author, 1 master's dissertation, and 1 book chapter as the third author

Chen, H. and Liu, S., 2013. Conversion of distillers grain to chemicals, liquid fuel and materials. Journal of Bioprocess Engineering and Biorefinery, 2(2), pp.85-93.

Chen, H. and Liu, S., 2015. A Kinetic Study of DDGS Hemicellulose Acid Hydrolysis and NMR Characterization of DDGS Hydrolysate. Applied biochemistry and biotechnology, 177(1), pp.162-174.

Chen, H. and Liu, S., 2015. Cooperative adsorption based kinetics for dichlorobenzene dechlorination over Pd/Fe bimetal. Chemical Engineering Science, 138, pp.510-515.

Chen, H., 2015. Hot water extraction and acid hydrolysis of dried distiller's grain (Master dissertation, State University of New York College of Environmental Science and Forestry).

Liu, S., Xing, Y., Chen, H., Tang, P., Jiang, J., Tang, S. and Liang, B., 2017. Sustainable Reactors for Biomass Conversion Using Pyrolysis and Fermentation.

Chen, H., Ni, L., Qu, X., Joshee, N. and Liu, S., The effect of hot water pretreatment on the heavy metal adsorption capacity of acid insoluble lignin from Paulownia elongata. Journal of Chemical Technology and Biotechnology.